JIMMA UNIVERSITY

JIMMA INSTITUTE OF TECHNOLOGY

FACULTY OF MECHANICAL ENGINEERING

THERMAL SYSTEMS ENGINEERING STREAM

Performance Investigation and Enhancement of Solar Ejector Cooling System

(Case study area: Addis Ababa, Ethiopia)

A Thesis Submitted to the School of Graduate Studies of Jimma University Institute of Technology in Partial Fulfillment of the Requirements for the Degree of Masters of Science in Thermal Systems of Mechanical Engineering.

By: Mihretab Woldetsadik

November, 2019

Jimma, Ethiopia

Jimma University

Jimma Institute of Technology

Faculty of Mechanical Engineering

Thermal Systems Engineering Stream

Performance Investigation and Enhancement of Solar Ejector Cooling System

(Case study area: Addis Ababa, Ethiopia)

A Thesis Submitted to the School of Graduate Studies of Jimma University Institute of Technology in Partial Fulfillment of the Requirements for the Degree of Masters of Science in Thermal Systems of Mechanical Engineering.

By: *Mihretab Woldetsadik*

Advisor: *Balewgize A. Zeru* (Asst.Prof.)

Co-Advisor: *Jemal Worku* (Msc.)

November, 2019

Jimma, Ethiopia

Declaration

I, the under signed, declare that this research entitled "Performance Investigation and Enhancement of Solar ejector cooling system in Addis Ababa, Ethiopia" is my original work and has not been submitted before for degree or Masters examination to any other University.

By - Mihretab Woldetsadik Ossa **Signature** _____ **Date** _____

This thesis has been submitted for examination with my approval as university supervisor.

Balewgize A. Zeru (Asst.Prof, PhD Candidate) _____ _____

Advisor **Signature** **Date**

Jemal Worku (M.sc) _____ _____

Co-Advisor **Signature** **Date**

Dr. Solomon Tesfamariam _____ _____

External Examiner **Signature** **Date**

Debela Geneti (M.sc) _____ _____

Internal Examiner **Signature** **Date**

Fikadu Kifle (M.Sc) _____ _____

Chairman **Signature** **Date**

Abstract

In this research performance investigation of solar ejector cooling system has been carried out in on-design and off-design operating conditions and enhancement of the ejector is studied. Addis Ababa is taken as a case study area and important data were gathered from the Ethiopian National Meteorology Agency (ENMA) of six consecutive years (2013-18). Hourly and monthly performance analysis of the system is carried out at on-design and it showed a good result. The hourly maximum overall coefficient of the performance and the cooling capacity were obtained as 0.2049 and 186.9 W/m^2, respectively, at 12:00 in March when the design points are (T_g = 90^{O}C, T_C = 30^{O}C and T_e = 12^{O}C). The collector area per ton cooling capacity is found to be 22.3 m^2 at noon for all cooling seasons in Addis Ababa. Off design operating condition map is derived for the system. The results are compared to related researches which is done previously in other countries and it showed good agreement. It was determined that the Solar ejector cooling system could be used for office-cooling purposes during the hours (8:00–15:00) in Addis Ababa/ Ethiopia.

The optimum dimension of Ejector is obtained using one-dimensional hung et al. theory with the help of flowchart with cooperation to EES code. Constant-pressure type ejector with steady state three-dimensional model has been carried out for the ejector (with and without mixer) numerical study in ANSYS 16.0 FLUENT. R-134a is the working fluid which is selected for the study and considered as an ideal gas. The results are compared between with and without mixer ejector. The performance of ejector is improved by 10.4 % and the mixing quality also enhanced.

Key words: Performance Analysis; Meteorological data; Cooling system; off-design operating conditions; Ejector

Nomenclature

Abbreviations

$SoECS$	Solar ejector cooling system
$ESMA$	Energy Sector Management Association program
NMA	National meteorology agency
WRS	World Radiation Center
EES	Engineering equation solver
CFD	Computational fluid dynamics
NXP	Nozzle exit position
COP	Coefficient of performance
COP_{ERS}	Performance of ejector cooling system
$COP_{overall}$	Overall coefficient of performance

Symbols

λ	Wavelength
G_{sc}	Solar constant
$\emptyset$	Latitude
δ	Declination angle
ω	Hour angle
ω_S	Sunrise hour angle
ST	Solar time
θ_Z	Zenith angle
β	Slope

θ_i	Angle of incidence
α_S	Solar altitude angle
n_s	Monthly average daily hours of bright sunshine hour
N_s	Monthly average of maximum possible daily hours of bright sunshine
H_O	Extraterrestrial radiation on a horizontal surface
$\acute{a}$, $\acute{b}$	Empirical constants
H	Monthly average daily radiation on horizontal surface
T_a	Ambient temperature
T_g	Generator temperature
T_c	Condenser temperature
T_e	Evaporator temperature
I_T	Total solar radiation in inclined surface
A_C	Collector area
η_C	Collector efficiency
η_P	Primary nozzle efficiency
η_N	Secondary nozzle efficiency
ϕ_p	Viscous loss arbitrary coefficient
ω	Entrainment ratio
Q_e	Cooling capacity
Q_{coll}	Collector useful energy
q_{coll}	Useful energy gain of the collector per unit of collector area

Biography

The author was born in May 1986 in South Nations Nationality People Region (SNNPR), Wolayita Zone, Soddo district from his mother Libework Babiso and his father Woldetsadik Ossa. He attended his elementary education at Otona elementary schools, and junior secondary education at Otona and senior and secondary school at Soddo Preparatory and high school. He then joined Jimma University in October 2005 and graduated with a B.Sc. degree in Mechanical Engineering in July 2009. After his graduation, he was awarded a merit scholarship from Jimma University due to his final year project was one of the three best technology transfer projects and has still been continued Masters in Thermal Systems Engineering.

Acknowledgement

First of all, I would like to thank almighty God for helping me in all. Secondly to my families that they are supporting me till now. It was impossible without my family to accomplish my study that they supported me in both morally and financially for more than two years. My special thanks to my family's Muluneh, Manuhe, Temesgen, Tsehay, and my mom.

I am very grateful to the Jimma Institute of Technology for giving me this merit scholarship. Also, I would like to express my appreciation to Jimma University Institutes of Technology Mechanical Engineering academic staff members for helping me. Particularly Mr. Abel, Mr. Keiyru, Mr. Bililign Ferihun for allowing me to use their office and Mr. Bisrat Melaku, Mr. Fraol, Mr. Yohanis, Mr. Eyosiyas, and my classmates duly acknowledged.

My exceptional thanks go to Ethiopian national meteorology agency staff members for helping me with full willingness during gathering data.

Next, I would like to thank my main ad-visor Mr. Balewgize and co-advisor Mr.Jemal Worku for their patience and their constructive comments that enriched me to work on this research. Their time and efforts have been a great contribution to my study.

Table of Contents **Page No**

List of Figures

List of Tables

Chapter one

1. Background and Introduction

Solar ejector cooling system (SoECS) is one of the attractive technologies in refrigeration and air conditioning system which uses low-grade energy so that it could be driven with solar energy, geothermal energy, waste heat, etc. The Ejector (Thermal compressor) technology has been used for over greater than one hundred years and has recently undergone a revival in interest for space conditioning applications and this technology offers an alternative whereby the electricity consumption is largely reduced. It is the oldest methods of producing a cooling effect [1].

A solar-driven refrigerator was first recorded in Paris in 1872 by Albel Pifre [2]. A solar boiler was used to supply heat to a crude absorption machine, producing a small amount of ice. Later, solar powered refrigeration systems have been installed worldwide in many countries e.g. Australia, Spain, and the USA. Most are thermally driven absorption systems, designed for air-conditioning purposes.

The energy needed to Refrigeration and Air Conditioning systems consists a vital role in this world. Approximately 15% of the world electrical consumption is used for refrigeration and air-conditioning applications, and additionally, the demand for air conditioning is proportional to solar radiation. Therefore, the utilization of solar energy is a logical way to meet the increasing demand for cooling and consequently, much research has been conducted on this subject in recent years but it was concentrated on the absorption cycle. [3]

Recently the direction in research in the area of refrigeration focusses on decreasing and/or elimination of adverse environmental effects. Refrigeration systems are the source of two types of pollution: ozone depletion from chlorofluorocarbon refrigerants and greenhouse gas emission from electricity production. This creates the crucial need to replace the conventional refrigerants with environment-friendly working fluids as well as applying renewable and non-polluting energies to run these systems.

The growing population and fast depleting reserves of fossil fuels have led scientists in the fields of engineering, meteorology, and industry to pursue the development and use of renewable energy

resources like solar energy. Solar power is pollution free and causes no greenhouse gases to be emitted after installation.

1.1 Energy potential of Ethiopia

Ethiopia uses hydro power as its main energy source for the purpose of cooling and heating mostly. The country should conserve energy by using solar power. Ethiopia is one of the developing countries and there is a significant solar energy potential available therefore rather than using an electrically driven cooling system it's better to use Solar driven cooling system from low-grade energy.

Ethiopia is in Tropical zone and lays between equator and tropic of cancer its solar resource is obviously of significant potential. This makes Ethiopia one of the highest solar energy potential. There are four climate seasons for Ethiopia such as summer (June-August), autonomy (Sept-Nov), winter (Dec-Feb) and spring (March-May). Winter and spring are the hot months and during Summer there is heavy rainfall According to Ethiopia National treasure (ENT), April 2019

The annual average daily radiation in Ethiopia reaching the ground is 5.8 KWh/m^2/day which varies from a minimum of a 4.8 KWh/m^2/day in July to a maximum value of 6.8 KWh/m^2/day in February and march. This is a long-term average Global Horizontal Irradiance for a period of 1994-2015 according to Solaris Energy Sector Management Association program (ESMA) 2019. Here in this research Addis Ababa is selected for the study due to its annual average daily radiation approximately the average of the country 5.789 KWh/m^2/day.

Several HVAC systems use electricity to drive their system depending on the efficiency of the unit and this increases the consumption of the electricity of the country. SoEC system uses ejector instead of compressor however compressor uses electricity power as a driving force due to this it increases the consumption of the electricity. Due to there is no moving parts inside the ejector and it's cheap to manufacture [4]. It has a certain advantage over a system which uses a compressor in terms of maintenance, duration, etc.

1.3 Ejector Technology

Solar Ejector Cooling System has two cycles the first is Power cycle and the second is Cooling cycle. SoEC system main components such as Solar collector, Pumps, Generator, Ejector (thermal compressor), Condenser and Evaporator. An ejector is a component which is added instead of a compressor. Ejector contains three main parts primary converging-diverging nozzle, mixing tube, and diffuser.

The steam produced by solar energy is used as a power to drive the system. The Generator sends the primary fluid (vapor) to the primary nozzle(converging-diverging) then the fluid gets choked inside the primary nozzle throat then it expands when it leaves the nozzle. After passing the nozzle the fluid becomes low pressure in another means it reaches to high velocity then vacuum will be formed. The vacuum formed will entrain the low-pressure vapor from the evaporator then both vapors mix with each other in the mixing section. After passing the mixing section it enters to the diffuser which helps to regain the pressure.

Amongst existing alternatives, ejector cooling seems to be an attractive technology because of its structural simplicity, low initial cost, long life span and relative flexibility in terms of refrigerant selection. In contrast to these advantages, ejector cooling has a relatively low Coefficient of performance (COP) therefore it is necessary to improve ejector performance in order to successfully compete with other heat driven technologies [5]. It is still a fascinating subject for researchers because of gradually decreasing fuel resources and increasing energy costs, even if it has a low coefficient of performance. When we come to the performance of Solar ejector cooling system ejector plays a major role but still, it needs further improvement [6]. The ejector cannot work efficiently in the off-design conditions and its mixing quality is less.

Note-Solar radiation is used interchangeably in this research instead of total solar radiation or Horizontal solar radiation.

1.4 Statement of the problem

Fossil fuels have served mankind for over several years. They have made our life simple as we can always have whatever we want and whenever we want. The big question that stands now if how far these fossil fuels can be used considering the fact that they are going to vanish soon from our lives.

Moreover, some serious environmental problems related to global warming and climate change have made people aware of the brutal consequences that they may have to face if a switch to green and clean energy is not made sooner. This led to use of sources. Sustainable energy should be widely encouraged as it does not cause any harm to the environment and is available widely free of cost. All renewable energy sources like solar, wind and geothermal are sustainable as they are stable and available in plenty [7].

Air conditioning system nowadays plays a major role in making the environment comfortable for human beings. The main driving force for this system is electricity and this will increase the consumption of electricity and its mention above in introduction that approximately 15% of the world electricity is consumed with heating, ventilating and air conditioning system.

The energy use of a central air conditioning and refrigeration highly depends on the climate of the region, a central air conditioning will run 3 to 7 months of the year depending on the outside temperature. An average central AC will use 3 Kw to 5 Kw of power every hour for around 9 hours a day during the hotter months according to (Energy Use 2019).

Ethiopia uses electricity to drive the refrigeration and air Conditioning system mostly and this consumes electricity of the country in addition to that Ethiopia has a high solar energy potential but there are no guidelines or roadmaps for designers and operators still in the country in order to show the way to install solar ejector cooling system with full confidence. Up to now in Ethiopia, performance of ejector cooling system has not been investigated but instead of ejector cooling system, solar absorption cooling system and solar water heating has been investigated.

Here in this research investigation of the performance analysis of Solar ejector cooling system for cooling system in selected city of Ethiopia specially in Addis Ababa is carried out. The

investigation will push the country to use sustainable energy for the application of the Refrigeration and Air conditioning system and shows a way for designers as well as becomes a resource for researchers.

Secondly, Ejector cooling technology has a very low coefficient of performance as compared to the Vapor compression Refrigeration system. Still, the Solar ejector cooling system lacks good performance and Ejector is one of the components that must be responsible. Mixing quality and entrainment ratio is the main parameters that affects the performance of the Ejector. Ejector is the main component for the solar ejector cooling system which is used as a compressor. Ejector still needs further improvement. Here in this research beside of investigation of the system improvement of ejector will be done by using Curved blade mixer inside the primary nozzle of the ejector. This increases the mixing quality and entrainment ratio this means performance of the system will be enhanced.

1.5 Objective of the study

1.5.1 General objective

The main objective of this research is to investigate and enhance the performance of solar ejector cooling system in Addis Ababa.

1.5.2 Specific objective

- ✓ Performance investigation of solar ejector cooling system in hourly and monthly bases of on-design and off-design conditions using engineering equation solver.
- ✓ Deriving performance map for different operating conditions.
- ✓ Designing ejector and obtaining optimum geometry dimensions.
- ✓ Enhancing ejector using Ansys software

1.6 Scope and limitations of the study

The research deals with the investigation of the performance analysis of solar ejector cooling systems in Addis Ababa in hourly and monthly bases using the computational models for the application of cooling system. The investigation has been studied using six years (2013-2018) consecutive meteorological data of selected site. The cooling season and period which are taken into consideration are all months with special focus on nine months (Sept-April) which has high solar radiation within a period of 8:00-15:00. Using genuine data from national meteorology agency monthly and hourly solar ration variation has been analyzed using excel. The performance analyses of the system have been studied in hourly and monthly bases at a design point. In addition to investigation of the system performance in on-design conditions, the off-design (different operating conditions) map derived for the system.

The performance investigation focused on collector area per ton of cooling capacity, cooling capacity per unit collector area, the useful energy output of collector per unit area, solar-collectors efficiency, coefficient of performance and overall coefficient of performance of solar ejector cooling system. The thermal energy storage system is beyond the scope of this research.

Steady state three-dimensional numerical analysis of supersonic steam ejector with and without mixer using computational software ansys fluent 16.0 has been carried out. Constant pressure - flow model is used with a working fluid of R-134a by considering it as an ideal gas. Governing equations of mass, momentum, energy and turbulence were solved with steady state flow. while turbulent kinetic energy and turbulent dissipation rate are discretized with second order upwind scheme. The results are compared between ejector with and without mixer.

Modelling and simulation have been analyzed by using CFD software in three-dimensional. Primary validation (experimental validation) is beyond the scope of this research. In this research only numerical and computational model has been studied.

1.7 Significance of the research

During modern times, we've become reliant on fossil fuels. This allowed us to develop our cultures and economies tremendously, but has come at a steep price. Due to the side-effects of using fossil fuels, the use of solar energy has become important to mankind once again. Some of the reasons solar energy is important are...

- ✓ Global energy demand is increasing
- ✓ Continued usage of fossil fuels is damaging our environment
- ✓ Solar energy is one of the most promising alternatives to fossil fuels

Refrigeration and air conditioning system uses the electricity to drive the compressor and this leads to an increase in the electricity consumption of the world. Solar ejector cooling system uses Solar Energy to drive the system. Due to this, it helps to reduce the consumption of the electricity. Still, it has disadvantages when compared to the compressor using the system, which is related to the performance.

Ethiopia is in the tropical zone lying between the Equator and the Tropic of Cancer due to this it has a high solar energy potential and it is better if the country uses this potential to the purpose of cooling system. Once analyzing the performance of this system will open the door to researchers, designers and operators to apply of the system.

Ejector or thermal compressor is the component which replaces the compressor in solar ejector cooling system. It has no moving parts, not uses the electricity and it is durable when compared to the compressors but it has a very low coefficient of performance. Still, ejector technology needs further improvements due to this it is better to focus on this amazing component.

1.8 Justification/Rationale/Motivation

Ejector Cooling System is an economic system so that could be driven with any kind of heat sources, such as solar energy, geothermal energy, waste heat, etc... [8]. As we know that Ethiopia has high solar energy potential because of its near to the Equator.

I am interested to investigate Solar Ejector cooling system performance analysis in this country which uses electricity instead of solar energy for the purpose of cooling system. Ethiopia didn't use solar energy to cooling system mostly this increases the consumption of electricity in the country.

Investigation of the performance analysis of a solar ejector cooling system in this country is needed due to this I want to investigate and put my role in order to show that this system can perform, this may help the Designers and Operators to install it with full confidence It is an attractive system SoECS because of gradually decreasing fuel resources and increasing energy costs, even if it has a low coefficient of performance. In addition, it requires lower operating and maintenance costs due to it has no moving parts.

Nowadays Compressor is the main device to drive the Refrigeration and Air conditioning system. The compressor uses electricity power in order to drive the fluids and due to moving parts which are inside the Compressor, it is subjected to failure. The maintenance which comes from the moving parts failure will consume the time as well as it increases the cost and the electricity power which drives the compressor will increase the consumption of electricity of the country.

Ejector or thermal compressor is an amazing device which is a gift of Engineering philosophy. It works instead of the compressor in the air Conditioning and refrigeration system. It doesn't use the electric city. It is driven by solar power easily and it has no moving parts due to this it is durable this makes it better than a compressor. It has a certain advantage but still, it has a low COP when compared to vapor compression system. Again, I am interested to improve this special system by adding mixer inside the primary nozzle of the ejector. This helps to increase the performance of the whole system.

Chapter Two

2. Methodology

2.1 Introduction and site selection

Availability of solar radiation data is a basic requirement to utilize solar energy economically. Knowledge of global solar radiation at a site is essential for the proper design and assessment of solar energy conversion systems. However, owing to the high cost of solar radiation measuring devices and owing to the shortage of skillful care, there are few locations in the developing countries where long-term irradiation measurements are available. For example, Ethiopia has only one solar radiation measuring center Addis Ababa, where measurements of daily and hourly values of global and diffuse radiation are carried out.

According to the Solaris Energy Sector Management Association Program (ESMAP) 2019, Ethiopia's solar radiation range is 4.8-6.8 KWh/m2/day. All cities solar radiation lays between the above solar radiation range and many cities solar radiation is very similar to each other so this will help us to predict for the whole country. Now except for Addis Ababa other cities in Ethiopia have no direct Solar radiation measuring device. Other cities except Addis Ababa have an instrument which measures Sunshine Hours, Ambient Temperature relative humidity and so on. Using bright sunshine hour and meteorological parameters solar radiation will be estimated using suitable empirical models.

Addis Ababa is the selected site for this research that which it is found in the in Ethiopia located at 9.02^0 latitude and 38.75^0 longitude and it is situated at elevation of 2,405 meters above sea level with its annual average daily solar radiation is 5.789 KWh/m2/day and Relevant data were acquired and processed using an Excel spreadsheet. The annual average daily solar radiation which reaches ground in Ethiopia is 5.8 KWh/m2/day which is mention in introduction and it is near to Addis Ababa. Due to this Addis Ababa is selected site and relatively to other cities it has a genuine data.

2.2 Data collection

Data has been collected from the Ethiopian National Meteorological Agency (ENMA). The collected data are geographical data latitude, longitude, declination angle in addition to that Meteorological data Sunshine hour, relative humidity, Ambient temperature for six consecutive years. The period to accomplish this research takes a minimum of four months starting from April up to September 2019.

2.3 Data analysis

To accomplish the desired objectives after gathering data by defining the problem the expected review has been carried out. Below there is a chart which contains the methodology of the

research which helps us to accomplish the desired objective.

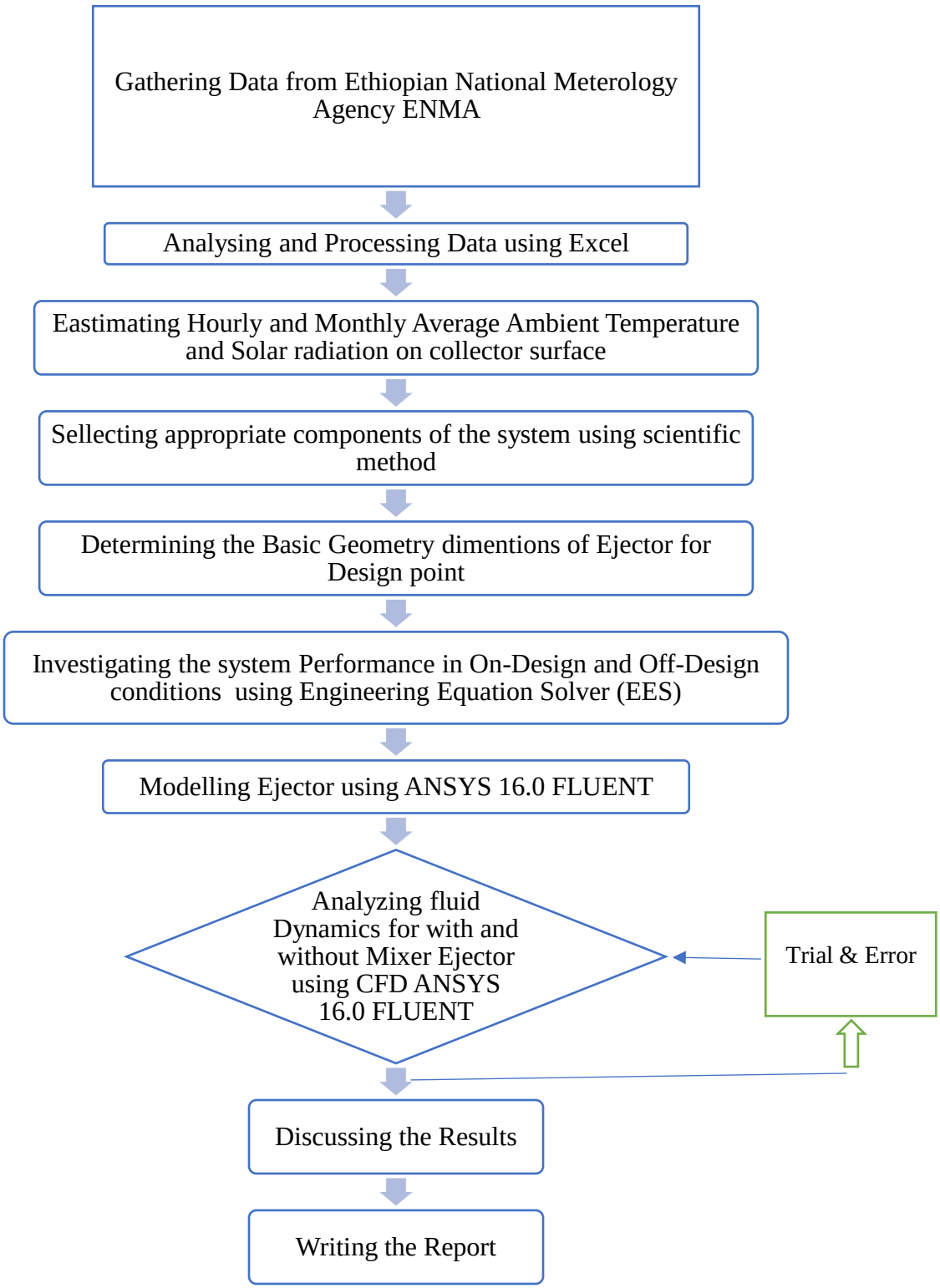

Figure 2.1 Flowchart of the methodology

Chapter Three

3. Literature review

3.1 Solar ejector cooling system in Ethiopia

Ethiopia is one of the tropical zone countries though it has high solar energy potential. Electricity is the main driving source for Refrigeration and Air conditioning system. Different country investigated the performance of the Solar Ejector Cooling System but Ethiopia is not. In general, investigation of this system will show some way to decrease the electricity consumption of the country in the side of Refrigeration and Air conditioning system secondly it will provide the necessary information or data to the Designers and Operators who want to install the system. Solar ejector cooling system is investigated for different countries in the world and this investigation helped those countries to use the system for cooling application.

Adnan, S., Mehmet, O., & Erol, A. (2004) the potential of solar energy in Turkey studied which can whether or not give a required heat for the generator of ejector absorption compression system can be obtained. Due to the country's location, it has high solar energy potential. Analysis of the 17 cities was gathered by using meteorological data. The optimum collector surface area and the maximum heat gain factor was found for all of the selected regions throughout the season. The results showed that there is a great potential for the utilization of solar cooling system for domestic heating and cooling application in Turkey. [9]

Erosy HK, Yalcin S, & Ozgoren M (2007) the performance of the solar ejector cooling system is investigated by taking the southern region of Turkey as the case study using computer programs. Meteorological data collected from Turkish meteorological agency for the study. It was seen that the hourly cooling capacity of Solar ejector cooling in the chosen cities changed from 162.50 W/m^2 - 178 W/m^2 at 12:00 in August. The monthly maximum average of the overall coefficient of performance and cooling load are 0.167 and 108 W/m^2, respectively in July. The problem faced them were to use this system in off-design conditions. Controlling mechanism is needed for the off - design conditions by varying one of the components of ejector. [10]

Pridasawas, W., & Lundqvist, P. (2007) studied solar-driven ejector refrigeration system using iso-butane(R600a) as a refrigerant. Operating at different working conditions and using different solar collector types influence on the performance of the system also examined. The climatic data were generated from METEONORM. The whole system is modeled under the TRNSYS environment, but the model of the ejector refrigeration subsystem is developed in the Engineering Equations Solver (EES) program. At the selected simulation location, Bangkok, condenser temperature 5K above the ambient temperature, evaporator temperature $+15^0$C, an evacuated collector area is 50 m^2 and a hot storage tank volume of 2 m^3, the average yearly system thermal ratio (STR) is about 0.22, the COP of ejector is about 0.48, and the solar collector efficiency is about 0.47. The solar fraction over one year for the system using evacuated tube is on the average 75% at the collector area of 80 m^2. They concluded that at high evaporator temperature ejector works efficiently and the COP of ejector component depends on the evaporator temperature. The operating condition and collector type also influence the performance of the ejector system according to their study.[11]

Kim, D.S., Infante Ferreira, C.A., (2008). They investigated the solar ejector system performance in hot season for six months using the meteorological data from the institute of the Tunis city by using three flat plate collector types. Different environmentally friendly refrigerants such as R141b, R142b, R152a, R245fa, R290, R600 and R717 analyzed based on empirical correlation. Thermodynamic properties of functioning fluids are obtained with a package REFPROP7. The daily period is between 8 and 17 h which the sun shines. In the present work, a computer program based on the above analyses is developed. Given the operating conditions, the software gave the system's performance. It appears that the refrigerant R717 offers the highest coefficient of performance. Coefficient of performance of the ejector air conditioning system was calculated using the data. Maximum COP was obtained is 0.408 for ejector air conditioning system and overall COP is varied from the 0.21 to 0.28. Total solar radiation varied in between 351-875 W/m^2 in July. The results obtained show that the COP of the studied system is mainly influenced by the type and the efficiency of the solar collector.[12]

Ethiopia is one of highest solar annual energy potential when compared to other non-tropical zone countries. The annual average daily radiation in Ethiopia reaching the ground is 5.8 KWh/m^2/day. The above research tells us that the importance of solar ejector cooling system and its performance

analysis in different countries. The application of SoECS is done in many countries and they are using it now. When we come to Ethiopia Solar ejector cooling system is not investigated till now. There are researches conducted in solar water heating and solar assisted vapor absorption refrigeration system but not in solar ejector refrigeration system specifically.

In this research, Investigation of solar ejector cooling system for Addis Ababa for the application of cooling system is carried out. Using computer programs investigation of performance analysis of the system is Determined. It will become a resource for the researchers and will show the way to designers, and operators in order to install the system in the country with confidence. It will fill the resource gaps of solar ejector cooling system performance analysis of the country a little bit.

3.3 Ejector or Thermal compressor background and recent reviews

Solar energy is a good alternative for electricity, fossil fuels, and geothermal energy on the basis of costs. Solar Ejector Cooling system is the system which is used to cool the required space by using solar energy as a source but it also uses waste heat and geothermal energy as its main driving power.

Henry Giffard invented the condensing-type injector in 1858. The background of Giffard‟s intention was to find a solution to the problem of feeding liquid water to replenish the reservoir of steam engine boilers. Since then, ejectors have been studied intensively for a large number of different applications. Typical applications are reviewed with a special emphasis on how ejectors can be utilized to improve the performance of air-conditioning and refrigeration systems. Solar ejector cooling system has a low coefficient of performance and it depends on the working condition but it decreases the consumption of electricity as an advantage. Still, the main problem that makes the system perform badly is the geometry of Ejector. The ejector has three main components such as Primary Nozzle, Mixing section and diffuser. A lot of researchers conducted research on the geometry optimization of Ejector but still, it needs further improvement. The operating conditions affect the performance of the Ejector system. Below there are some researches that are related to the Ejector cooling system and its details.

Alexis, G. K., & Karayiannis, E. K. (2005) they analyzed the influence of the generator, condenser and evaporator temperature including the compression ratio on the entrainment ratio (secondary

fluid to primary fluid). Describes the performance of an ejector cooling system driven by solar energy using R134a as working fluid in the Athens area. COP of ejector cooling system varied from 0.035 to 0.199 when the operating conditions of the generator temperature are (82-90^{0}C), condenser temperature (32-40^{0}C) and evaporator temperature is (-10-0^{0}C). Overall COP varied between 0.014 - 0.101 within total solar radiation of 536 W/m^2 - 838 W/m^2 in July. The system performance calculation proceeded by a sequential simulation process, following the information-flow diagram. Still the gap in this research is that coefficient of performance is low but the solar energy is available in Athens. They concluded that COP of the ejector cooling system is an exponential function of generator, condenser and evaporator temperature.[13]

Khaled A, & Charles, G. (2005) they carried out the flow induction in non-steady supersonic fluid in which steam is working fluid. By varying the throat diameter of the ejector, they analyzed the induction related processes. Especially with regard to pressure exchange moment, studied the complex fluid mechanisms in three-dimensional supersonic, non-steady, viscous flow using computational fluid dynamics (CFD). In this paper a numerical analysis was conducted to study the actual behavior of the steam supersonic pressure exchange ejector and how this is related to throat diameter ratio. The relation between the primary fluid and secondary fluid on the induction process is also studied. 2.90 throat diameter is performed better for the desired cooling effect. They concluded that one can choose the best ejector configuration for a flow induction device which utilizes the principle of pressure exchange.[14]

SzabolcsVarga, Armando C. Oliveir, Bogdan Diaconu (2 0 0 9), they investigated numerical assessment of the steam ejector efficiency using an axi-symmetric CFD model. Water is used as a working fluid and operating conditions were selected in a range that would be suitable for an air-conditioner powered by solar thermal energy. The efficiency of the primary nozzle, suction, mixing, and diffuser was determined for the first time through a most fundamental approach, using the results of a CFD model. It was found that while nozzle efficiency can be considered as constant, the efficiencies related to the suction, mixing and diffuser sections of the ejector depend on operating conditions. They concluded that entrainment ratio increases when constant area chamber cross section decreases at the constant generator and condenser temperature but it results in smaller critical back pressure. CFD analysis has proved its usefulness in analyzing the complex flow behavior in ejectors. It can provide a more fundamental approach for the assessment of ejector

efficiencies and their dependence on operating and geometrical factors that are used in 1D models, which are very useful for ejector design. Gaps found from this journal is that this work can be extended to include the effect of the working fluid, as well as other geometrical factors.[15]

Jean-Marie, S., & Yann, B. (2009) they investigated experimentally and numerically the supersonic air ejector operation and the relation between global operation and local flow features. The software which they used to investigate the numerical analysis is CFD model. The flow in the air-ejector is governed by the ideal gas compressible steady-state axisymmetric form of the viscous fluid flow conservation equations. For variable density flows, the Favre averaged Navier-Stokes (FANS) equations are more suitable and used in this work. Results clearly demonstrate that good predictions of the entrainment rate, even over a wide range of operating conditions, do not necessarily mean a good prediction of the local flow features. This issue is shown through the results obtained for two turbulence models, and also raises the problem of their assessment. Mixing quality and entrainment rate affects the performance of the ejector due to this the two parameters must be improved. In this paper, the analysis of the sonic line location together with the Mach number field and operation curve was proposed as a key parameter to understand the link between local flow features and the entrainment rate. Furthermore, this parameter allowed to locate the position of the critical section where the ejector becomes choked. This method has never been proposed in previous CFD studies.[16]

Dennis, M., &Garzoli, K. (2011) they studied the solar fraction by using variable geometry ejector and cold store in order to get a maximum solar fraction. A computer model of the solar ejector cooler coupled to a cooling load and cold store was constructed in the TRNSYS. They Studied the performance of the ejector by varying secondary duct diameter in the range of 10-20 mm. The variable geometry ejector has increased the yield by 8-13 % compared with the fixed one but this alone is insufficient to achieve acceptable solar fraction for a real system at moderate sized collectors. If a 70% solar fraction is desired and a solar collector area of 20 m^2 is available, a fixed ejector system would require 18 MJ of cold store capacity whereas a variable geometry ejector would require only 12 MJ of cold store capacity. The results showed that using the cold store will decrease the area needed by the solar collector. Furthermore, the study has assumed that, due to the low theoretical COP of the ejector system, cold storage would be more appropriate than storage of high temperature heat as a mechanism for providing cooling into the evening. The study has

variable ejectors with only a variable secondary duct whereas it may be possible to vary the primary jet throat also.[17]

Oliveira and Bogdan Diaconu (2009) analyzed the a solar-assisted ejector cooling system based on a simplified 1D approach numerically. Using water as a working fluid the system performance and required collector area are studied in a Mediterranean country using meteorological data. To get acceptable values, generator temperature should not be below 90^0C for good COP and system efficiency. For the require collector output temperature of 100^0C evacuated tube collectors are better suited for the ejector cooling system. Evaporator temperatures below 10^0C also resulted in very poor system performance (COP < 0.1). Using water as a working fluid is not appropriate at very low temperatures (below 4^0C) for Ejector cooling system. For greater than 35^0C of condenser temperature and for evaporator temperature which is below 10^0C the required collector area is greater than 50 m^2. In the case of Mediterranean country auxiliary heating needed is even relatively high solar radiation (800 W/m^2). It is believed that using a more detailed approach is will give good results. Ejector geometry can be optimized to improve COP by increasing the entrainment ratio using CFD software.[18]

Oliveira , Xiaoli Ma (2 0 1 1) they carried out CFD and experimental analysis by comparing a variable area ratio of steam ejector. Results for 5 kW capacity steam ejector with variable primary nozzle geometry has been studied. Working fluid is water and air conditioning working conditions are considered. The experimental entrainment ratio varied in the range of 0.1- 0.5 depending on operating conditions and spindle tip position. Experimental and CFD results agreed well, with an average relative error of 7.7% for the successful adjustment of the primary flow rate. Secondary flow rate and entrainment ratio were simulated resulted in acceptable accuracy for only 70% of the cases. Small adjustments in the evaporator pressure (<0.2 KPa) resulted in very good agreement between simulated and experimental entrainment ratio. A more complete sensitivity analysis should be carried out in order to analyze the influence of uncertainty in experimentally measured variables (e.g. temperatures, pressures and flow rates) on the validation of steam ejector CFD models, under design and off-design operating conditions this are the gaps of this journal.[19]

Varga, S. & Oliveira Armando, C. (2013) they studied the variable area ratio ejector using environmentally friendly refrigerants R600a and R152a in CFD model numerically. They

improved the performance of the ejector by using variable area ratio by changing the distance of the Spindle from the primary nozzle as a reference. R600a and R152a are the working fluids and R152a performed better COP of 0.21. The results indicated that using a fixed geometry ejector is very sensitive to variations in operating conditions which can have a very negative impact on its performance. When the generator temperature increases by 10^0C it resulted in a 41% decrease in the entrainment ratio for R600a. Along the operating path of the spindle (1-7mm) position from the primary nozzle, the eject performance can be successfully controlled. The movable spindle controls ejector operation by changing the cross-section area for the motive flow in the primary nozzle and thus the primary flow rate. The spindle position obtained in optimal operation was 4mm from the ensuring the critical operation with entrainment ratio of 0.30 in contrast the fixed geometry ejector has entrainment ratio is 0.20. Opening further the spindle resulted in stronger shock waves downstream the nozzle exits as well as in a stronger final wave in the diffuser Simulation results were obtained with a CFD model using FLUENT (ANSYS) package. Research gap is that the study which is done with CFD study must verify the performance improvement of variable area ratio ejector over a fixed geometry design in addition to that it has to develop an adequate control strategy depending on operating conditions.[20]

R.H. Yen , B.J. Huang , C.Y. Chen (2013) they Proposed a variable throat ejector and analyzed its performance using CFD simulations to improve ejector performance. The regressive equation is used to relate optimum throat area ratio for operating range of generator temperature 90-110^{0}C, Condenser temperature 35 - 40^0 C and evaporator temperature 8-20^{0}C. conclusion made is that an ejector with a greater throat area and larger solar collector allows a wider operating range of generator temperatures but may be over-designed and expensive. Decreasing the throat area limits the operating range of the generator temperature, and the resulting system may be unable to use solar energy as a heat source. To make the system better, curve-fitting relationship between the optimum throat area ratio and the operating temperatures should be derived.[21]

Akiko, M., & Haruki, S. (2014). They designed methods of ejector configuration for the solar cooling system. The numerical and experimental approaches are used in ordered to configure the parameters of four sets of mixing section area and nozzle exit area of the ejector are considered. CFD and the experimental test was applied to get the best geometry parameters of ejector through a trial and error approach. The results showed that the performances of the ejector cycle having

four different sets of configuration parameters cannot exceed a linear relationship between cooling capacity and condenser temperature so far. In addition to that ejector cooling system provides cooling using solar energy being higher than 60^0C. The gap that found in this journal is that using CFD and experimental test the best geometry of ejector in the side of an appropriate combination of nozzle exit area, mixing-section area and the length of those parts should be done.[22]

Dennis, M., &Garzoli, K. (2011). They prescribed primary nozzle diameter for a range of operating conditions of solar driven ejectors prescribed using experimental and analytical ejector model. They extended the works of others by providing a means to design the primary nozzle with variable primary throat diameter and nozzle exit diameter. A correlation is provided to determine an optimal nozzle throat diameter as a function of the ejector operating conditions of ambient temperature and solar radiation. The results showed that using fixed geometry ejector for the solar driven cooling system is not likely to be able to produce high cooling yield but for variable geometry ejector its better. The authors documented that there are several other parameters that affect ejector performance, such as the nozzle position relative to the mixing chamber and the mixing chamber geometry. The 1-D model used in this work does not capture the effects of these parameters therefore 2D and 3D model should be recommended. However, in principle, the method presented in this paper could be combined into any analytical ejector mode [23]

Raghavan KS and Murthy Ch (2017) they employed CFD technique to investigate the effect of diverging angle of nozzle, Nozzle exit position (NXP) and throat of the ejector on the entrainment ratio using the steam jet refrigeration cycle. Geometry was created in the Ansys 16.0 workbench. The gird elements were initially created in the form of quadrilateral. The convective terms were discredited with a second order upwind scheme. Ideal gas is selected as working fluid in the ejector three cases were analyzed in this work. The results showed that whenever the diameter of the throat is decreased the entrainment ratio also decreases and whenever the divergent angle of the primary nozzle has increased a series of oblique shocks found in the portion of the divergent section. They used velocity as a dependent variable for the analysis in steam jet refrigeration system the throat diameter, diverging angle and Distance between the nozzle exit to mixing chamber inlet (NXP) plays a major role. Only one fixed mixing chamber is used in this case for different divergent primary nozzle, NXP and throat of an ejector and it is better if variable mixing chamber is tested for the future.[24]

Generally, the above researches worked on the improvement of the ejector and studied the different conditions that affect the overall system. The main issue that made the ejector cooling technology to not perform at an optimum level is Ejector. As we see from the above researches Ejector is the main component which helps the working fluid to be compressed by substituting the compressor. In the introduction part above, it tells the significance of Ejector in Refrigeration and Air Conditioning system. According to Global parameter which increases the coefficient of performance of Ejector is Entrainment ratio, which is the amount of Secondary fluid to the primary fluid [25]. In addition to that, the performance of the Ejector is evaluated by using the Entrainment ratio. The Normal design which exists now has a problem in terms of mixing quality and has low entrainment ratio. In this research, the hollow type mixer which is added will increase the performance by improving the Entrainment ratio in addition to that the mixing quality will be enhanced. Mixer will be modelled and inserted inside the primary nozzle to increase entrainment ratio as well as to enhances the mixing quality and this will increase the overall performance of the system.

CFD technique is the mostly used method for the researchers above to study the ejector performance. Computational Fluid Dynamics is an effective diagnosing numerical tool which aids in understanding the real flow physics inside the ejector and also in achieving optimum ejector geometry for maximum efficiency without causing harm to the environment compared to experimental studies. The CFD technique will be used for this research in order to Model the component in addition to simulate.

3.5 Summarize

The above two research gaps are important gaps which must be fulfilled in the research study because of two reasons the first is Engineering is the field which makes things simpler and effective in short. Nowadays global warming is increasing in the world in the same way the solar incidence is increasing in parallel, due to this we have to use solar energy to cooling applications instead of using electricity power, because solar energy is sustainable energy resource

A country like Ethiopia should use solar energy because of there is a high potential. Ethiopia is developing country therefore rather than consuming electricity it is better if they conserve it using available renewable energy resources. Since we are academician, we should have to investigate

the possibilities of such systems in our countries. Secondly, Ejector is a component which is used in Refrigeration and Air Conditioning system instead of Compressor but it has low COP due to this it must be improved in ordered to perform better.

Ethiopia has not investigated the performance analysis of solar ejector cooling system till now in addition to that Ejector is a component which is the backbone of SoEC system but it has low coefficient of performance. In this research those two gaps will be investigated and enhanced.

Performance of the ejector could be improved by incorporating various techniques like unconventional nozzles, movable primary nozzle or variable throat nozzle, rotor vane pressure exchange ejector, ejector as thermal expansion device, swirl flows, mixer etc. Gupta 1984 et al. Aero foil type blade mixer is used to enhance the ejector and 6% improvement has been shown. figure 3.1 shows the mixer types used in the literature which enhanced the entrainment ratio are shown below

The ejector is designed with fixed mixer with a camber angle of 15° placed at a distance of 5 mm from the primary nozzle entry

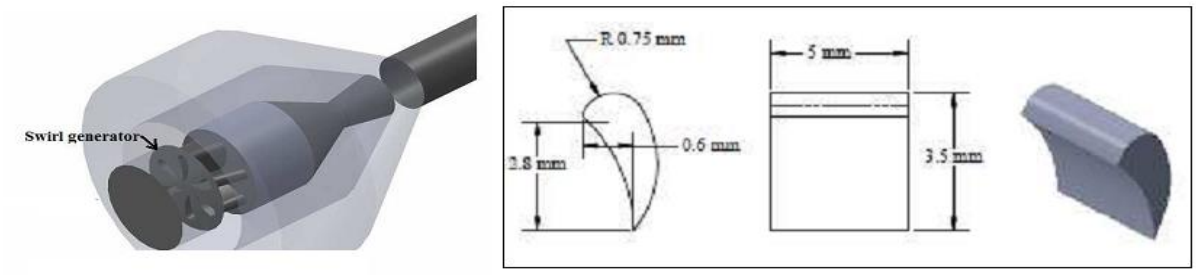

Fig 3.1 Pictorial representation of mixer incorporated in the primary nozzle with aero foil blade type taken from and entrainment ratio enhanced by 6% [26]

Figure 3.2 a, and b shows the two types of mixer the cavity type and solid vane type. Cavity type, in which vanes are arranged in a fashion that it act as a separate duct through which air flow occurs. It enhances the performance by around 5 %.[27]

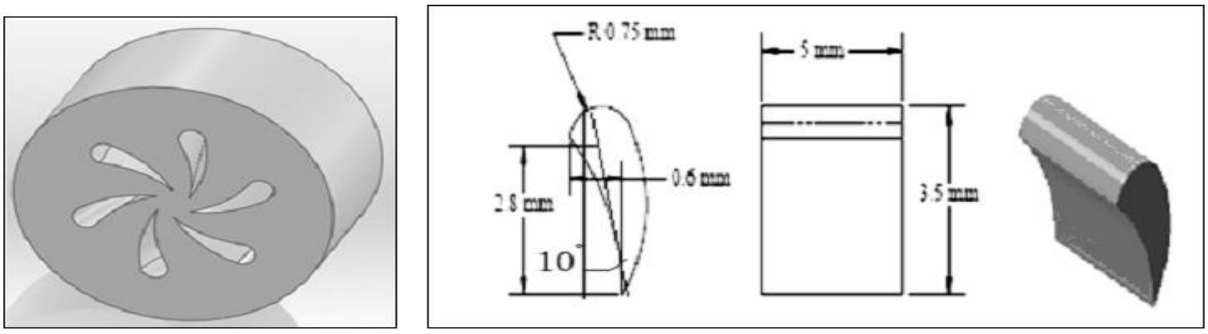

a. Cavity type

Mixer which is shown below is a solid type mixer with 10° camber angle, which induces turbulance of low magnitude, that it has a less significant improvement in the ejector performance only 2% enhancement, similar to the observation made by the author on the studies of turbulent mixing of jets by Schetz and Swanson.

b. Solid vane type

Fig 3.2 a and b Pictorial representation of two types of mixer incorporated in the primary nozzle taken from Maharudrappa 2016

Here in this research curved blade type mixer is used which is shown below

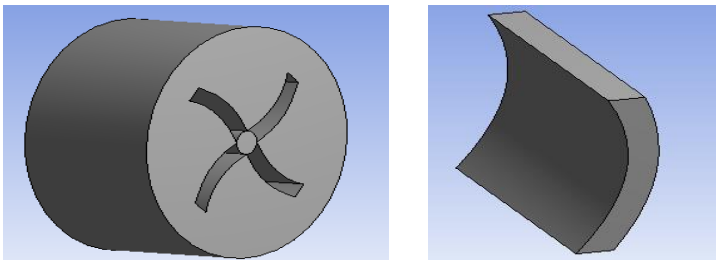

Fig 3.3 Pictorial representation of Mixer incorporated in the primary nozzle with curved blade with hollow type mixer which is used in this research

Using curved blade type mixer which is easy to manufacture. Curved blade with hollow type mixer is used in the present work to investigate the flow behavior and performance prediction of ejector.

Note: -The cavity type mixer is used with four mini channels. It is not a blade but it is a channel which fluid flows. Blade specification is used in ordered to design it easily. The name mixer is used because it enhances mixing qualities.

The two gaps will come together First by investigating the performance analysis of the system in country and after that, using design points of the system Ejector will be enhanced by inserting mixer inside the primary nozzle.

Chapter Four

Mathematical modelling and Analysis

4. Availability of Solar radiation

4.1 The sun

The sun's structure and appearances determine the nature of the energy it radiates into space. The sun is a sphere of intensely hot gaseous matter with a diameter of 1.39×10^9 m and is, on the average, at a mean sun distance 1.5×10^{11}m from the earth. The sun has an effective blackbody temperature of 5777 K. The temperature in the central interior regions of the sun is severally estimated at 80 - 40 $\times 10^6$ K and the density is estimated to be about 100 times that of water.[28]

The energy produced in the interior of the solar sphere at temperatures of many millions of degrees must be transferred out to the surface and then be radiated into space. A succession of radiative and convective processes occurs with successive emission, absorption, and reradiation; the radiation in the sun's core is in the x-ray and gamma-ray parts of the spectrum, with the wavelengths of the radiation increasing as the temperature drops at larger radial distances.

This simplified picture of the sun, its physical structure, and its temperature and density gradients will serve as a basis for appreciating that the sun does not, in fact, function as a blackbody radiator at a fixed temperature. Rather, the emitted solar radiation is the composite result of the several layers that emit and absorb radiation of various wavelengths. The resulting extraterrestrial solar radiation and its spectral distribution have now been measured by various methods in several experiments.

Solar energy is the result of electromagnetic radiation released from the sun by the thermonuclear reactions occurring inside its core. All of the energy resources on earth originate from the sun (directly or indirectly), except for nuclear, tidal, and geothermal energy [28]

4.2 Spectral Distribution of Extraterrestrial Radiation

The sun's energy is emitted constantly in all directions, and it is divided into two forms; extraterrestrial and terrestrial. Radiation in a wavelength range of 0.25 to 3.0 μm, the portion of the electromagnetic radiation that includes most of the energy radiated by the sun.

As you see from above figure that the maximum spectral intensity occurs at about a wavelength $\lambda = 0.48$ μm. About 6.4 % of the total energy is contained in ultraviolet region (< 0.38 μm); Another 48 % is contained in the visible region ($0.38 < \lambda <$ O. 78 μm); and the remaining 45.6 % is contained in the infrared region ($\lambda >$ O. 78 μm).

4.3 The Solar Constant

The solar constant G_{sc} is the energy from the sun per unit time received on a unit area of surface perpendicular to the direction of propagation of the radiation at mean earth-sun distance outside the atmosphere. The availability of very high-altitude aircraft, balloons, and spacecraft has permitted direct measurements of solar radiation outside most or all of the earth's atmosphere. Additional spacecraft measurements have been made with Hickey et al. (1982) reporting 1373 W/m^2 and Willson et al. (1981) reporting 1368 W/m^2. Measurements from three rocket flights reported by Duncan et al. (1982) were 1367, 1372, and 1374 W/m2. The World Radiation Center (WRC) has adopted a value of 1367 W/m2, with an uncertainty of the order of 1% [26]. Here in this research 1367 W/m^2 is also used to calculate the values. Below there is schematically the geometry of the sun-earth relationships.

4.4 Basic Sun-Earth Angles

The geometric relationships between a plane of any particular orientation relative to the earth at any time (whether that plane is fixed or moving relative to the earth) and the incoming beam solar radiation, that is, the position of the sun relative to that plane, can be described in terms of several angles. Some of the angles are indicated in figure below.

4.4.1 Latitude (∅)

The latitude of a location is the angle made by the radial line joining the given location to the center of the earth with its projection on the equatorial plane and it is between $-90^0 \leq \varphi \leq 90^0$.

The angular location north or south of the equator, north positive and south is negative. Addis Ababa is found in northern hemisphere and should face towards the south in order to receive sufficient irradiation. Therefore, the latitude angle is positive.

Addis Ababa which is located on: Latitude is $\emptyset$ =9.01891 due to south

4.4.2 Declination angle (δ)

It's the angular position of the sun at solar noon (i.e., when the sun on the local meridian) with respect to the plane of equator, north positive. The angle between the earth's equatorial plane and the line drawn between the center of the earth and the sun. Declination angle of the sun varies daily and is calculated from the following relation [28]:

$$\delta = 23.45 \sin\left[\frac{360}{365}(284 + N)\right] \quad (4.1)$$

Where N- is year day, with January 1+1.

$1 \leq N \leq 365$

Varies between -23.45 $\leq \delta \leq$ 23.45.

4.4.3 Hour angle (ω)

The angular displacement of the sun east or west of the local meridian due to rotation of the earth on its axis at 15^0 per hour; morning negative, after noon positive.

Solar time and hour angle are related as

$$\omega = (ST - 12)\ x\ 15^0 \quad (4.2)$$

Where ST is the solar time from 1-24 hours

4.4.4 Zenith angle(θ_z)

It is an angle that describes the position of the sun in the sky. the angle between the vertical and the line to the sun, that is, the angle of incidence of beam radiation on a horizontal surface. For horizontal surfaces, the angle of incidence is the zenith angle of the sun, θ_z Its value must be between 0^0 and 90^0 when the sun is above the horizon.

$$\text{Cos}\ \theta_z = \text{Cos}\emptyset\ \text{Cos}\delta\ \text{Cos}\ \omega + \text{Sin}\ \emptyset\ \text{Sin}\ \delta \qquad (4.3)$$

$\boldsymbol{\beta}$ **Slope**, the angle between the plane of the surface in question and the horizontal; $0^0 \leq \beta \leq 180^0$. ($\beta > 90^0$ means that the surface has a downward-facing component.)

4.4.5 Angle of Incidence (θ)

The angle between the beam radiation on a surface and normal to that surface

$$Cos\ \theta = Sin\ \delta\ Sin\ \emptyset\ Cos\ \beta - Sin\ \delta\ \ Cos\ \emptyset\ Sin\ \beta\ Cos\ \gamma + Cos\ \delta\ Cos\ \emptyset\ Cos\ \beta\ Cos\ \omega + Cos\ \delta\ Sin\ \emptyset\ Sin\ \beta\ Cos\ \gamma\ Cos\ \omega + Cos\ \ \delta\ Sin\ \beta\ Sin\ \gamma\ Sin\ \omega \qquad (4.4)$$

The angle θ may exceed 90^0, which means that the sun is behind the surface.[26]

For the horizontal surface, the angle of incidence is the zenith angle of the sun, θ_z. Its value must be between 0^0 and 90^0 when the sun is above the horizon. For this Situation, $\beta = 0$ and the above equation becomes

$$\text{Cos}\ \theta_z = \text{Cos}\emptyset\ \text{Cos}\delta\ \text{Cos}\ \omega + \text{Sin}\ \emptyset\ \text{Sin}\ \delta \qquad (4.5)$$

4.4.6 Surface azimuth angle (γ)

The deviation of the projection on a horizontal plane of the normal to the surface from the local meridian, with zero due south, east negative, and west positive; $-180^0 \leq \gamma \leq 180^0$. Shown in the figure above

4.4.7 Solar azimuth angle (γ_s)

The angular displacement from the south of the projection of the beam radiation on the horizontal plane

4.4.8 Solar altitude angle (α_s)

the angle between the horizontal and the line to the sun, that is, the complement of the zenith angle.[29]

$$\alpha_s = 90^0 - \theta_z \quad (4.6)$$

4.5 Solar radiation in Addis Ababa

Addis Ababa is the city which is found in Ethiopia which is the capital city of the country. It is located 9.02 latitude and 38.7475 longitude and it is situated at elevation 2405 meters above sea level. The annual average daily solar radiation which reaches ground in Addis Ababa is 5.789 KWh/m^2/day which is approximately the average of Ethiopia solar radiation according to Energy Sector Management Association program 2019. Now except for Addis Ababa other cities in Ethiopia have no direct Solar radiation measuring device. Other cities except Addis Ababa have an instrument which measures Sunshine Hours, Ambient Temperature relative humidity and so on. Using bright sunshine hour and meteorological parameters solar radiation will be estimated using suitable empirical models. The average annual solar radiation is needed for this research in ordered to predict for the country.

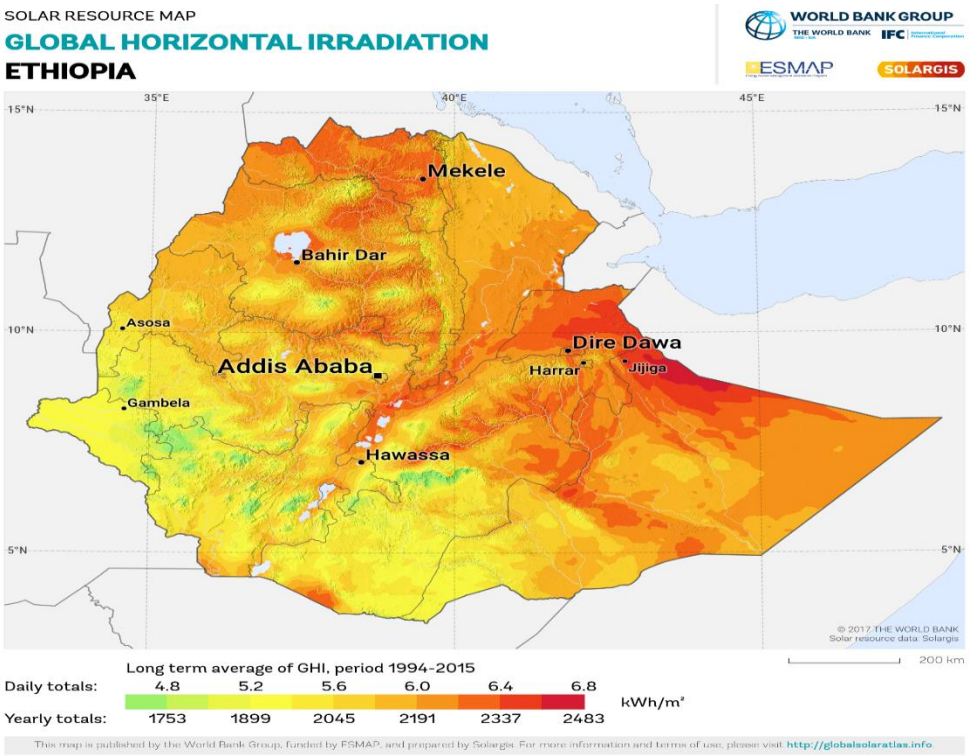

Fig 4.1 The variation of Global Horizontal Radiation in Ethiopia ESMA 2019

According to the above information approximately the average Global horizontal radiation of the country lies in Addis Ababa not only this we can get genuine data relative to other cities in Ethiopia.

4.6 Sunshine hour duration data

Sunshine hour is a climatological indicator, measuring duration of sunshine in a given period (usually a day or a year) for a given location on earth, typically expressed as an averaged value over several years. It is a general indicator of cloudiness of a location, and thus differs from isolation, which measures the total energy delivered by sunlight over a given period.

Two instruments have been or are widely used. The Campbell-Stokes sunshine recorder uses a solid glass sphere of approximately 10 cm diameter as a lens that produces an image of the sun on the opposite surface of the sphere. A strip of standard treated paper is mounted around the appropriate part of the sphere, and the solar image burns a mark on the paper whenever the beam radiation is above a critical level. The lengths of the burned portions of the paper provide an index of the duration of ‘‘bright sunshine.’’ These measurements are uncertain on several counts: The

interpretation of what constitutes a burned portion is uncertain, the instrument does not respond to low levels of radiation early and late in the day, and the condition of the paper may be dependent on humidity.[28] Ethiopia measures bright sunshine hour using Actinographies and Campbell-strokes recorders. Let us see the measure values which are put in graphs

Monthly average daily hours of bright sunshine hour (n_s) variation of Addis Ababa in 2013-2018

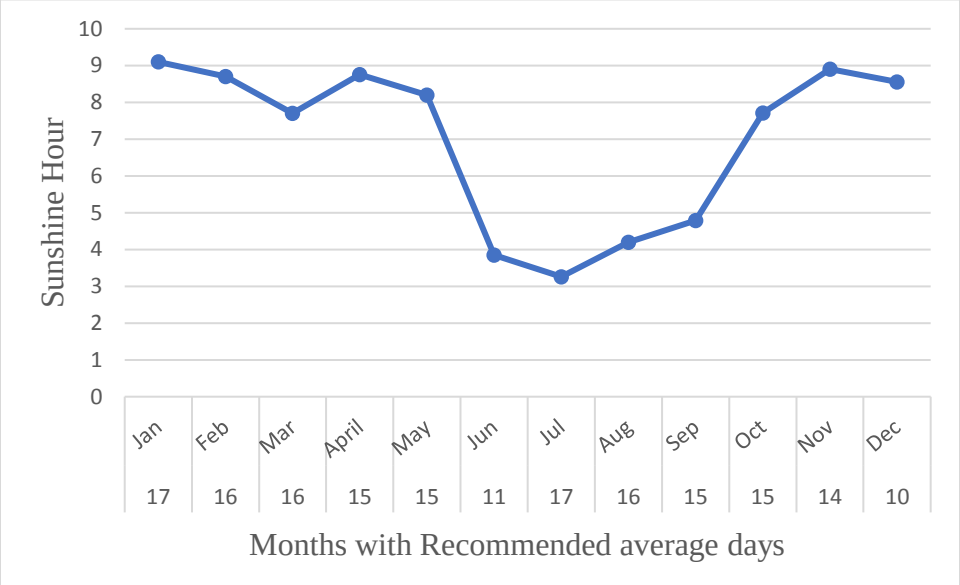

Fig 4.2 Sunshine hour

Monthly average of maximum possible daily hours of bright sunshine (N_s) is calculated using

The length of sunshine hours $\overline{N_s}$ is computed from Cooper's formula:

$$\overline{N_s} = \frac{2}{15} x\, \overline{\omega_s} \qquad (4.7)$$

Where $\overline{\omega_s} = Cos^{-1}(-\tan \emptyset \tan \delta)$ (4.8)

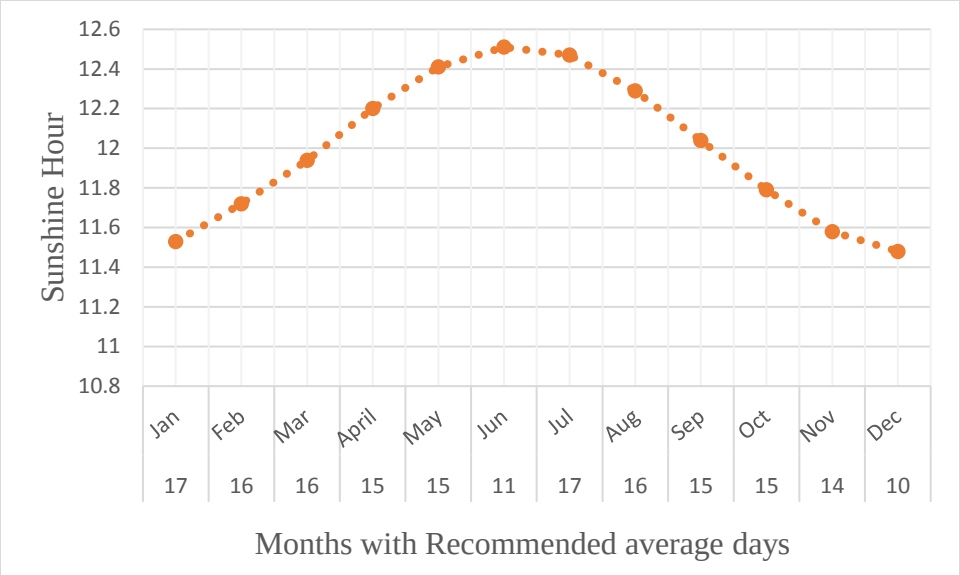

Fig 4.3 Monthly average of maximum possible daily hours of bright sunshine (N_s)

4.7 Extraterrestrial Radiation on a Horizontal Surface

At any point in time, the solar radiation incident on a horizontal plane outside of the atmosphere is the normal incident solar radiation as given by [28]

$$\text{Cos}\ \theta_z = \text{Cos}\emptyset\ \text{Cos}\delta\ \text{Cos}\ \omega + \text{Sin}\ \emptyset\ \text{Sin}\ \delta \tag{4.9}$$

$$G_o = I_{SC}\left(1 + 0.033\ Cos\ \frac{360\ n}{365}\right)\ Cos\ \theta_z \tag{4.10}$$

where - I_{SC} is the solar constant and n is the day of the year Combining Zenith angle for cos θ_z with Equation above gives H_O for a horizontal surface at any time between sunrise and sunset: where $H_O\ and\ G_o$ are same including I_{sc} and G_{sc}

For horizontal surfaces, the angle of incidence is the zenith angle of the sun, θ_z. Its value must be between 0^0 and 90^0 when the sun is above the horizon. For this situation, β = 0

$$H_o = I_{SC}\left(1 + 0.033\ Cos\ \frac{360\ n}{365}\right)\ x\ (\text{Cos}\emptyset\ \text{Cos}\delta\ \text{Cos}\ \omega + \text{Sin}\ \emptyset\ \text{Sin}\ \delta) \tag{4.11}$$

Where- I_{SC} is the solar constant 1367 W/m^2 and n is the day of the year.

For horizontal surfaces, the angle of incidence is the zenith angle of the sun, θ_z. Its value must be between 0^0 and 90^0 when the sun is above the horizon. For this situation, $\beta = 0$

It is often necessary for calculation of daily solar radiation to have the integrated daily extraterrestrial radiation on a horizontal surface, H_o. This is obtained by integrating above Equation over the period from sunrise to sunset. If I_{SC} is in watts per square meter, H_O in daily joules per square meter per day is

$$H_o = \frac{24\ x\ 3600\ x\ I_{SC}}{\pi}\left(1 + 0.033\ Cos\ \frac{360\ n}{365}\right)\ x\ (\text{Cos}\emptyset\ \text{Cos}\delta\ \text{Sin}\omega_s\ + \frac{\pi\omega_s}{180}\text{Sin}\ \emptyset\ \text{Sin}\ \delta) \qquad (4.12)$$

ω_S - sunrise hour angle which is negative of sunset hour angle - $\omega_S = Cos^{-1}(-\tan\emptyset\tan\delta)$

Monthly average daily global radiation in Horizontal surface MJ/m^2-day

4.8 Estimation of the monthly average daily solar radiation in Horizontal surface

Radiation data are the best source of information for estimating average incident radiation. Lacking these or data from nearby locations of similar climate, it is possible to use empirical relationships to estimate radiation from hours of sunshine or cloudiness. Data on average hours of sunshine or average percentage of possible sunshine hours are widely available from many hundreds of stations in many countries and are usually based on data taken with Campbell-Stokes instruments.

The original Angstr˚om-type regression equation related monthly average daily radiation to clear-day radiation at the location in question and average fraction of possible sunshine hours.

$$\frac{\text{H}}{\text{H}_\text{C}} = \acute{\text{a}} + \acute{\text{b}}\frac{\text{n}}{\text{N}} \qquad (4.13)$$

H = monthly average daily radiation on horizontal surface

H_C= average clear-sky daily radiation for location and month in question

$\acute{a}$, $\acute{b}$ = empirical constants

n_s= monthly average daily hours of bright sunshine

N_s = monthly average of maximum possible daily hours of bright sunshine

(i.e., recommended days of the month)

A basic difficulty with Equation above lies in the ambiguity of the term's $\frac{n}{N}$ and H_c. The former is an instrumental problem (records from sunshine recorders are open to interpretation). The latter stems from uncertainty in the definition of a clear day. Researchers have modified the method to base it on extraterrestrial radiation on a horizontal surface rather than on clear-day radiation.

$$\frac{\bar{H}}{H_O} a + b \frac{\bar{n}_s}{\bar{N}_s} \tag{4.14}$$

where H_O is the extraterrestrial radiation for the location averaged over the time period in question and *a* and *b* are constants depending on location.

The regression parameters a and b can be obtained from

Tiwari et al, (1997) Tiwari, R.F and Sangeeta, T.H. 1997. developed a relationship for a and b coefficients that are function of ∅, the location latitude as follows:

$$a = -0.11 + 0.235\ Cos\ \emptyset + 0.323 \frac{\bar{n}_s}{\bar{N}_s} \tag{4.15}$$

$$b = 1.449 - 0.553\ Cos\ \emptyset + 0.694 \frac{\bar{n}_s}{\bar{N}_s} \tag{4.16}$$

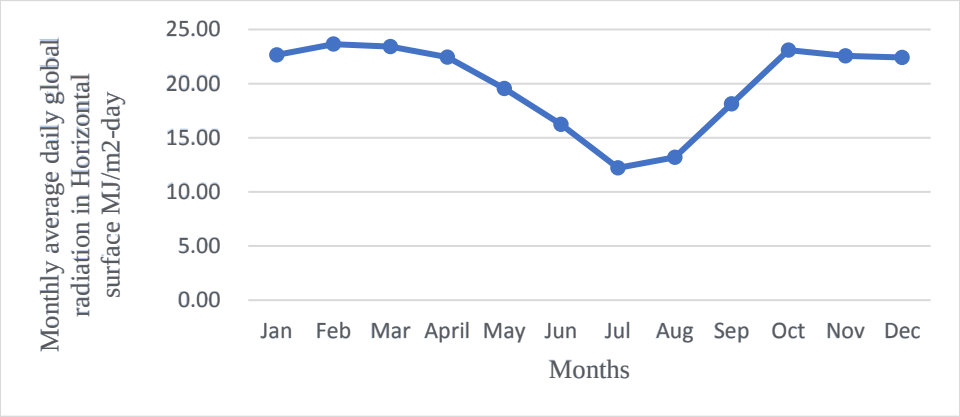

Fig 4.4 Solar radiation in horizontal surface

4.9 Optimum tilt angle of the Collector surface

Addis Ababa which is found in the northern hemisphere should face towards the south in order to receive sufficient irradiation. The collector must face towards the equator with tilt angle of the local latitude of the site is recommended.

The solar radiation reaches pick at solar noon when the sun just becomes at meridian of the point. So, to utilize this pick solar radiation, our solar collector surface must face south with zero azimuth angle (i.e. no tilting of the collector towards west or east).

For south facing collector incident angle of solar rays is given as. Useful relationships for the angle of incidence of surfaces sloped due north or due south can be derived from the fact that surfaces with slope β to the north or south have the same angular relationship to beam radiation as a horizontal surface at an artificial latitude of $\emptyset - \beta$. The relationship is shown in Figure below for the northern hemisphere. Modifying Zenith angle yields

$$Cos\ \theta = Cos\ (\emptyset - \beta)\ Cos\ \delta\ Cos\ \omega + Sin\ (\emptyset - \beta)\ Sin\ \delta \qquad (4.17)$$

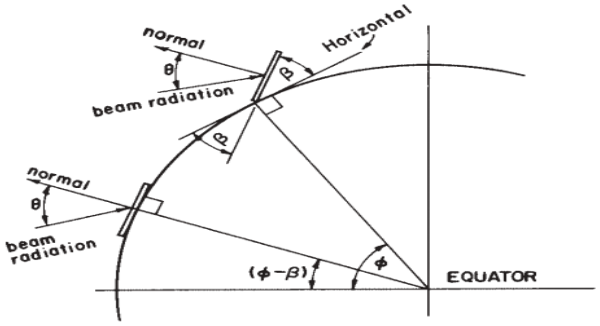

Fig 4.5 Section of earth showing $\beta, \theta, \emptyset, and\ (\emptyset - \beta) for\ a\ south - facing\ surface$

Collector orientation may be affected by which load dominates; optimum orientation is approximately $\beta = \emptyset + 15$ degrees for winter use, $\beta = \emptyset - 15$ degrees for summer use, and $\beta = \emptyset$ for all-year use.[29] but here the assumption is ± 13

Winter $\beta = \emptyset + 13$ (Dec, Jan, Feb) 9.02+13=22.02

Summer $\beta = \emptyset - 13$ (June July Aug) 9.02-13=-3.98

For other $\beta = \emptyset$ (sept, oct, Nov march April may) Spring and autonym =9.02

4.10 Estimation of the monthly average daily solar radiation in Inclined surface

The procedure for calculating H_T is parallel to that for I_T, that is, by summing the contributions of the beam radiation, the components of the diffuse radiation, and the radiation reflected from the ground. The first method is that of Liu and Jordan (1962) as extended by Klein (1977), which has been widely used.

$$\bar{H}_T = \bar{H}_b \bar{R}_b + \bar{H}_d \left(\frac{1+\text{Cos}\,\beta}{2}\right) + \bar{H}\rho_g \left(\frac{1-\text{Cos}\,\beta}{2}\right) \quad (4.18)$$

$$\text{And } \bar{R} = \frac{\bar{H}_T}{\bar{H}} = \left(1 - \frac{\bar{H}_d}{\bar{H}}\right)\bar{R}_b + \frac{\bar{H}_d}{\bar{H}}\left(\frac{1+\text{Cos}\,\beta}{2}\right) + \rho_g \left(\frac{1-\text{Cos}\,\beta}{2}\right) \quad (4.19)$$

where $\frac{H_d}{H}$ is a function of K_T

$\bar{R}_b$-The ratio of the average daily beam radiation on the tilted surface to that on a horizontal surface for the month.

For surfaces that are sloped toward the equator in the northern hemisphere, that is, for surfaces with $\gamma = 0^0$

$$\bar{R}_b = \frac{Cos\,(\emptyset-\beta)\,Cos\,\delta\,Sin\,\acute{\omega}_s + \left(\frac{\pi}{180}\right)\acute{\omega}_s\,Sin\,(\emptyset-\beta)\,Sin\,\delta}{Cos\,\emptyset\,Cos\,\delta\,Sin\,\omega_s + \frac{\pi}{180}\omega_s\,Sin\,\emptyset\,Sin\delta} \quad (4.20)$$

where $\acute{\omega}_s$ is the sunset hour angle for the tilted surface for the mean day of the month, which is given by

$$\acute{\omega}_s = min\begin{bmatrix} Cos^{-1}(-tan\,\emptyset\,tan\delta) \\ Cos^{-1}(-tan\,(\emptyset-\beta)\,tan\delta) \end{bmatrix} \quad (4.21)$$

where ‘‘min’’ means the smaller of the two items in the brackets.

Assumed typical value of the ground reflectance is 0.2

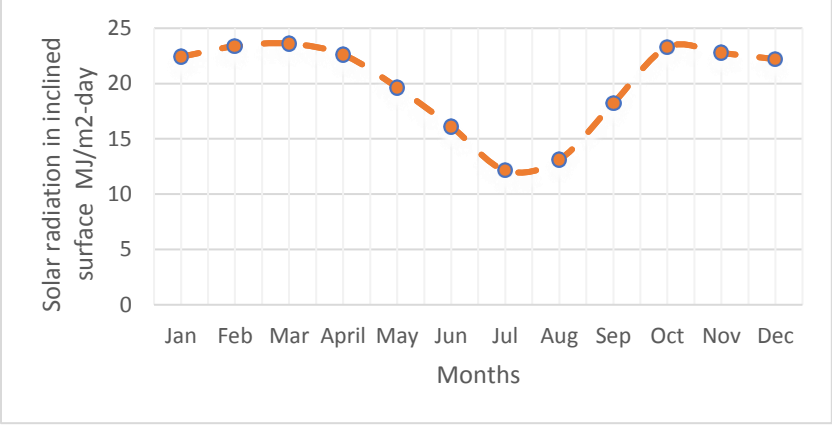

Fig 4.6 Solar radiation in inclined surface

4.11 Estimation of Hourly Average daily Solar Radiation from daily data

The monthly average hourly solar radiation on a horizontal surface can be calculated from the knowledge of the monthly average daily Solar radiation on a horizontal surface.

$$\frac{\bar{I}}{\bar{H}} = Rt = \frac{\pi}{24}(a + b\,Cos\,\omega)\frac{cos\,\omega - cos\,\omega_s}{sin\,\omega_s - \frac{\pi\omega_s}{180}cos\,\omega_s} \quad (4.22)$$

The coefficients a and b are given by

$$a = 0.409 + 0.5016\sin(\omega_s - 60) \quad (4.23)$$

$$b = 0.6609 - 0.4767\sin(\omega_s - 60) \quad (4.24)$$

In the above equations ω is the hour angle in degrees for the time in question (i.e., the midpoint of the hour for which the calculation is made) and ω_S is the sunset hour angle.

Monthly Average Hourly Global Radiation on a Horizontal Surface of all months

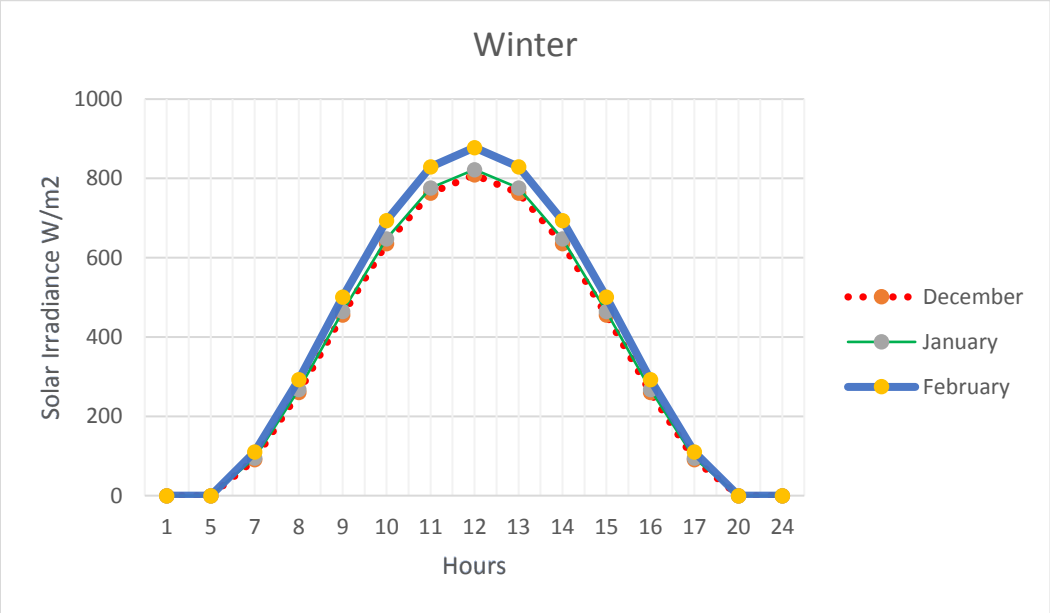

Fig 4.7 Monthly average hourly Solar radiation of winter

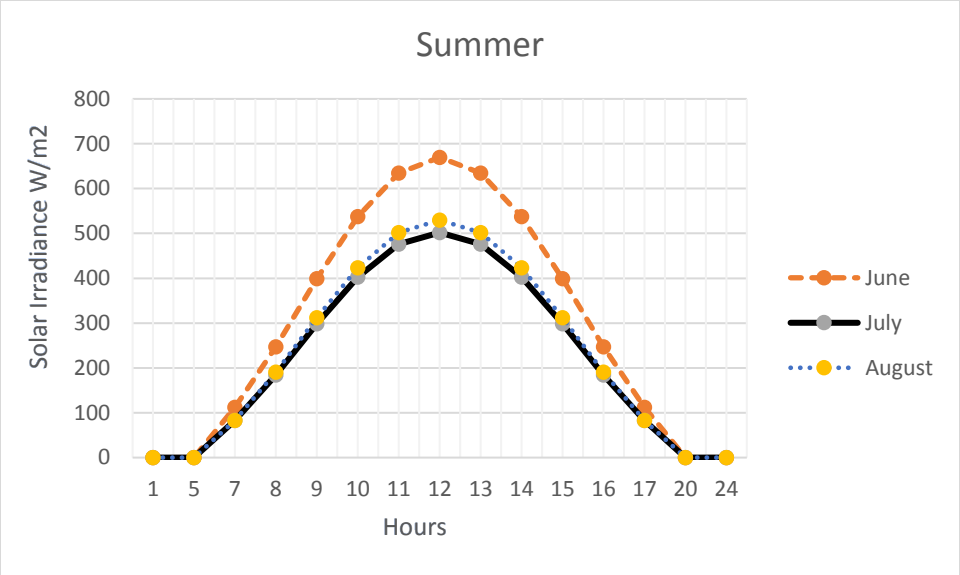

Fig 4.8 Monthly average hourly Solar radiation of summer

It is obvious that the solar radiation is becomes maximum in the solar noon time the above graphs shows that in detail. All months are analyzed winter and spring has high radiation than summer.

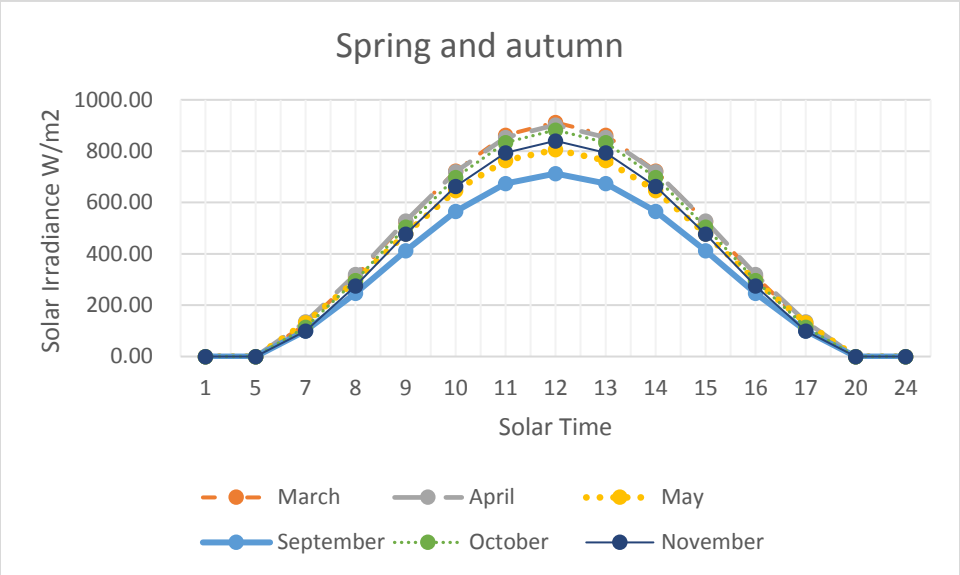

Fig 4.9 monthly average hourly Solar radiation of spring and autumn Each month data is available in appendix A

4.12 Estimation of Monthly Average daily Maximum, Minimum and Average Temperature on Horizontal Surface in Addis Ababa

The monthly average daily Maximum, Minimum and Average Temperature on Horizontal Surface can be calculated by the knowledge of the monthly average hourly variation of temperature on the year 2013 to 2018 from collected data.

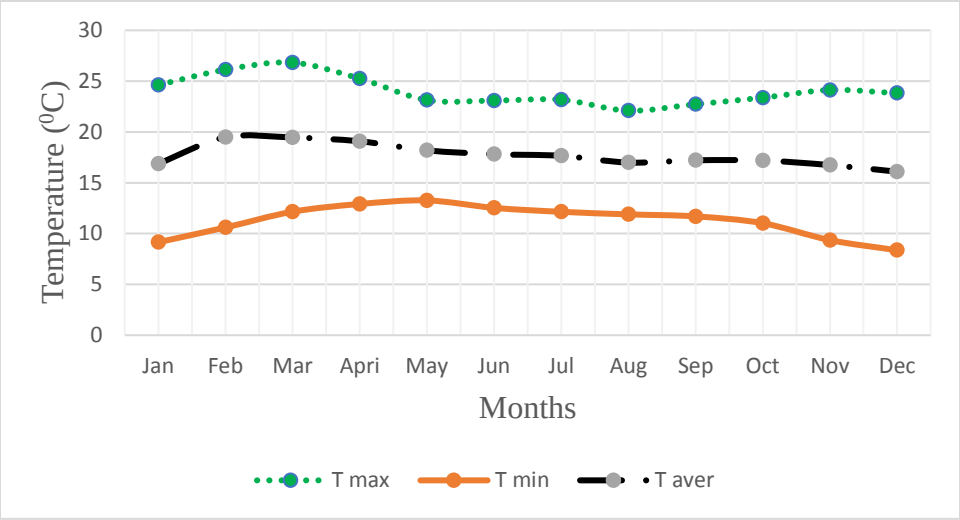

Fig 4.10 Monthly Ambient Temperature Form in Addis Ababa, from 2013 to 2018 Years

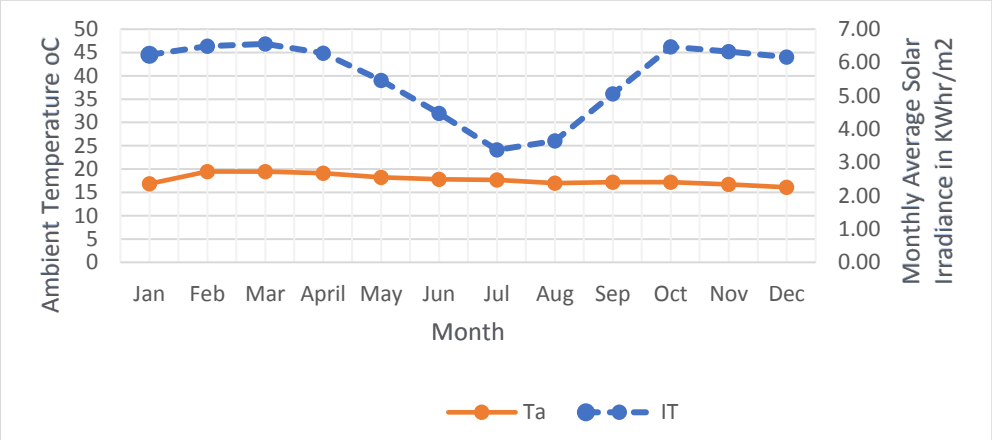

Fig 4.11 Monthly average daily radiation and monthly average ambient temperature on inclined surface.

June, July and August have low monthly average solar radiation than the others. March has high monthly average radiation than all months. The above figure shows the temperature and solar radiation relation. Using the above figure 4.11, we can able to calculate the collector efficiency

4.13 Solar collector performance Analysis

4.13.1 Introduction to collector

Solar thermal collectors are a special kind of heat exchangers that convert solar radiation into thermal energy through a transport medium or a heat transfer fluid (HTF). The major component of any solar system is the solar collector. This is a device that absorbs the incoming solar radiation, converts it into heat energy, and transfers it through a fluid (usually water, air, or oil) for useful purpose/applications.[29]

There are basically two types of solar thermal collectors: non-concentrating or stationery and concentrating. A non-concentrating collector has the same area for intercepting and for absorbing solar radiation, whereas a Sun-tracking concentrating solar collector usually has concave reflecting surfaces to intercept and focus the sun's beam radiation to a smaller receiving area, thereby increasing the radiation flux.

Non-concentrated collectors are mechanically simpler than concentrating collectors. The major applications of these units are in solar water heating, building heating, air conditioning, and industrial process heat. Passively heated buildings can be viewed as special cases of flat-plate collectors with the room or storage wall as the absorber.

Here in this research non-concentrating collector type is used rather than concentrating type. Non-concentrating type solar collector is preferable for the solar ejector cooling system and it is able to reach the temperature to greater than 90^{O}. It is stationary type collector which is fixed in one place

Table 4.1 Types of non-concentrating collector

Motion	Collector type	Absorber type	Concentration ratio	Indicative Temperature Range (^{0}C)
Stationary	Flat plate collector	Flat	1	30- 80
	Evacuated tube collector	Flat	1	50-200
	Compound parabolic collector (CPC)	Tabular	1-5	60-240

[10-13] & [30-36] all used Evacuated tube collector and they concluded that Evacuated tube collector performs better than flat plate collector for the application of solar ejector cooling system. They recommended the collector to use for the solar ejector cooling system.

4.13.2 Evacuated tube collector (ETC)

ETC consists of single tubes that are connected to a header pipe. To reduce heat losses of the water-bearing pipes to the ambient air, each single tube is evacuated. Besides different geometrical configurations, it has to be considered that the collector must always be mounted with a certain tilt angle in order to allow the condensed internal fluid of the heat pipe to return to the hot absorber.

The ETCs provide the combined effects of a highly selective surface coating and vacuum insulation of the absorber element so that they can have high heat extraction efficiency compared with FPCs in the temperature range above 80^{O}C. [37]

At present, the glass-evacuated tube has become the key component in solar thermal utilization, and they are proved to be very useful especially in residential applications for higher temperatures. So, ETCs are widely used to supply the DHW or heating, including heat pipe-evacuated solar collectors and U-tube glass ETCs [39]

These collectors feature a heat pipe (a highly efficient thermal conductor) placed inside a vacuum-sealed tube. The pipe, which is a sealed copper pipe

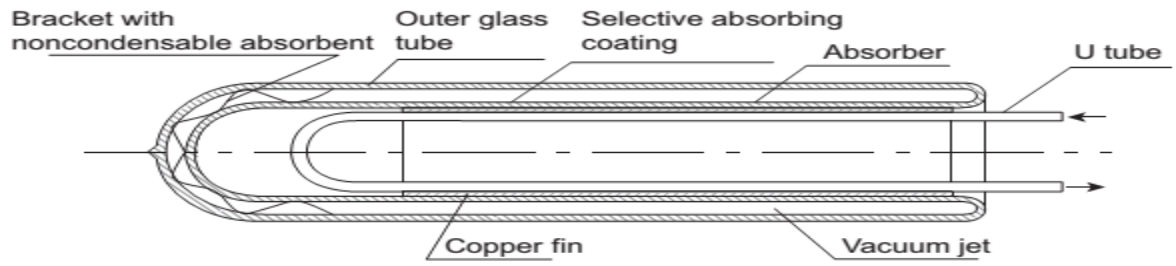

Fig 4.12 Glass ETC with U-tube illustration of the glass evacuated tube

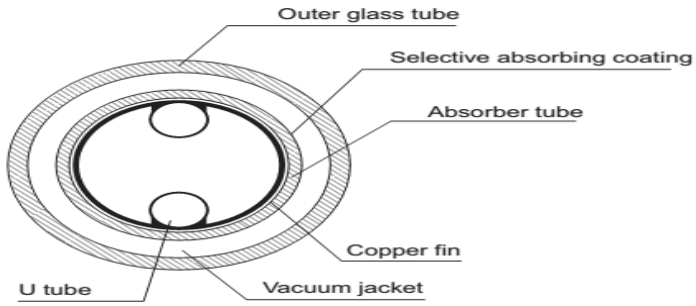

Fig 4.13 Glass ETC with U-tube cross section.

attached to a black copper fin that fills the tube (absorber plate) is a metal tip attached to the sealed pipe (condenser). The heat pipe contains a small amount of fluid that undergoes an evaporating condensing cycle.

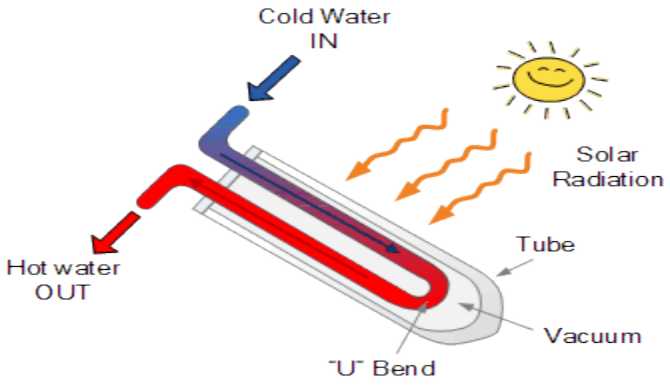

Fig 4.14 Evacuated Tube Collector with U-tube cross section.

In this cycle, solar heat evaporates the liquid, and the vapor travels to the heat sink region where it condenses and releases its latent heat. The condensed fluid return back to the solar collector and the process is repeated. When these tubes are mounted, the metal tips up into a heat exchanger (manifold).

All these collectors are installed at a fixed tilt that optimizes the performance for a specified period; for a summer use, a tilt equal to the latitude ∅ minus 13 degrees can be considered as optimal in this study.

The solar collector efficiency η_C is defined as the ratio of gain of the useful heat over any time period to the solar radiation over the same period [28]. The below equation is providing the basis for simulation models of a collector operating under steady conditions.[40]

$$\eta_C = F_R(\tau\alpha) - F_R U_L \left(\frac{T_i - T_a}{I_T}\right) \quad (4.25)$$

where $F_R(\tau\alpha)$and $F_R U_L$ are the average heat removal factor and the heat loss coefficient W/m^2 ^{0}C respectively. They change depending on the collector type.

T_a the ambient temperature (^{0} C); assumed that after two hours of the solar noon the ambient temperature will become maximum [41].

I_T the total solar radiation on an inclined surface per unit area W/m^2 and

T_i is the collector's inlet temperature:

as an assumption, it could be commonly taken as 10^{0}C greater than the generator temperature. That is, assumed as

$$T_i = T_g + 10^0 C \quad (4.26)$$

Where T_g- Generator Temperature

Table 4.2 Solar collector Characteristic's [10][42] & [43]

Collector type	**Collector description**	$F_R(\tau\alpha)$ **W/ m^2-^{0}C**	$F_R U_L$ **(W/m^2-^{0}C)**
Type-1	Evacuated selective surface	0.70	3.3
Type-2	Double Glazed	0.75	6.5
Type-3	Single Glazed	0.90	10.0

Collector characteristic coefficients and they change depending on the collector type. These values are Selected as $F_R(\tau\alpha)$ = 0.70 and $F_R U_L$ = 3.3 for the evacuated tube collector.

$$\eta_C = 0.70 - 3.3\left(\frac{T_i - T_a}{I_T}\right) \quad (4.27)$$

The solar radiation incident upon the collector surface at 22.01^0 on Winter at -3.99^0 for the summer and for others 9.01^0 or which is equal to altitude and the ambient temperature values, all found in solar calculated data, were used to calculate the solar collector efficiency η_c , the overall coefficient of performance(COP) , the useful energy output of the collector per unit collector area Q_{coll} and the maximum cooling capacity per unit collector area Q_e will be analyzed in the next chapter

Designed point Generator temperature is T_g=90^0C there for the collector efficiency will become

$$\eta_C = 0.70 - 3.3\left(\frac{100^0C - T_a}{I_T}\right) \quad (4.28)$$

By using the calculated value of solar irradiance and ambient temperature we can analyze the collector performance in Addis Ababa.

4.14 Total solar radiation and ambient temperature hourly variation

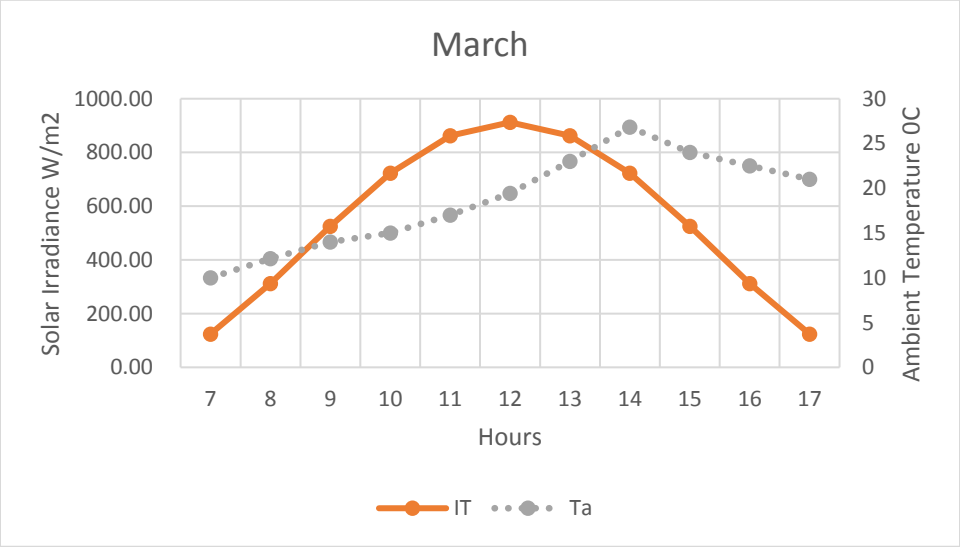

Fig 4.15 Total solar radiation and ambient temperature variation the rests are in appendix

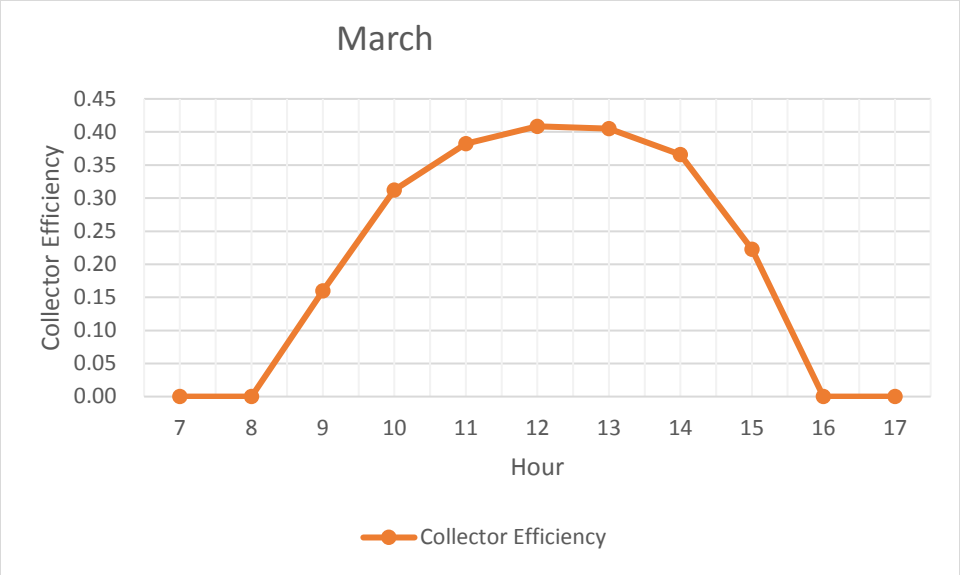

Fig 4.16 Collector efficiency hourly variation of March

4.15 The useful energy output

The performance of a solar collector is described by an energy balance that indicates the distribution of incident solar energy into useful energy gain thermal losses, and optical losses. In steady state the useful energy output of a collector of area A_C is the difference between the absorbed solar radiation and the thermal loss. [28]

$$Q_u = A_c[S - U_L(T_{pm} - T_a)] \quad (4.29)$$

Where Q_u – useful collector output energy, S- is absorbed radiation per unit collector area, T_{pm} – the mean absorber plate temperature, T_a –ambient temperature heat transfer coefficient U_L

A measure of collector performance is the collection efficiency, defined as the ratio of the useful gain over some specified time period to the incident solar energy over the same time period:

$$\eta = \frac{\int \dot{Q}_u dt}{A_c \int G_T dt} \quad (4.30)$$

Since our conditions is constant over a time period, the efficiency reduces. The useful energy output of the collector per unit collector area q_{coll} are [28].

Average useful energy gain of the collector per unit of collector area

$$q_{coll} = \frac{Q_{coll}}{A_c}, \qquad q_{coll} = \eta_C \, x \, I \quad (4.31)$$

Hourly average collector useful energy gain per unit collector area of four months

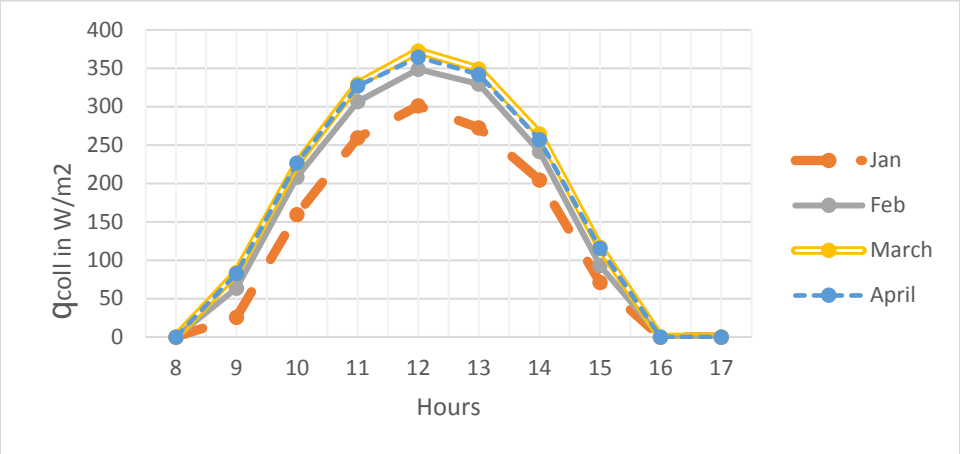

Fig 4.17 Hourly collector useful energy output of four months

4.15 Theoretical studies of SoECS

4.15.1 Steady-State Solar Ejector Cooling system (SoECS) Performance Analysis

HVAC systems use electricity to drive their system depending on the efficiency of the unit and this increases the consumption of the electric city of the country. SoEC system uses ejector instead of compressor however compressor uses electric city power as a driving force due to this it increases the consumption of the electric city. Because off there are no moving parts inside the ejector and it's cheap to manufacture as mention in introduction in chapter one. It has a certain advantage over a system which uses a compressor in terms of maintenance, duration, etc.

Solar ejector cooling system is one of the alternatives of the technology in refrigeration and air conditioning application which uses low-grade energy so that it could be driven with solar energy geothermal energy, waste heat, etc. It has two cycles. The first is the power cycle and the second is cooling cycle. It consists of five main parts such as Solar collector, Generator, Ejector, Condenser and Evaporator. The working principle is explained below.

4.15.2 System description

A schematic view of the SoECS is shown in fig 4.18. The system consists of the solar energy and ejector cooling cycles. A solar collector, a generator and a circulation pump are the main parts of the former cycle. Main components of the latter cycle are a vapor generator, an ejector, a condenser, an evaporator, an expansion valve and a liquid pump.

The refrigeration cycle is divided into two interconnected power and cooling cycles. The power cycle occurs in clockwise direction and the refrigerant passes, in sequence, the generator, the ejector, the condenser and the liquid pump.

The cooling cycle takes place in anticlockwise direction. The refrigerant leaving the evaporator sequentially passes through the ejector, the condenser and the expansion valve and returns back to the evaporator. The energy taken from the power cycle is used to drive the cooling cycle. A compressor, to be used in a vapor-compression system, is replaced with the ejector in the Ejector Cooling System.

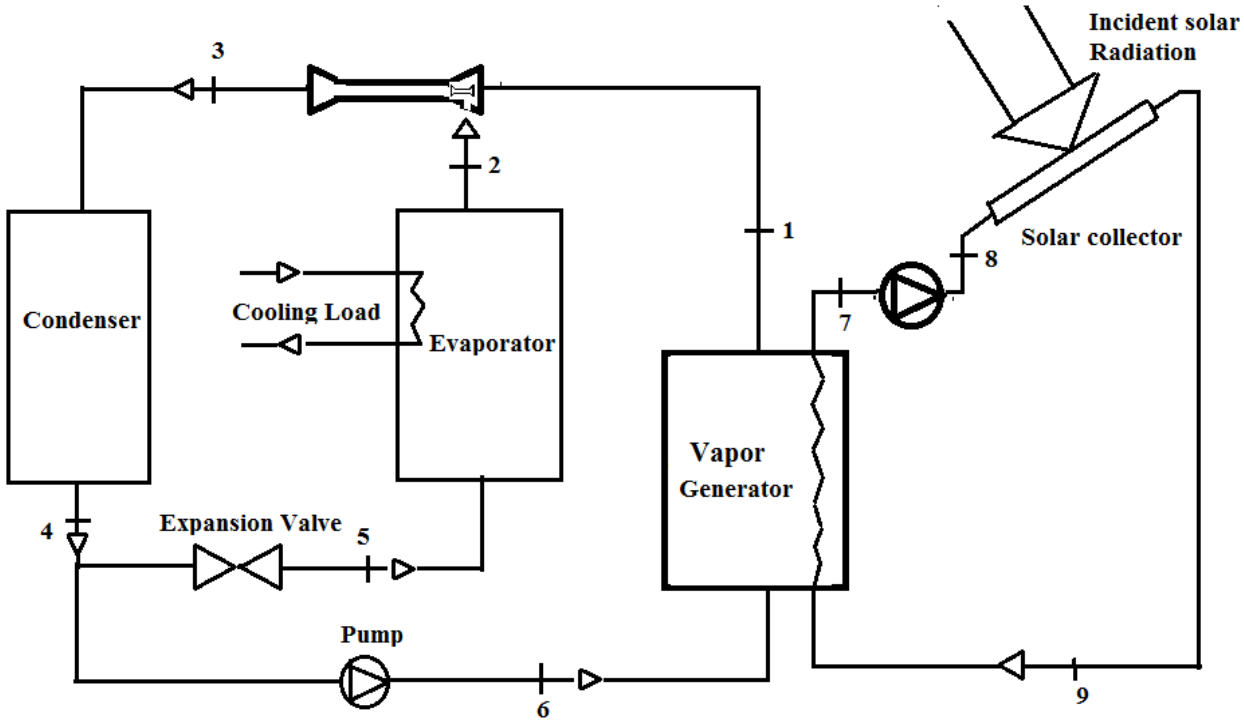

Fig 4.18 Solar ejector cooling system cycle

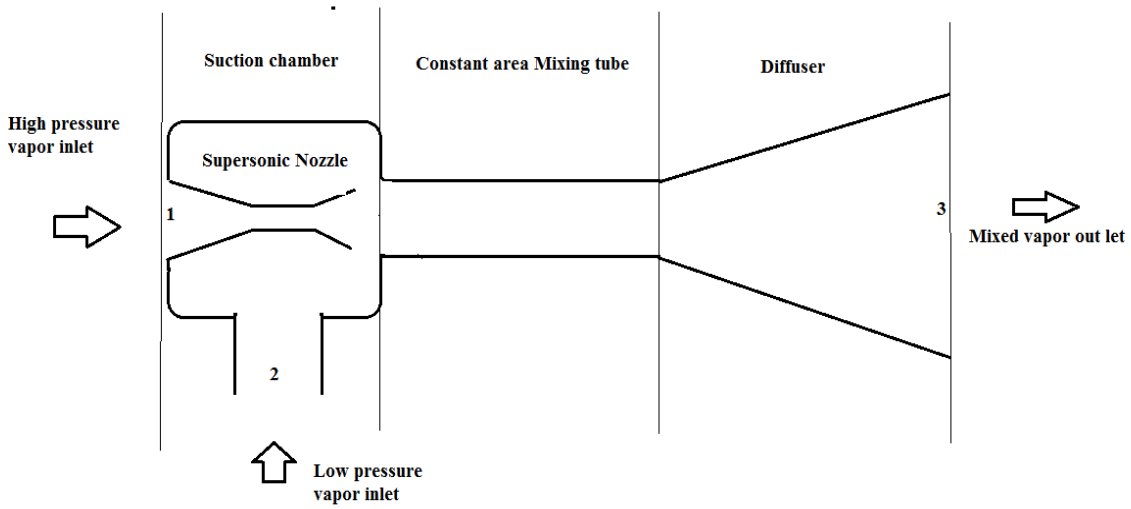

Fig 4.19 Ejector

4.15.3 The working principle of the System explained in detail as follows

- ✓ The refrigerant vapor at the state -1 with high pressure and temperature is produced or generated by using solar energy in the vapor Generator. At this point the vapor is called the primary fluid which helps the system to activate.
- ✓ After passing the Vapor generator it becomes saturated vapor and enters to the ejector with high pressure and temperature. The Ejector is a component which is called thermal compressor which compresses the fluid to desired point. There is a supersonic nozzle inside the ejector which helps to increases the primary fluid velocity. This supersonic nozzle expands the primary vapor which means the primary vapor become low-pressure after passing the supersonic nozzle. This causes the suction of the secondary fluid from the Evaporator state 2
- ✓ At state -2 the low-pressure vapor from the evaporator will be entrained due to the high velocity formed supersonic nozzle outlet.
- ✓ The two vapors then mix with each other in mixing chamber. After passing the mixing section it enters to the diffuser in ordered to regain its pressure. This mixed vapor is then compressed to the condenser pressure in diffuser state -3

- ✓ The mixed vapor which leaves the ejector enters to the condenser in order to reject the heat to the surroundings and condenses to state -4
- ✓ After passing state-4 the fluid divided into two parts one enters to the evaporator by expansion process (4-5) to state -5 and the other go back to the vapor generator at state -6 through the liquid pump.
- ✓ Since the pressure difference between the Vapor generator and condenser is higher the liquid pump is used in state (4-6)
- ✓ The liquid entering the vapor generator is vaporized from states '6' to '1' by the solar radiation
- ✓ The low temperature fluid inside the Evaporator produces the cooling effect by absorbing heat from the cooling space. After absorbing heat from the cooling space, the fluid enters to the Ejector again

4.16 Ejector Design and performance analysis

4.16.1 Theoretical analysis

Ejector design is generally classified into two categories, depending on the position of the nozzle, as

1. Constant-Area Mixing Ejector: the exit of the supersonic nozzle is inside the constant area of the ejector. Primary and secondary fluids mix at the constant area.
2. Constant-Pressure Mixing Ejector: the exit of the nozzle is in the suction chamber, before the constant area. Primary and secondary flows mix in the suction chamber at a specific pressure. Pressure of the mixing streams remains constant along the chamber from the nozzle exit to the inlet of the constant area section.

In this research Constant-pressure mixing type ejector is used which is more promising than constant-area mixing ejector because of it generates better performance [45]

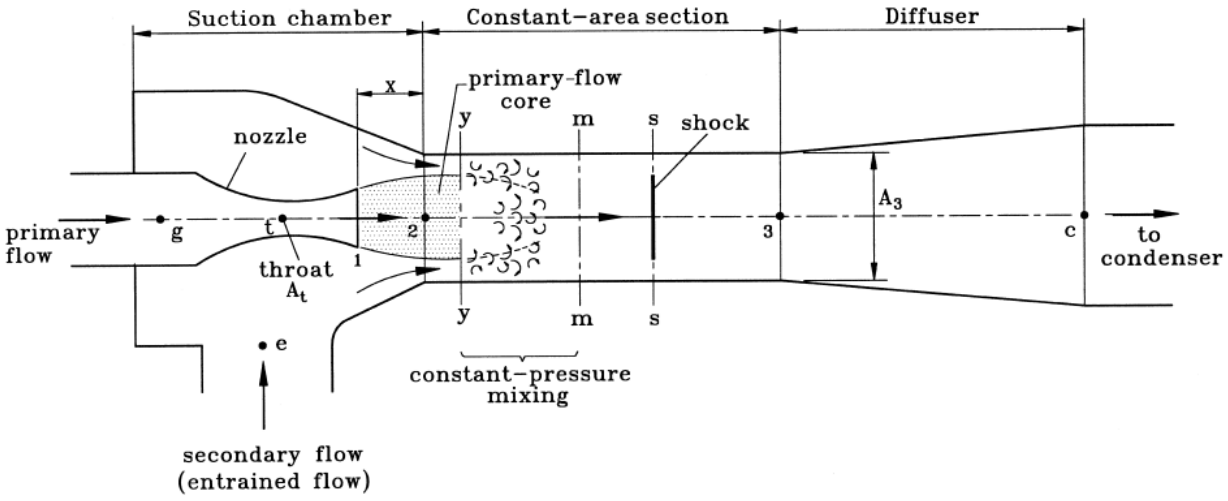

Fig 4.20 Schematic diagram of ejector performance.

Even if the model introduced by Munday [46]and improved by Huang et al. [47] has some rather artificial assumptions. it is still used by many authors (Huang et al. have been cited by about 400 authors till May 2017) and, by careful calibration of some parameters, may

be brought in good agreement with the experimental results. The symbols for the model and the reference locations within the ejectors are defined in Fig 4.25

The following assumptions are made for the analysis using:

- ✓ The working fluid is an ideal gas with constant properties cp and γ =cp/cv.
- ✓ The ejector operates at steady state and one-dimensional.
- ✓ The kinetic energy at ejector inlet/outlet ports is negligible.
- ✓ The flow is modeled as isentropic, and irreversibility's are taken into account by using experimentally determined coefficients.
- ✓ After exhausting from the nozzle, the primary flow fans out by mixing with the entrained flow.
- ✓ The entrained flow is choked at the cross-section *y–y* (hypothetical throat).
- ✓ The ejector wall is adiabatic.

According to a wide range of publications about hydraulic losses and efficiency coefficients of the ejector flow field elements, the following assumptions regarding ejector element efficiency [54]

$$\eta_P = 0.95\,, \eta_N = 0.85, \phi_p = 0.88$$

4.17 Working fluid selection

Working fluid is an essential part in the ejector refrigeration cycle. Different refrigerants have distinct characteristics and perform differently. Appropriate refrigerants can provide good system performance in selected operating conditions.

4.17.1 R-134a (1,1,1,2-Tetrafluoroethane)

Use of halocarbon compounds is found suitable to operate vapor ejector refrigeration system (VERS) satisfactorily at generator temperature as low as 65^0C However, refrigerants in the families of CFCs (Chlorofluorocarbons) and HCFCs(hydrofluorocarbons) have been identified as a cause of the depletion of ozone layer and as a potential source of global warming according to Minnesota pollution control agency 2017.

Considerable interest was developed during the end of the last century in probing for environmentally acceptable refrigerants with the thermodynamic properties. From the enlisted group of alternative refrigerants, R134a is found to be a leading substance that provides good chemical and thermal stability [48] Also, Vapor Ejector Refrigeration System with R134a gives a better performance in comparison with many other environment friendly refrigerants [49-51]. It is environmentally friendly refrigerant R134a [50]

In the present study, R134a is selected as the working fluid for the ejector cooling system. R134a has a low boiling point (-26.5^{0}C) and critical temperature (101.1 ^{0}C). For thermodynamic properties of R134a,

Table 4.3 Physical properties

Physical properties	**Unit**	**R-134a**
Chemical name	-	CH_2FCF_3
Molecular weight	g/mol	102.03
Boiling Point at 1 atm (101.3 kPa or 1.013 bar)	^{0}C	-26.1
Critical Temperature	^{0}C	101.1
Critical pressure	KPa	4060
Thermal conductivity at 25^{0}C Vapor at 1 atm (101.3 kPa or 1.013 bar)	W/m-k	0.0145
Heat of Vaporization at Normal Boiling Point	KJ/Kg	217.2
Viscosity at 25^{0}C Vapor at 1 atm (101.3 kPa or 1.013 bar)	MPa-S(cp)	0.012

4.18 Governing equations

The expansion process of the primary flow through the nozzle vapor from the generator expands irreversibly in the primary nozzle creating a partial vacuum at the nozzle exit. Applying the first law of thermodynamics by using the energy balance equation:

$$q = W + H_B - H_A + \frac{U_B{}^2 - U_A{}^2}{2} + g.(Z_B - Z_A) \quad (4.32)$$

With the assumption of adiabatic condition (q = 0), no work (W=0), and no influence of elevation change ($Z_B = Z_A$),

- ✓ Primary flow through nozzle

For a given inlet stagnant pressure P_g and temperature T_g the mass flow through the nozzle at choking condition follows the gas dynamic equation [47 &54].

$$\acute{m}_p = \frac{P_g A_t}{\sqrt{T_g}} x \sqrt{\frac{\gamma \eta_p}{R}\left(\frac{2}{\gamma+1}\right)^{(\gamma+1)/(\gamma-1)}} \quad (4.33)$$

Where $\acute{m}_p -$ primary fluid mass flow rate A_t −Nozzle throat area

P_{g-}Generator pressure, T_g −Ggenerator temperature, γ −specific ratio, R- Gas constant

The gas dynamic relations between the Mach number at the exit of nozzle *M* p1 and the exit cross section area *A*p1 and pressure *P*p1 are, using isentropic relations as.

$$\left(\frac{A_{p1}}{A_t}\right)^2 = \frac{1}{M_{p1}{}^2}\left[\frac{2}{\gamma+1}\left(1 + \frac{(\gamma-1)}{2} M_{p1}{}^2\right)\right]^{(\gamma+1)/(\gamma-1)} \quad (4.34)$$

$$\frac{P_g}{P_{p1}} = \left(1 + \frac{(\gamma-1)}{2} M_{p1}{}^2\right)^{\gamma/(\gamma-1)} \quad (4.35)$$

- ✓ Primary-flow core from section 1–1 to section y–y
  The Mach number M_{py} of the primary flow at the *y–y* section follows the isentropic relations as:

$$\frac{P_{py}}{P_{p1}} = \frac{\left(1+((\gamma-1)/2)M^2{}_{p1}\right)^{\gamma/(\gamma-1)}}{\left(1+((\gamma-1)/2)M^2{}_{py}\right)^{\gamma/(\gamma-1)}} \quad (4.36)$$

For the calculation of the area of the primary flow core at the *y–y* section, we use the following isentropic relation, but an arbitrary coefficient ϕ_p should account for viscous loss at the boundary between primary and secondary flow:

$$\frac{A_{py}}{A_{p1}} = \frac{\phi_p M_{p1}}{M_{py}}\left[\frac{2}{\gamma+1}\left(\frac{1+\frac{\gamma-1}{2}M^2{}_{py}}{1+\frac{\gamma-1}{2}M^2{}_{p1}}\right)\right]^{\frac{\gamma+1}{2(\gamma-1)}} \quad (4.37)$$

- ✓ Secondary flow from inlet to section y–y

$$\frac{P_e}{P_{sy}} = \left(1+\frac{(\gamma-1)}{2}M_{sy}{}^2\right)^{\gamma/(\gamma-1)} \quad (4.38)$$

$$\acute{m}_e = \frac{P_e A_{sy}}{\sqrt{T_e}}\, x \sqrt{\frac{\gamma\eta_N}{R}\left(\frac{2}{\gamma+1}\right)^{(\gamma+1)/(\gamma-1)}} \quad (4.39)$$

Where $\acute{m}_e -$ Secondary fluid mass flow rate $A_{sy} -$ location of choking area

P_{e-} Evaporator pressure, $T_e -$Evaporator temperature

The isentropic efficiency of the secondary flow expansion is a third parameter to be specified.

- ✓ Cross-sectional area at section y–y

The geometrical cross-sectional area at section *y–y* is A_3 that is the sum of the areas for the primary flow A_{py} and for the entrained flow A_{sy}.

$$\mathrm{A_3} = \mathrm{A_{py}} + \mathrm{A_{sy}} \quad (4.40)$$

- ✓ Temperature and Mach number at section y–y

The temperatures of the two streams are related to the Mach numbers and stagnation conditions:

$$\frac{\mathrm{T_g}}{\mathrm{T_{PY}}} = 1+\frac{\gamma-1}{2}\mathrm{M_{py}}^2 \quad (4.41)$$

$$\frac{T_e}{T_{sy}} = 1 + \frac{\gamma-1}{2} M_{sy}^{\ 2} \tag{4.42}$$

- ✓ Mixed flow at section m–m

Two streams start to mix from section *y–y*. A shock then takes place with a sharp pressure rise at section *s–s*. A momentum balance relation thus can be derived as

$$\phi_m\left[\acute{m}_p U_{py} + \acute{m}_s U_{sy}\right] = (\acute{m}_p + \acute{m}_s) U_m \tag{4.43}$$

Where- U_m is the velocity of the mixed flow and ϕ_m is the coefficient accounting for the frictional loss [45]

$$\phi_m = \left\{ \begin{array}{c} 0.80, \quad for\ A_3/A_t > 8.3, \\ 0.82, \quad for\ 6.9 \le A_3/A_t \le 8.3, \\ 0.84, \quad for\ A_3/A_t \le 6.9. \end{array} \right\} \tag{4.44}$$

- ✓ Energy balance relation can be derived as

$$\acute{m}_p \left(h_{py} + \frac{U_{py}^{\ 2}}{2}\right) + \acute{m}_s \left(h_{sy} + \frac{U_{sy}^{\ 2}}{2}\right) = (\acute{m}_p + \acute{m}_s) \left(h_m + \frac{U_m^{\ 2}}{2}\right) \tag{4.45}$$

where U_{py} and U_{sy} are the gas velocities of the Primary and Secondary flow at the section *y–y*:

Primary, secondary, and mixed stream velocities are also obviously related to Mach numbers;

$$a_{py} = \sqrt{\gamma R T_{py}} \qquad U_{py} = M_{py}\ x\ a_{py} \tag{4.46}$$

$$a_{sy} = \sqrt{\gamma R T_{sy}} \qquad U_{sy} = M_{sy}\ x\ a_{sy} \tag{4.47}$$

$$a_m = \sqrt{\gamma R T_m} \qquad M_m = \frac{U_m}{a_m} \tag{4.48}$$

After mixing, the flow undergoes a normal shock in section s. Assuming an isentropic flow before and after the shock, the pressure rise is concentrated in this section and brings the stream from the mixed flow pressure $P_m = P_{py} = P_{sy}$ to the final value P_3 at the end of the cylindrical duct. Mixed flow across the section m-m to 3-3

$$\frac{P_3}{P_m} = 1 + \frac{2\gamma}{\gamma+1}(M_m{}^2 + 1) \quad (4.49)$$

$$M_3{}^2 = \frac{1+\frac{\gamma-1}{2}xM_m{}^2}{\gamma M_m{}^2 - \frac{\gamma-1}{2}} \quad (4.50)$$

- ✓ Finally, the Diffuser produces a further pressure recovery using isentropic relation up to

$$\frac{P_C}{P_3} = \left[1 + \frac{\gamma-1}{2}M_3{}^2\right]^{\frac{\gamma}{\gamma-1}} \quad (4.51)$$

The performance of an ejector is generally defined in terms of the mass flow rate ratio between the streams from the evaporator and generator, called the entrainment ratio (ω).

$$\omega = \frac{m_e}{m_g} \quad (4.52)$$

The basic geometry of ejector is arrived by solving mass, momentum and energy conservation equations for Design point of $P_g = 3.237$ MPa $T_g = 363\ K$, $P_e = 0.44$ MPa $T_e = \mathbf{2}8\mathbf{5}\ \boldsymbol{K}$, and $P_{con} = 0.77$ MPa $T_{Con} = 303$ K using one dimensional analysis with the working fluid of R-134a with the help of EES codes . The dimensions of ejector are shown below

Table 4.4 Optimum dimensions obtained for the design points

Names	**Dimensions in mm**
Throat diameter	2.24
Primary Nozzle outlet diameter	3.5
Primary nozzle area- ratio	2.44
Mixing section entrance diameter (NEP)	5.12
Distance of primary nozzle tip from mixing tube entrance	8
Motive nozzle converging angle α	35^0
Motive nozzle diverging angle β	10^0
Area ratio	5.225
Mixing section length	44
Diffuser angle of divergence angle	6^0
Diffuser diameter	13
Diffuser length	38

4.19 Modelling of Ejector cooling cycle

The system performance calculation proceeds by a sequential simulation process. There are important assumptions which are considered here

- ✓ Ejector performance analysis, the design calculation follows the method developed by Huang et al. [47]
- ✓ Steady-state operation
- ✓ Pressure losses in all components and connecting pipes are negligible.
- ✓ Refrigerant kinetic energy at the ejector inlet/exit are negligible
- ✓ Heat losses to the ambient are negligible except for the components exchanging energy with the environment
- ✓ The working fluid R-134a at the outlets of the generator, evaporator is considered saturated vapor and Condenser outlet is saturated liquid state.
- ✓ The expansion through the expansion valve is a throttling process,
- ✓ The refrigerant properties are obtained directly from data bank of thermodynamic and transport properties built into EES.

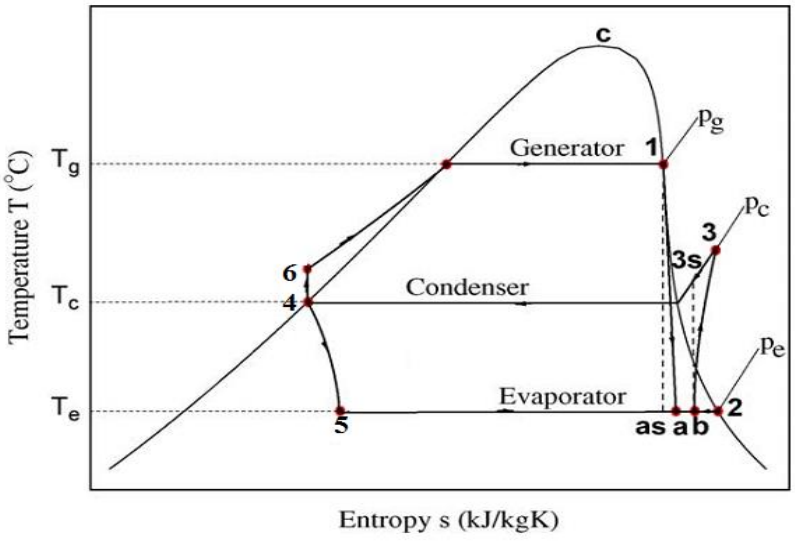

Fig 4.22 T-s diagram

4.19.1 Thermodynamics Energy equations

For design points of $P_g = 3.237$ MPa $T = 363\ K$, $P_e = 0.44$ MPa $T_e = 285$ K, and $P_{con} = 0.77$ MPa $T_{Con} = 303$ K and using the Refrigerant R-134a the performance analysis is carried out in monthly and hourly bases for cooling seasons the off-design operating conditions discussed in the coming chapter

The efficiency of an ejector cooling cycle can be represented by a thermal coefficient of performance derived as

$$h_1 = enthalpy = h_g@(T = T_g, x = 1),$$

$$h_2 = enthalpy = h_e\ @(T = T_e, x = 1),$$

$$h_4 = enthalpy = h_c@(T = T_c, x = 0),$$

$$h_5 = h_4 \text{ (throttling)},$$

$$v_4 = Specific\ Volume\ @(T = T_c, x = 0),$$

$$W_{pump} = v_4(P_g - P_c),$$

$$h_6 = h_4 + W_{pump}$$

- Evaporator: $\dot{Q}_e = \acute{m}_e \text{ x } (h_2 - h_5)$
- Generator: $\dot{Q}_g = \acute{m}_g \text{ x } (h_1 - h_6)$

$$COP_{ECS} = \frac{\dot{Q}_e}{\dot{Q}_g} = \omega\left(\frac{h_2 - h_5}{h_1 - h_6}\right)$$

$$COP_{overall} = \eta_C x\ COP_{ECS}$$

$$Q_e = COP_{overall}\ x\ I$$

Where h_1- Enthalpy at the exit of the generator, h_2- Enthalpy at the exit of the Evaporator

h_3- Enthalpy at the inlet of the condenser, h_4- Enthalpy at the exit of the condenser

h_5- Enthalpy at the entrance of the Evaporator, h_6- Enthalpy at the entrance of the Generator

x- Quality, W_{pump}- pump work,

Q_g-Heat added at the Generator, Q_e-Heat rejected at the evaporator,

COP_{ECS} is the coefficient of performance of the Ejector cooling system,

$COP_{overall}$-Overall coefficient of performance the SECS.

The useful energy output of the collector per unit collector area Q_{coll} and the cooling capacity per unit collector area Q_e

4.20 On-design and off-design operating conditions

Parameters are used to analyze the performance of the solar ejector cooling system. The on-design operating conditions are taken in this research are 90^0 C generator temperature, 30^0 C, condenser temperature and 12^0C Evaporator temperature. In the same way for off-design operating conditions using the above three parameters the performance investigation is carried out. In off design operating conditions, the performance is investigated by varying these three parameters. For generator the temperature range taken into account is 65-100^0C for condenser it is 25-40^0C and for evaporator 6-14^0C.

4.21 Predicting performance map for Off-Design Operating Conditions

Thermal systems are like all engineering systems too which are designed for a certain operating condition. Though, in actual practice these conditions may be encountered only for few hours in a day. Most of the time the thermal systems operate at off-design conditions This is due to a geometry of the components or the Environment conditions. The ambient temperature would

usually be different from the design conditions not only that the required temperature to drive a system is also. System simulation procedures enable us to predict the "off-design" performance of thermal systems and thus help identify any "harmful" consequences (like not able to give what we want, the problem which affects the component and the main parameter which varies more) that might occur. This information is useful in designing suitable control strategies to ensure safe and optimal operation over a wide range of operating conditions.[55]

The results obtained from simulation under off-design conditions would indicate the versatility and robustness of the system. It is obviously desirable to have a wide range of off-design conditions for which the system performance is satisfactory. A narrow range of acceptability is generally not suitable for consumer products because large variations in the operating conditions are often expected to arise.

The Ejector Cooling System cannot always operate at the optimum design conditions. Therefore, the performance of the system should also be investigated under the changing operating conditions (i.e. off-design). The main parameters here in this research considered are which varies in ECS are:

- Generator temperature
- Condenser temperature
- Evaporator temperature

Of course, the above parameters are related with other parameters indirectly such as variations in energy input, differences in raw materials fed into the system, changes in the characteristics of the components with time, changes in environmental conditions, and shifts in energy load on the system.

4.22 Enhancement of Ejector performance

4.22.1 Numerical CFD Analysis

Computational fluid dynamics (CFD) is a branch of fluid mechanics that uses numerical analysis and data structures to analyze and solve problems that involves fluid flows. CFD is applied to a wide range of research and Engineering problems in many fields of study and industries.

4.22.2 Goals of the study

The current study aims the flow through the ejector with Mixer and without. The optimum dimensions of the ejector have been found using Huang et al [56] model which is mostly used mathematical modelling for ejector. Using the obtained dimensions here the simulation is carried out for with and without mixer in ANSYS 16.0 FLUENT and the differences between both is compared using pressure, Velocity, Mach number and TKE mainly. There are mixer types which are used in the literature which enhanced the system performance which are shown in chapter three.

4.22.3 Modelling the geometry of the Ejector using ANSYS 16.0 FLUENT

The basic geometry of ejector is arrived by solving mass, momentum and energy conservation equations for Design point of $P_g = 3.237$ MPa $T = 90\ ^0$C, $P_e = 0.44$ MPa $T_e = 12^0$C, and $P_{con} = 0.77$ MPa $T_{Con} = 30^0$C using one dimensional analysis with the working fluid of R-134a with the help of EES codes in chapter four. The dimensions of ejector are shown below

Table 4.5 Optimum geometry Obtained

Names	**Dimensions in mm**
Throat diameter	2.24
Primary Nozzle outlet diameter	3.5
Primary nozzle area- ratio	2.44
Mixing section entrance diameter (NEP)	5.12
Distance of primary nozzle tip from mixing tube entrance	8
Motive nozzle converging angle α	35^0
Motive nozzle diverging angle β	10^0
Area ratio	5.225
Mixing section length	44
Diffuser angle of divergence angle	6^0
Diffuser diameter	13
Diffuser length	38

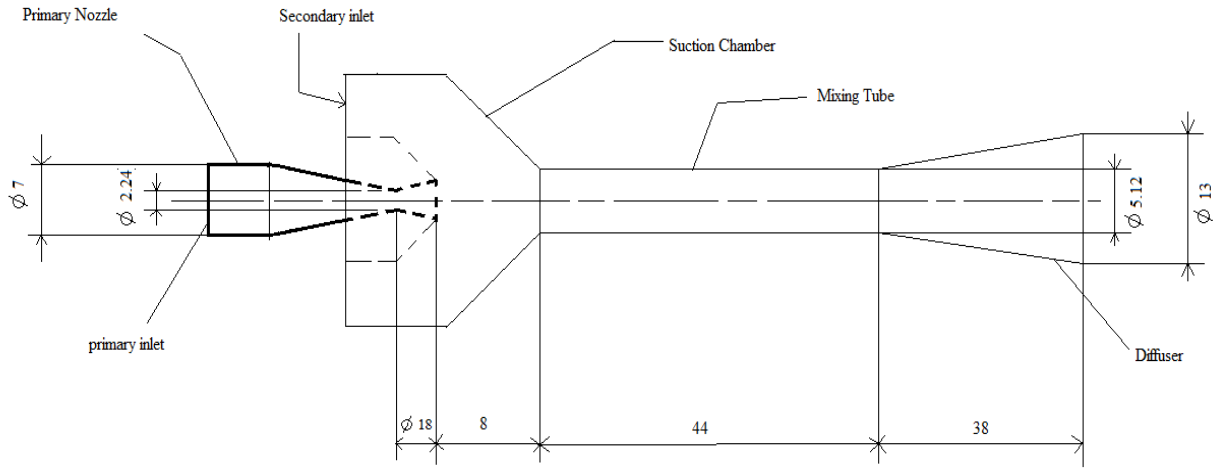

Fig 4.23 Schematic diagram of ejector

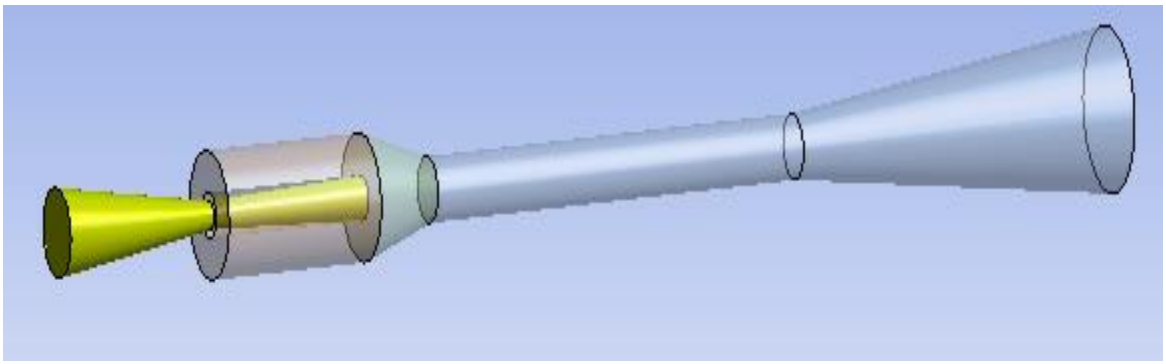

Fig 4.24 Normal ejector

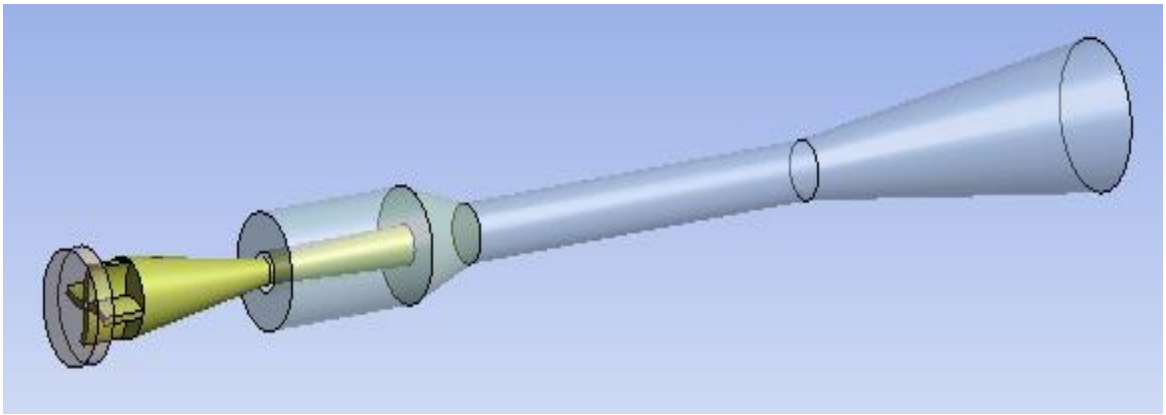

Fig 4.25 With Mixer Ejector

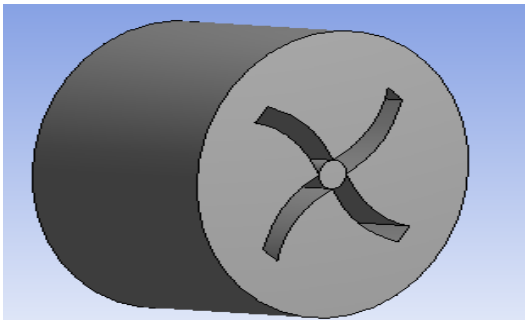

Fig 4.26 Mixer isometric view

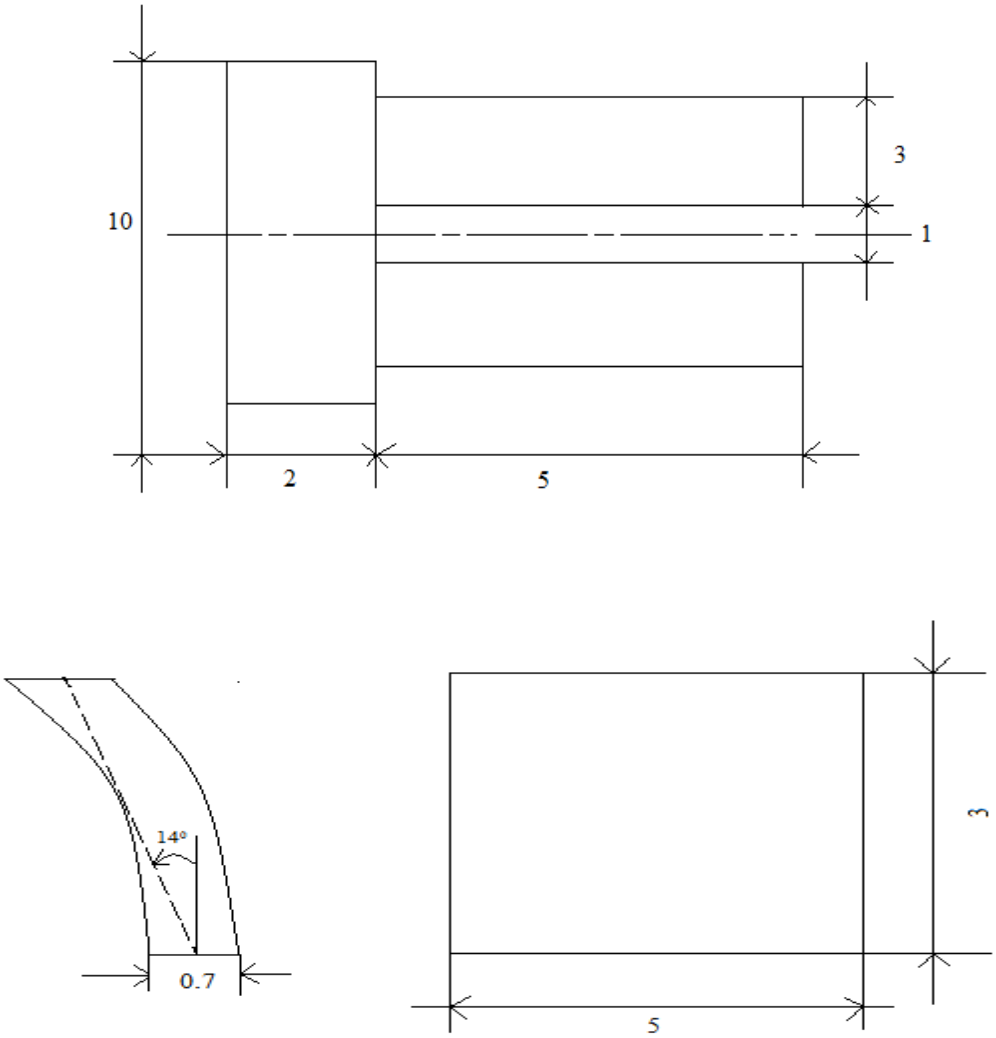

Fig 4.27 Curved blade profile specification

The Ejector is modelled with fixed four curved blade channel Mixer with a camber angle of 14° placed at a distance of 5 mm from the primary nozzle entry

Table 4.6 Mixer specification

Name	Dimension in mm
Chord (C)	3
Pitch (s)	5
Blade thickness	0.7
Blade tip diameter	7
Number of Blades	4

4.22.4 Numerical analysis of Ejector using CFD software

One dimensional numerical study has been studied in the chapter four using mass, momentum and energy governing equations using EES code. Critical dimensions arrived for on-design operating conditions. Numerical analysis of the supersonic ejector has been carried out for the arrived geometry with mixer and without using computational commercial software.

The following assumptions has been considered

- Steady state
- Turbulent and Compressible flow
- The thermodynamic and transport properties of refrigerant R134a considering as ideal gas behavior with constant properties.
- Governing equations of mass, momentum, energy and turbulence were solved using three-dimensional flow.

A general schematic drawing of the ejectors used in the numerical simulations is shown in figure 4.20

4.22.5 Computational domain with mesh details

Mesh is a general-purpose, intelligent automated high-performance product. It produces the most appropriate mesh for accurate efficient Multiphysics solutions.

Mesh of unstructured nature has been generated using the ANSYS software with advanced sizing function. Mesh quality for both orthogonal and skewness factor is excellent with average values of 0.97566 and 0.1543 respectively.

Mesh Quality:

Minimum Orthogonal Quality = 7.21069e-01

(Orthogonal Quality ranges from 0 to 1, where values close to 0 correspond to low quality.)

Maximum Ortho Skew = 2.78931e-01

(Ortho Skew ranges from 0 to 1, where values close to 1 correspond to low quality.)

Maximum Aspect Ratio = 5.02490e+00

4.22.6 ANSYS Fluent Solver

General Setting

Under steady state conditions, derivatives with respect to time can be neglected and the governing equations can be expressed in the following general form:[57]

$$\frac{\partial}{\partial x_k}\left(\rho U\varphi - \Gamma_\varphi \frac{\partial \varphi}{\partial x_k}\right) = S_\varphi \qquad (4.53)$$

Specific definitions of the variables φ, Γ_φ and S_φ for the cases of the continuity, momentum and energy equations are provided in Table below.

Table 4.7 Specific definitions of the variables

Variables	φ	Γ_φ	S_φ
Continuity	1	0	0
Z-momentum	w	$\rho(v_t + v_L)$	$-\frac{\partial p}{\partial z} + gravity + friction$
r-momentum	v	$\rho(v_t + v_L)$	$-\frac{\partial p}{\partial r} + gravity + friction$
Energy	h	$\rho(\frac{v_t}{Pr_t} + \frac{v_L}{PrL})$	$-\frac{Dp}{Dt} + heat\ sources + ..$

Where

Pr-Prandtl number, r-radial direction, S_φ-source term for φ , where φ- variable to be solved

L-laminar, t- turbulent, ρ-density (Kg/m^3), v- kinematic viscosity (m^2/s), Γ- diffusion coefficient for φ

U- velocity vector(m/s), v- radial direction velocity vector (m/s), w- axial direction velocity vector (m/s) and z axial direction (m)

Models- Turbulence is modeled using the $k - e$ turbulence model with realizable -scalable wall function with compressible effect and heat transfer using the thermal energy model. The turbulence model is a commonly used model and is suitable for a wide range of applications.

Material- R134a is used as an ideal gas with its constant physical properties, Specific heat = 489 J/Kg-k, Thermal conductivity =0.0145 W/m-K, Viscosity 1.2e-05 Kg/m-s and molar weight 102.03 Kg/K-mol.

Boundary condition- is set for On-design points with primary, secondary and outlet as Pressure

Primary inlet 3.237 MPa and total temperature 363 K

Secondary inlet 0.441131 MPa and temperature total 285 K

Outlet 0.7788 MPa and total temperature 303 K

Solution – Pressure coupling with velocity and all spatial discretization momentum, energy, turbulence kinetic energy and turbulence dissipation energy were discretized with second-order upwind scheme

For both with mixer and without ejectors has been studied. With mixer ejector showed better performance than normal ejector. Pressure, Velocity, Mach number and Turbulent kinetic energy are compared below

.

Chapter Five

5. Results and Discussion

5.1 Design point solar ejector cooling system performance analysis

5.1.1 Monthly performance variation of the SoECS in Addis Ababa at design point

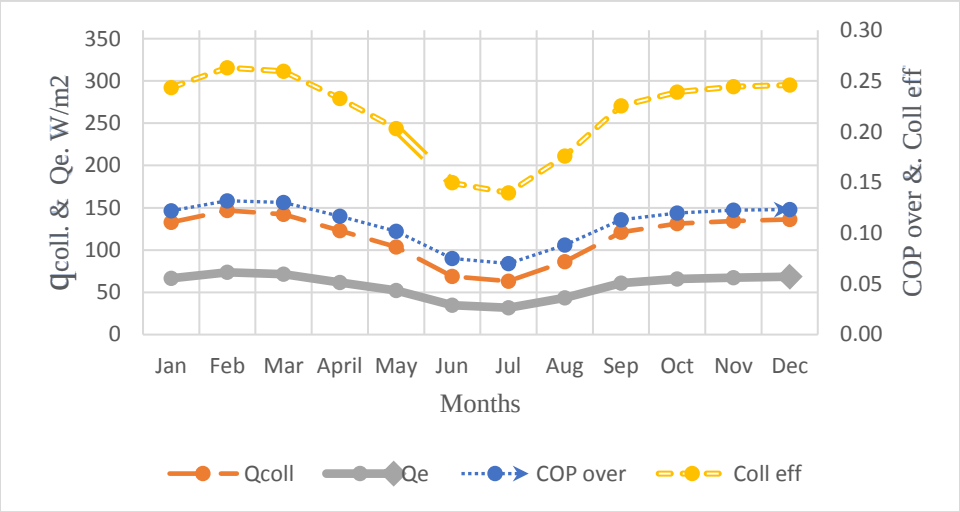

Fig 5.1 Monthly performances of the SECS for Addis Ababa at designed conditions of (T_g = 90^{0}C, T_C = 30^{0}C and T_e= 12^{0}C).

The above figure shows monthly average solar ejector cooling system performance variation for the design point (T_g = 90^{0}C, T_C = 30^{0}C and T_e= 12^{0}C). On the left side of the graph there is collector useful energy and the cooling capacity per unit collector area. According to design point temperatures, different cooling capacities are obtained for each month because of the variations of the solar radiation and the ambient temperature in fig 4.16. The highest monthly $COP_{overall}$ and Q_e are determined as 0.1319 and 73.62 W/m^2 for February, respectively. For the given operating conditions, the collector efficiency varies from 0.1397 to 0.2631 in February. February is the month which has maximum collector efficiency. The useful collector energy per unit collector area (q_{coll}) varies from 146.8 W/m^2 in February to 63.21 W/m^2 in July. Collector efficiency is directly related with cooling capacity, overall coefficient of performance and useful collector energy.

5.1.2 Hourly performance Variation of the SoECS in Addis Ababa at design point in March

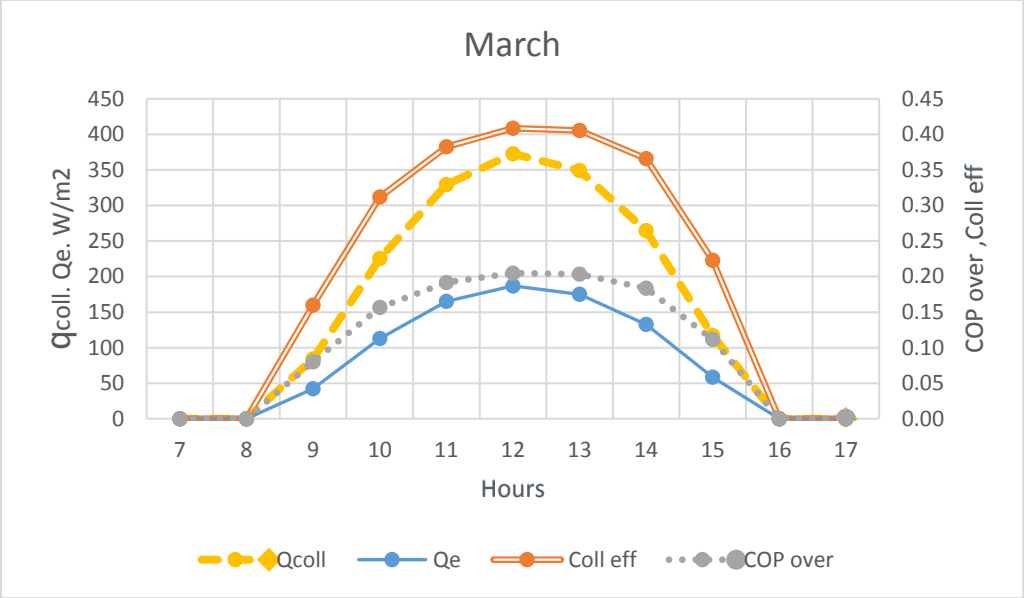

Fig 5.2 Hourly Average performances of the SECS for Addis Ababa at designed conditions of (T_g = 90^{0}C, T_C = 30^{0}C and T_e = 12^{0}C). The rest months graphs are in appendix A

Similarly, in fig 5.2 there is hourly performance of the SoECS through cooling season is carried out. The collector efficiency becomes smaller on version of the lower solar-radiation and the ambient-temperature in the morning hours. For march the performance increases and reaches a maximum value at 12:00 with the rise of the solar radiation. After that time, it decreases during the day and becomes zero around 16:00. The highest hourly $COP_{overall}$ and Q_e are determined as 0.20 and 186.9 W/m^2 respectively. For the given operating conditions, the maximum collector efficiency 0.41 at 12:00. The maximum useful collector energy per unit collector area (q_{coll}) is 372.7 W/m^2 at noon time. The variation of collector efficiency affected the $COP_{overall}$. Q_e and q_{coll}as shown in the above graph.

5.2 Cooling capacity (Q_e)

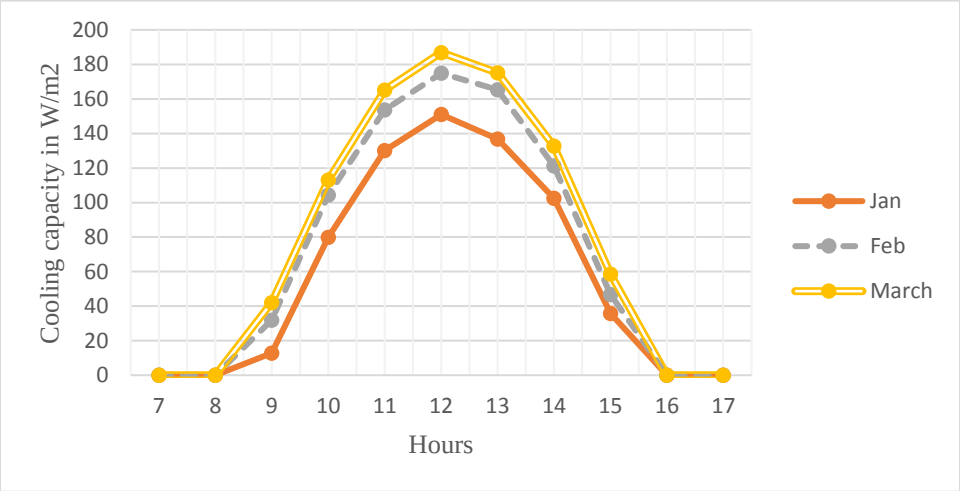

a.

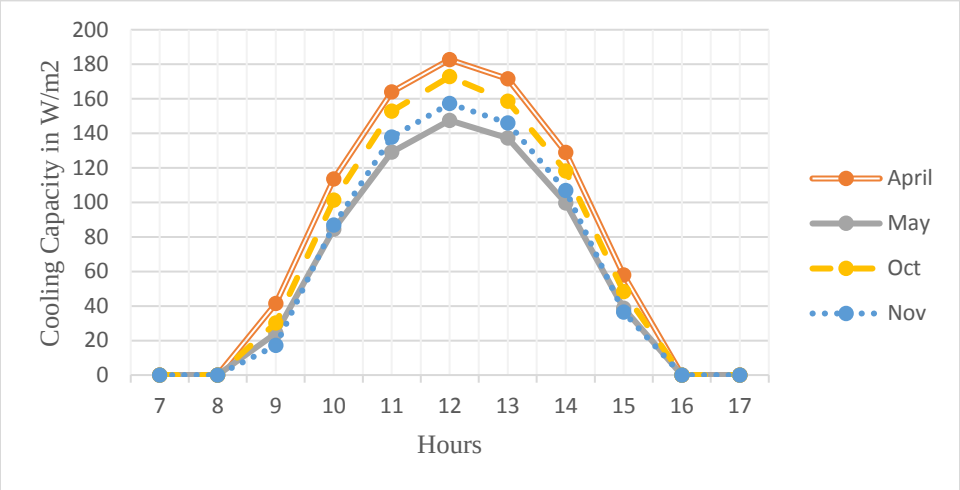

b.

Fig 5. 3 a and b are Hourly variations of the cooling capacity of the SoECS through the cooling season for Addis Ababa (T_g = 90^{0}C, T_c = 30^{0}C and T_e = 12^{0}C). cooling capacity

Here in the above figure 5.3 a and b shows hourly cooling capacity per unit collector area variation of seven months. The above figure includes a month which has good performance than the other months which are not shown above fig. The maximum hourly cooling capacity found to be 186.9 W/m^2 in March at 12:00 in fig 5.3 a. The maximum hourly cooling capacity for Jan 151 W/m^2, Feb 174.9 W/m^2, March 186.9 W/m^2, Apr 182.7 W/m^2, May 147.5 W/m^2, Oct 172.7 W/m^2 and

Nov 157.2 W/m^2 at 12:00 and now it is easy to differentiate the maximum and minimum hourly cooling capacity. For the given operating conditions, it is found that the Solar ejector cooling system would not provide a cooling effect in any examined months at 17:00. Therefore, in order to operate the system after 15:00, an auxiliary heat source (resistance heater, etc.) instead of the solar energy is necessary.

5.3 Necessary collector surface areas per ton cooling capacity

According to the obtained results, the necessary collector surface area per ton cooling capacity for Addis Ababa at 12:00.

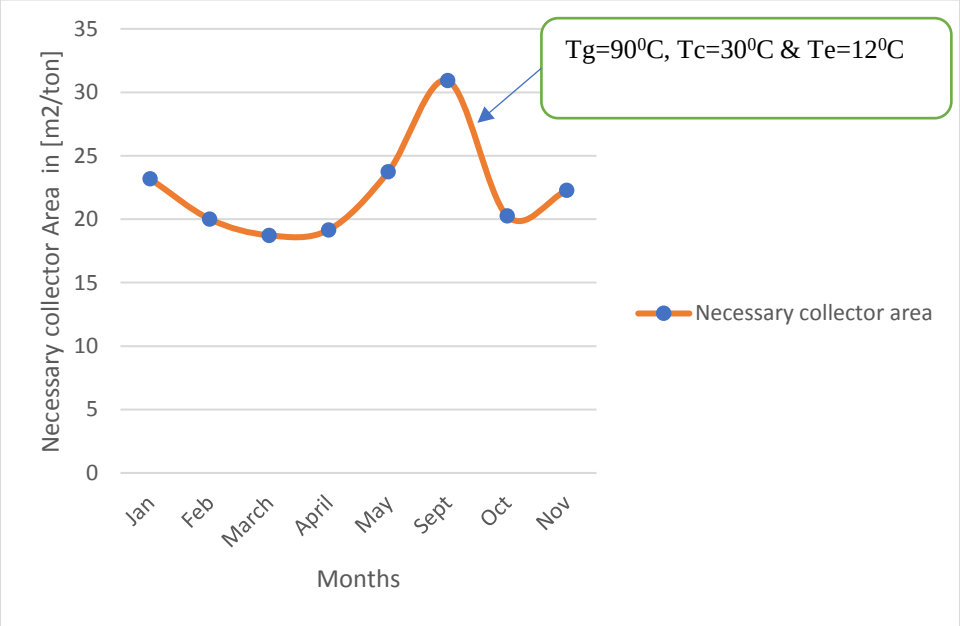

Fig 5.4 Necessary collector area per ton cooling capacity of eight months at 12:00

According to the obtained results, the necessary collector surface areas per ton cooling capacity for Addis Ababa at on-design operating condition (Tg=90^{0}C, Tc=30^{0}C & Te=12^{0}C) in Jan, Feb, March, April, May Sept, Oct and Nov are 23.18 m^2, 20.01 m^2, 18.72 m^2, 19.15 m^2, 23.72 m^2, 30.91 m^2, 20.25 m^2 and 22.26 m^2 at 12:00 in, respectively.

5.4 Performance of the system at different operating (Off-design) conditions

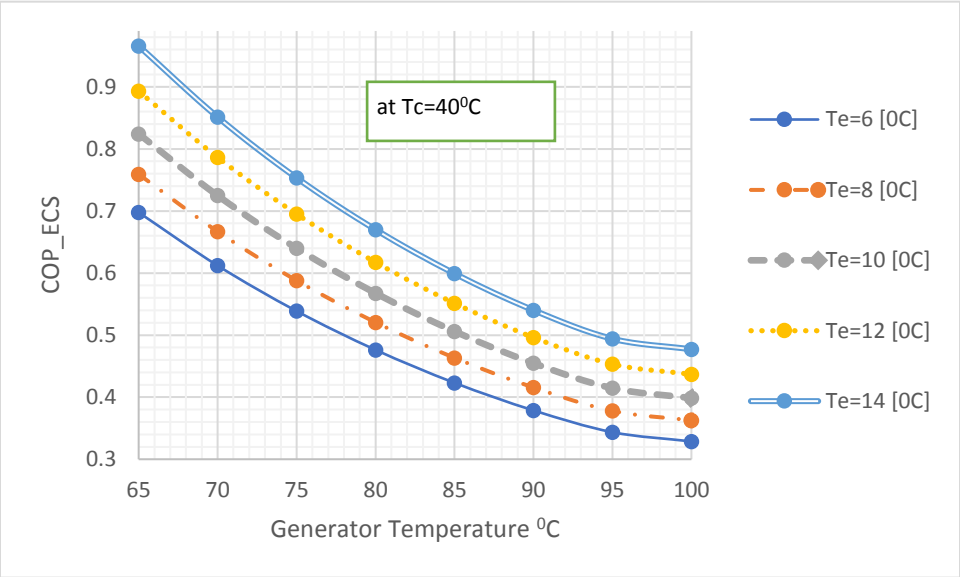

a,

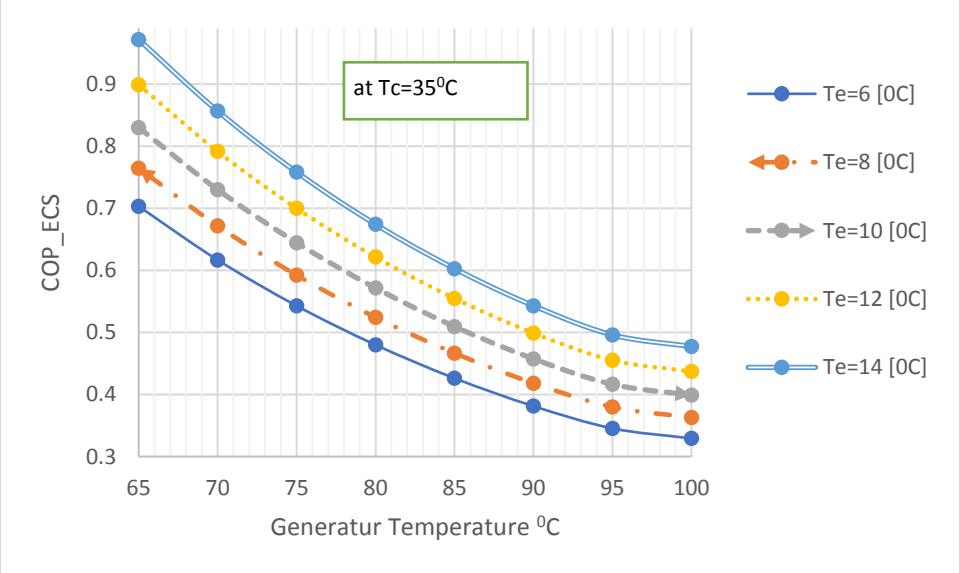

b,

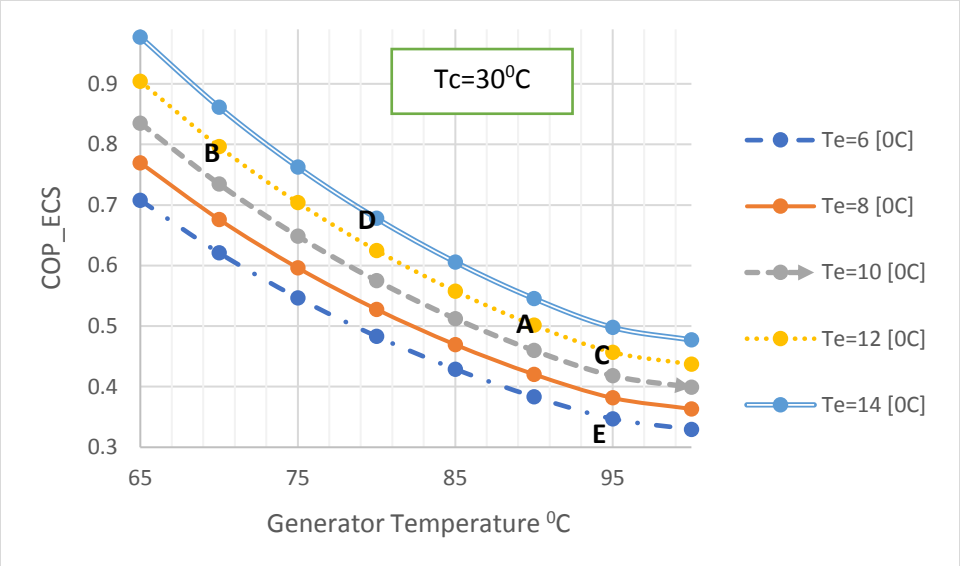

c,

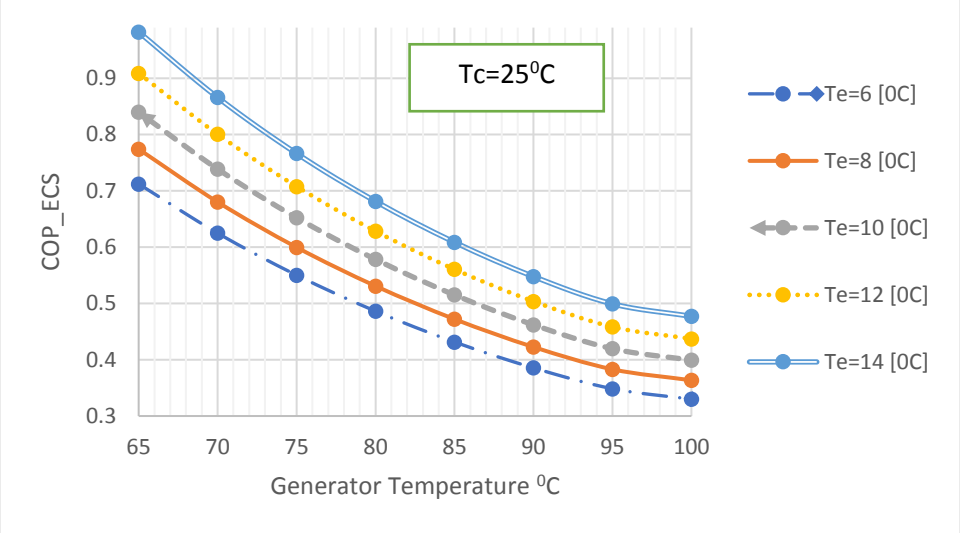

d,

Fig 5.5 Performance of the ECS during operation (a, Tc=40^{0}C, b, Tc=35^{0}C, c, Tc=30^{0}C and c, Tc=25^{0}C)

The above figures (a, b, c and d) shows the coefficient of performance (COP) variation of the system for different operating conditions. The above graphs show a performance at constant condenser temperature when the generator temperature decreases with slight increase in evaporator temperature the performance of the system increases. The figure c is better explaining the rest figures due to the map which is represented by the letters[A-E].

Figure 5.5 c shows the design points as well as and it is different from the others and it shows the performance map depending on the operating condition temperature's denoted with A, B, C, D & E. Point A represents the design point of the system B, C, D and E are the off-design operating conditions.

When the temperatures changes from one to point to the another for instance

- ✓ From A-B the coefficient of performance of the system (COP_ECS) increased this is because of the Generator temperature decreased with constant condenser and evaporator temperature.
- ✓ In the same way when from A-C the performance is decreased when the generator temperature increased with constant condenser and evaporator temperature.
- ✓ From A-D happened when both evaporator and generator temperature is changed means with decreasing temperatures of generator and increasing evaporator resulted in increasing the performance
- ✓ From A-E Performance is decreased due increasing generator temperature with decreasing evaporator temperature with constant temperature

Therefore, to increase the performance of the system generator temperature must decrease with constant evaporator and condenser temperature present study demonstrates a similar trend to the experimental research findings of Huang et al. [56] & Ersoy et al. [60]

5.4.1 Variation of the cooling capacity versus hour of day corresponding to the performance map and operating conditions (A–E) in March

A, B and C

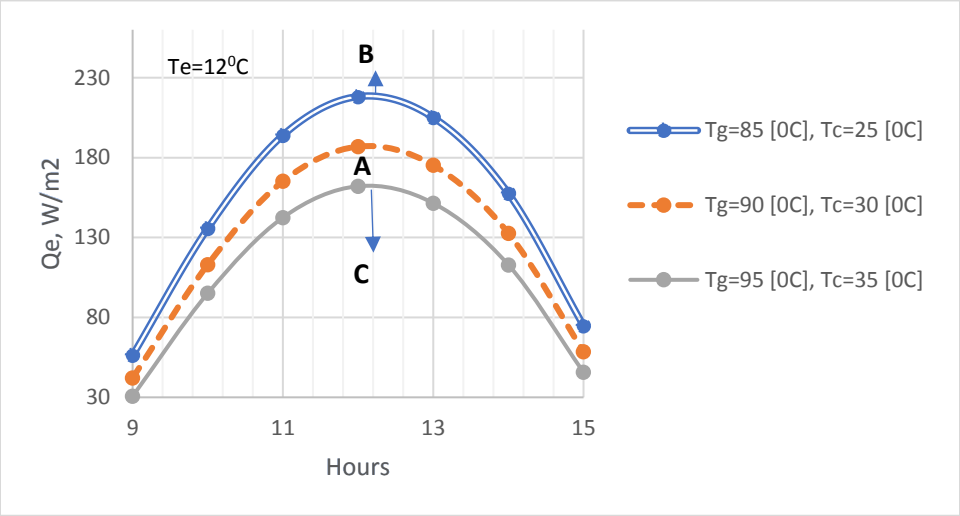

Fig 5.6 The cooling capacity hourly variation at different generator and condenser temperature with constant evaporator temperature.

D, E and F

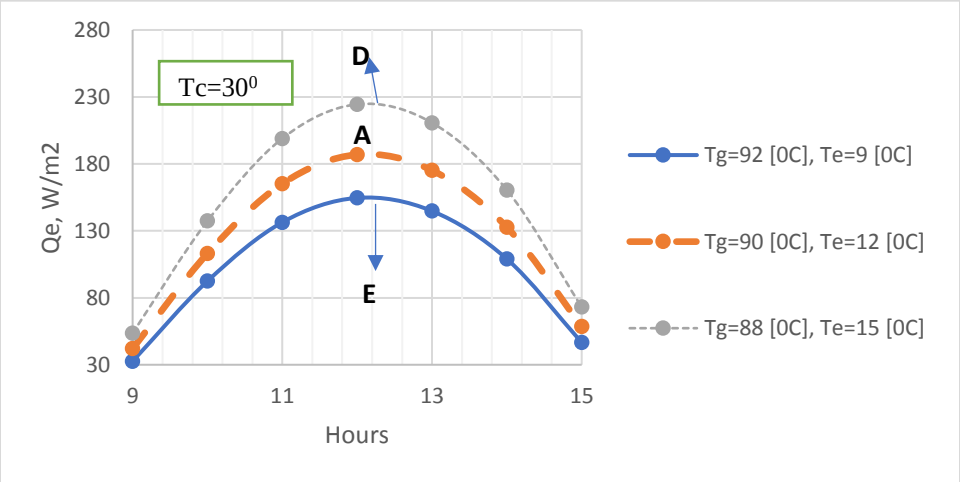

Fig 5.7 The cooling capacity hourly variation at different generator and Evaporator temperature with constant Condenser temperature.

Both figures (5.6 & 5.7) above shows the cooling effects variation with different operating conditions that;

Fig 5.6

- ✓ Letter A shows cooling capacity variation of the design point at hourly
- ✓ A to B the cooling capacity is increased due to that both generator and condenser temperature decreased with constant evaporator temperature
- ✓ A to C the cooling capacity is decreased because of the generator and condenser temperature is increased with constant evaporator temperature

Fig 5.7

- ✓ Letter A shows cooling capacity variation of the design point at hourly
- ✓ (A to D) the cooling capacity is increased due to decreased generator and increased evaporator temperature with constant condenser temperature
- ✓ (A to E) the cooling capacity is decreased because of the increased generator and decreased evaporator temperature with constant Condenser temperature

Therefore, to increase the cooling capacity of the system generator and condenser temperature must decrease with constant evaporator temperature. In addition to that again to increase the cooling capacity of the system it is must to decrease the generator temperature and slight increase in evaporator temperature with constant condenser temperature. The results presented here demonstrates a similar trend to the experimental research findings of Huang et al. [56] & Ersoy et al. [60].

The best results from the performance map of the system can be easily observed under various operating conditions. To achieve the highest operation-efficiency, the temperatures of generator, condenser and evaporator should be automatically controlled according to the performance map [54]. Therefore, the performance map will guide the automatic-control system of the Ejector Cooling System and helps the designers or operators to plant the system easily. By using this analysis researchers can enhance the system performance figuring out the problems easily.

5.5 CFD results with discussion

The Mixer is placed in the upstream of the primary nozzle entry which helps introduces a turbulence flow which increases the amount of energy, momentum exchange between two fluid and the contact time of the fluids as well as heat transfer. The results are expressed in terms pressure, Velocity, Mach number and turbulent kinetic energy (TKE) below and there is a difference between two ejectors illustrated.

5.5.1 Pressure variation along the ejector length

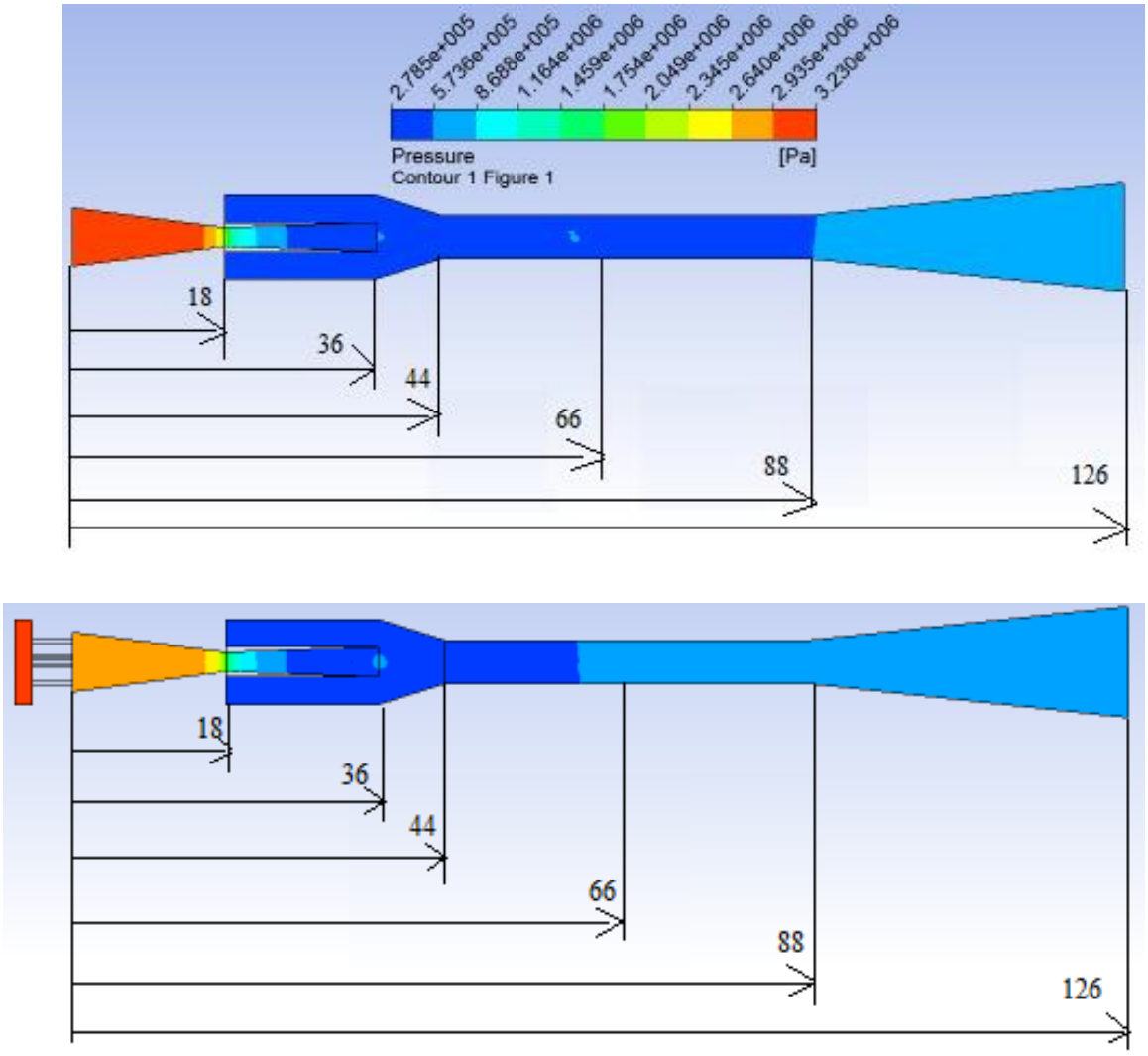

Fig 5.8 Pressure contour

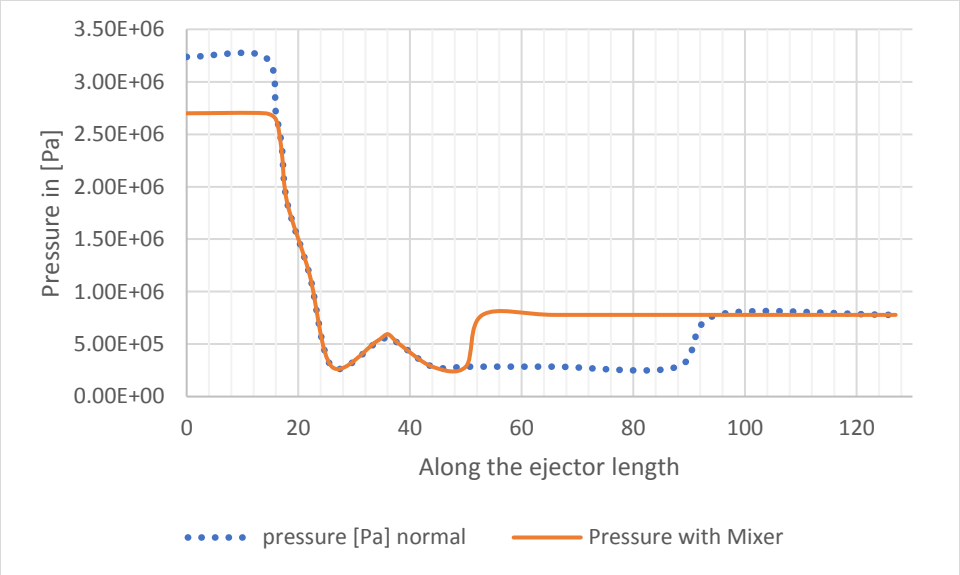

Fig 5.9 Graphs of normal and with mixer Ejector

The pressure in the above graph is reduced for the ejector with Mixer along the converging primary nozzle. The pressure of the normal ejector along the primary nozzle is higher than with Mixer and after passing the primary nozzle it becomes lower than with Mixer due to the mixer effect. The pressure increase in the mixing tube helps to suck more secondary fluid from the evaporator. This increased the entrainment ratio and enhanced the mixing quality. The mixing of the two streams occurs near the mixing tube at constant pressure exchange. Since the fluid travels with supersonic speed means with speed higher than local speed of sound it produces normal shock. It has been observed that shock occurs for both ejector along the primary nozzle outlet but for ejector with mixer has relatively higher.

It indicates that mixing effect improves mixing of the two streams, thereby better momentum exchange occurs and pressure recovery has been obtained for a relatively shorter distance of mixing tube for ejector with mixer than the normal ejector. Mixing of two streams occurs at constant pressure in both suction chamber and mixing tube followed by a sudden pressure rise due to shock. In the diffuser, further pressure rise takes place or it regains its pressure.

5.5.2 Velocity variation along the ejector length

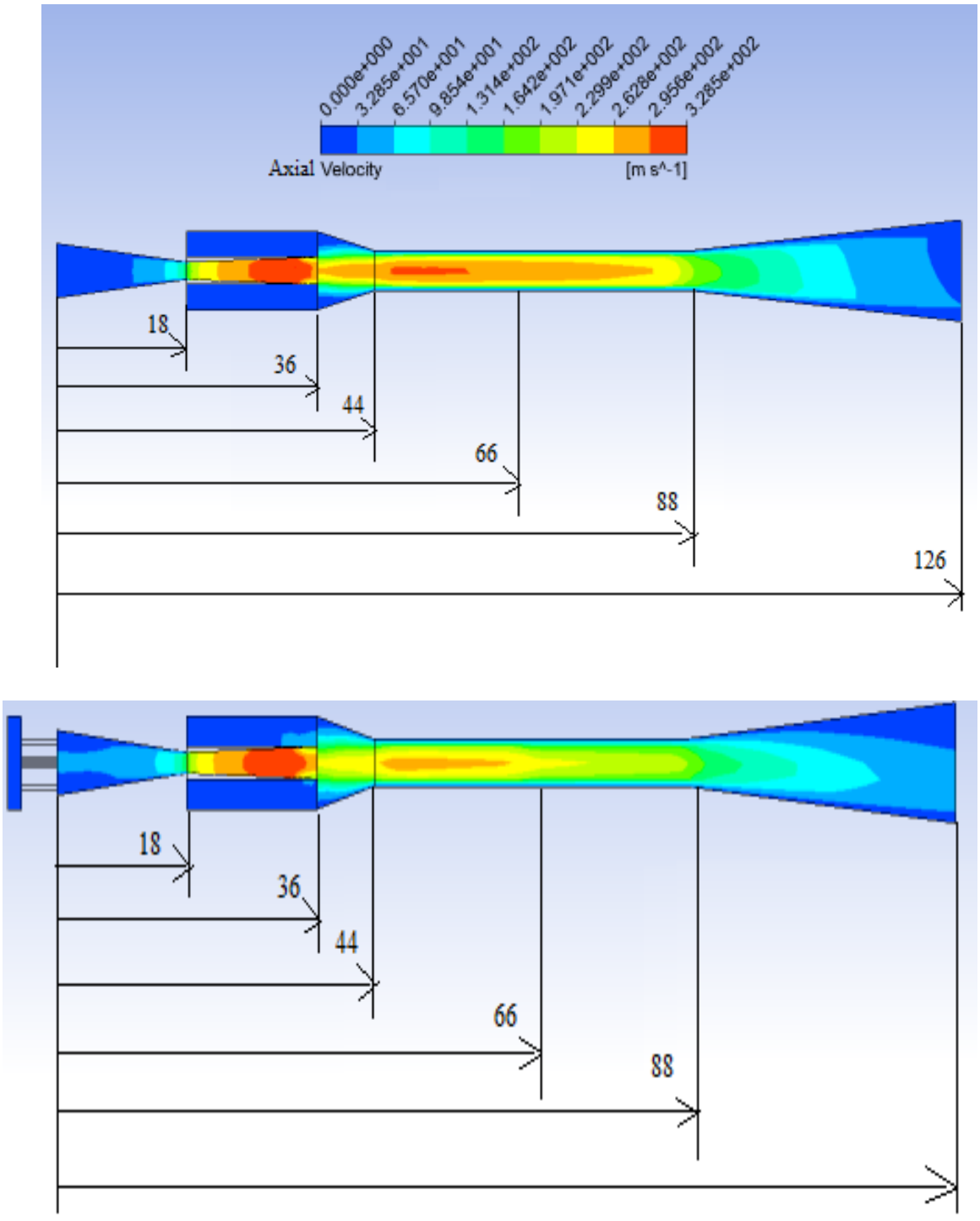

Fig 5.10 Axial velocity contour

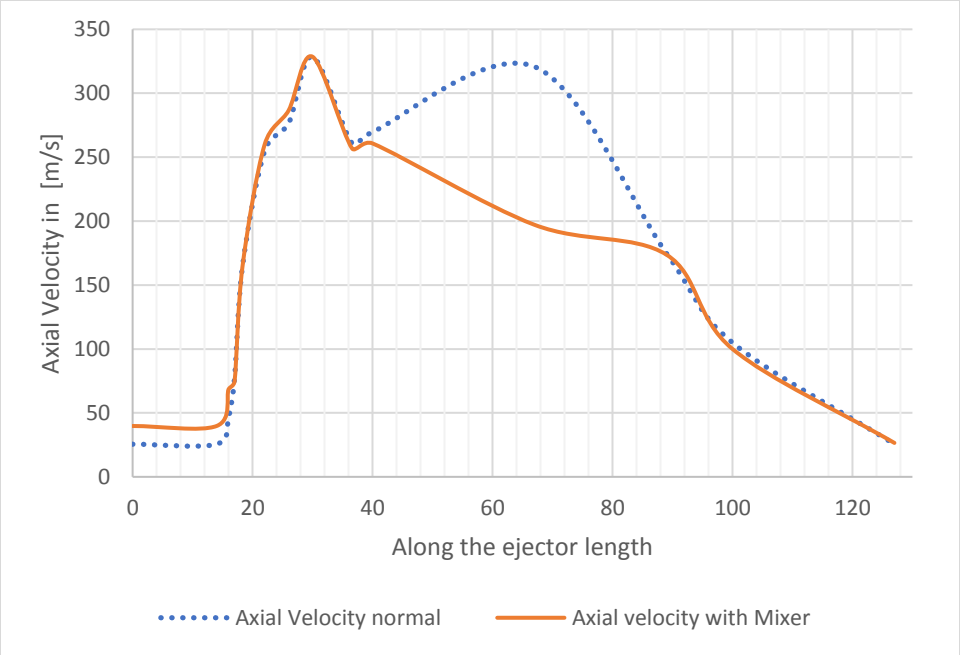

Fig 5.11 Axial velocity with and without Mixer Ejector

Axial velocity is increased in the above graph for the ejector which uses mixer inside the primary nozzle along the converging nozzle due to a mixer effect. The axial velocity difference occurs again after primary nozzle outlet. Axial velocity for the ejector with mixer is decreased due to the mixing effect. The Mixer reduces the axial velocity to the flow that means velocity in other direction is higher due to that suction of the secondary fluid increases which is in radial direction [58]. Axial velocity decreased due to turbulence effect and mixing quality also enhanced fig 5.14. Primary stream expands to supersonic velocity in the convergent-divergent primary nozzle and entrains the secondary stream which has low velocity. The secondary stream is accelerated to sonic condition due to momentum exchange between primary and secondary streams.

5.5.3 Mach number variation along the ejector length

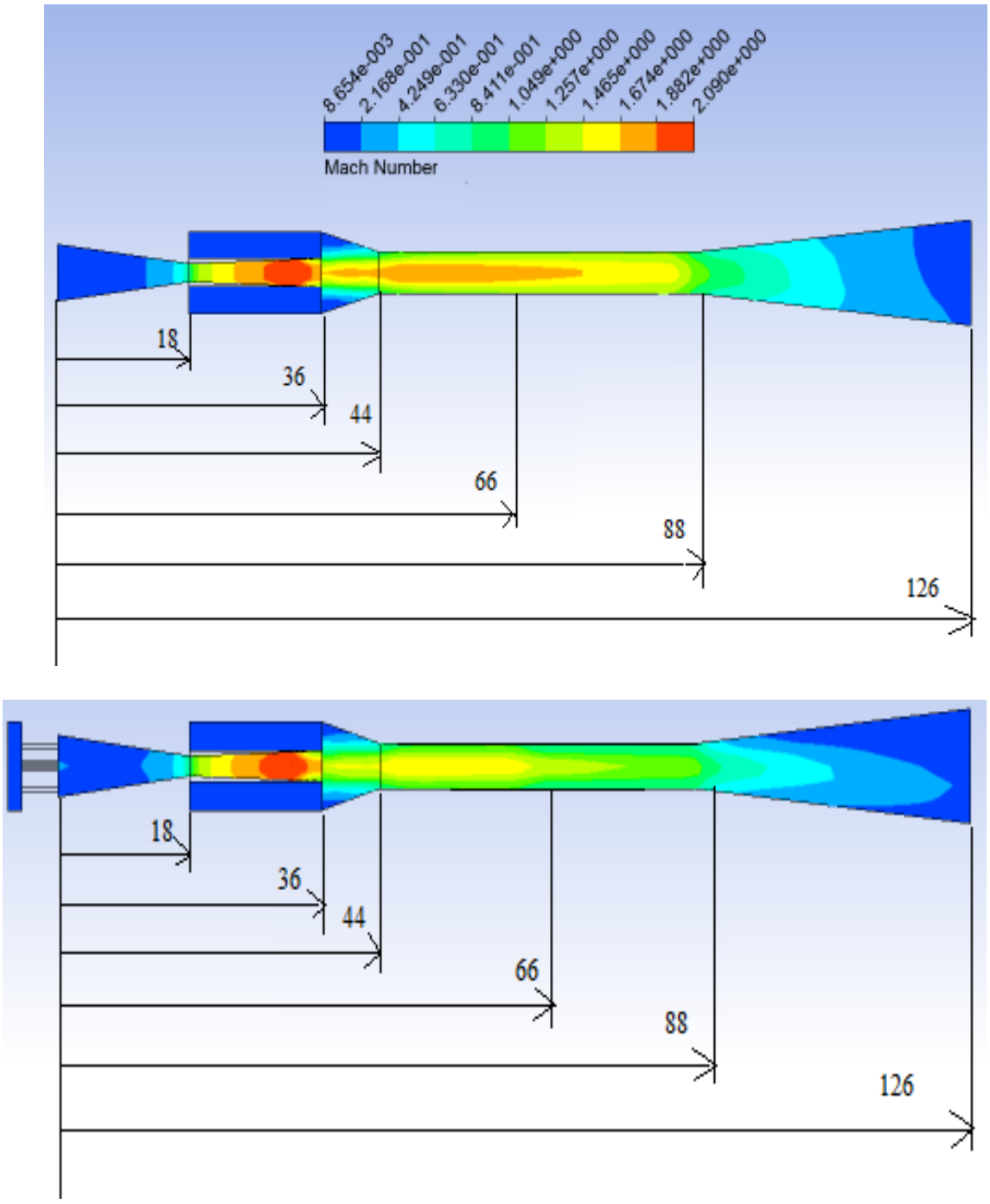

Fig 5.12 Mach number contour

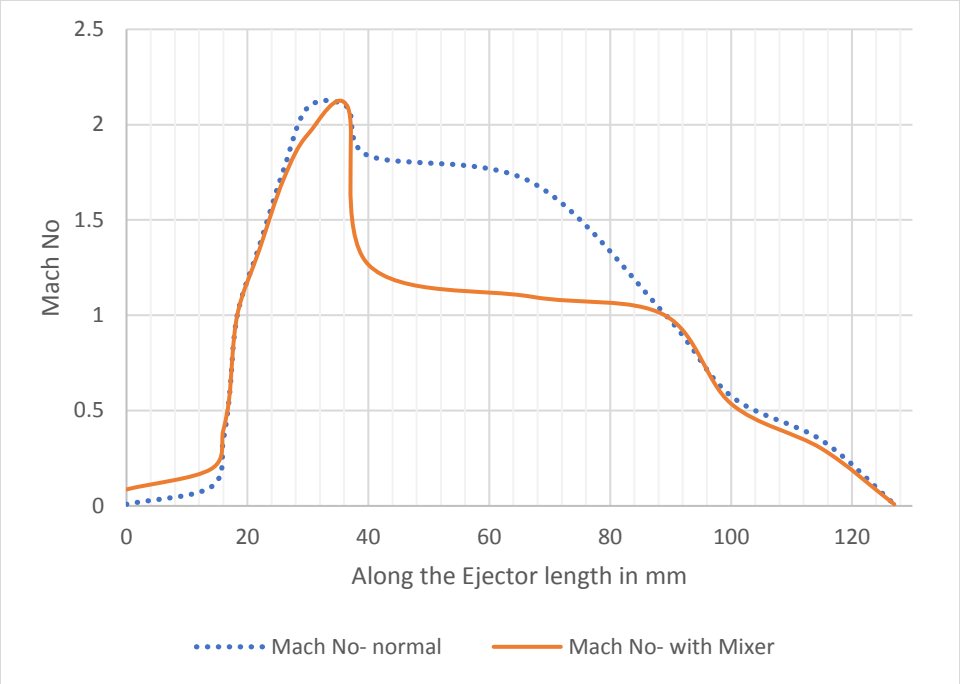

Fig 5.13 Mach number for normal and with mixer Ejector

Mach number is higher for the ejector with mixer along the primary nozzle in converging nozzle due to a pressure drop. Mach number is increased along the converging primary nozzle for ejector with mixer and it becomes one in the throat of converging diverging nozzle. After passing the primary nozzle it reduced largely due to momentum exchange between the two streams and axial velocity decreased. The speed becomes sonic along the throats of the primary converging-diverging nozzle and between the mixing tube and diffuser.

5.5.4 Turbulent kinetic energy (K) Variation along the length of ejector

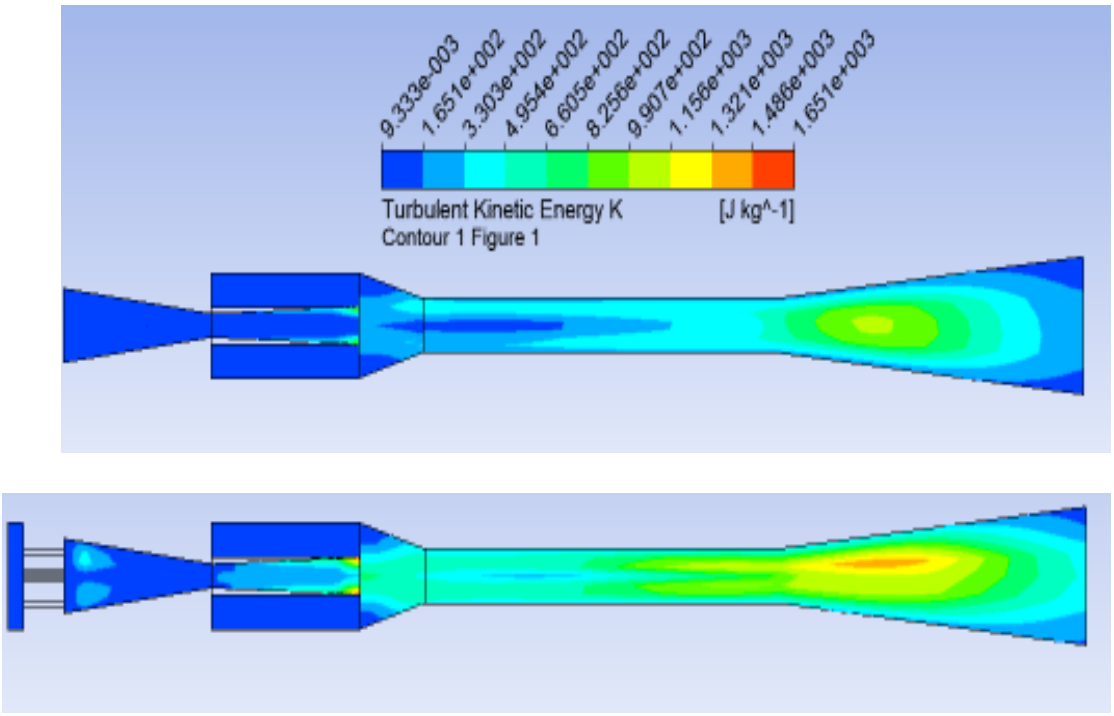

Fig 5.14 Turbulent kinetic energy K

In the above fig 5.14 it shows the Turbulent kinetic energy variation along the ejector length for with and without Mixer. The ejector without Mixer starts the turbulence around the primary nozzle exit this is due to the sudden shock which is occurred at the primary nozzle exit. Turbulence kinetic energy which is increased after passing the primary nozzle for without mixer because it is the place where secondary vapor is mixed to the primary vapor. In the same way for with mixer ejector the turbulence starts along the converging nozzle of the primary nozzle which is earlier than without ejector and this is due to a mixer effect and this increases the mixing quality along the constant mixing section. The turbulence kinetic energy of the without mixer ejector is less when compared to the ejector with mixer. Turbulence kinetic energy is high for the ejector with the mixer this helps to increase the entrainment ratio means performance is enhanced.

Summarize

The CFD results obtained here are compared to the International Refrigeration and Air Conditioning journals and it showed a good agreement. [58] & [59]

Table 5.1 The entrainment ratio increased from 0.551846 to 0.609046

Types	***ω***
Normal ejector	0.551846
With Mixer ejector	0.609046

The mathematical modelling (Huang et al model) which is well known phenomena in ejector performance design result entrainment ratio is 0.5564 and CFD result which is done in present work is 0.551846 of normal ejector. The model is no more than 5% deviation. This means the model is effective for analysis. The entrainment ratio is increased 10.4 % this means that ejector with mixer has better performance than ejector without. By using this Mixer, we can enhance the system performance in addition to that it increases mixing quality. The investigators T. Shaligram [58] 2014 & M, Jawali [59] in 2016 studied the numerical and experimental analysis using Mixer with aero foil blade type and solid blade type and enhanced the system to 6%. But here by using Curved blade hollow type mixer it is improved to 10.4% percent. For future the influence of Mixer and blade angle on the ejector performance will be studied.

5.6 Enhanced cooling capacity per unit collector area of the system

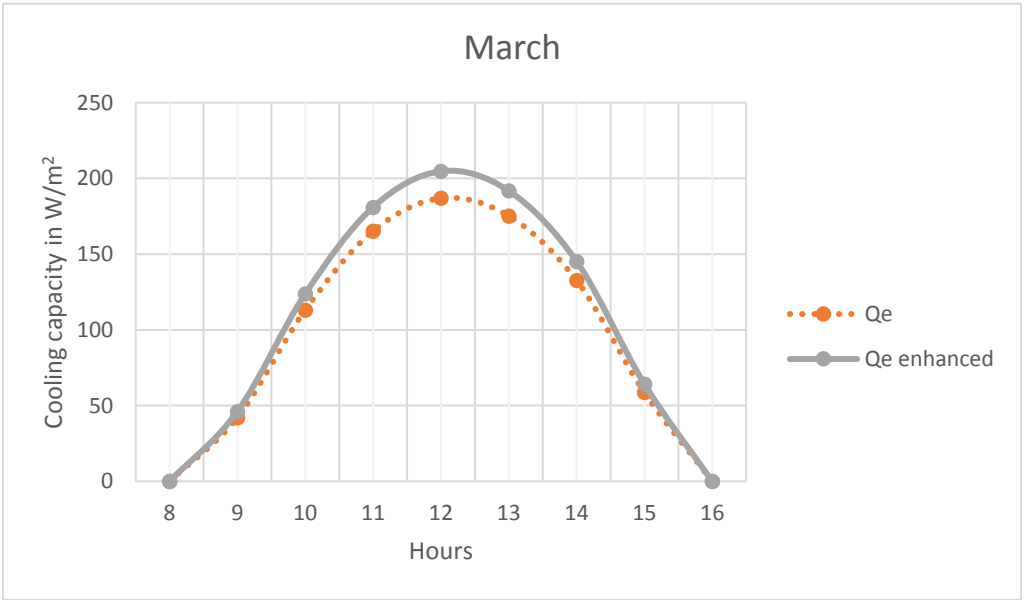

Fig 5.15 Hourly enhanced cooling capacity of the system on march

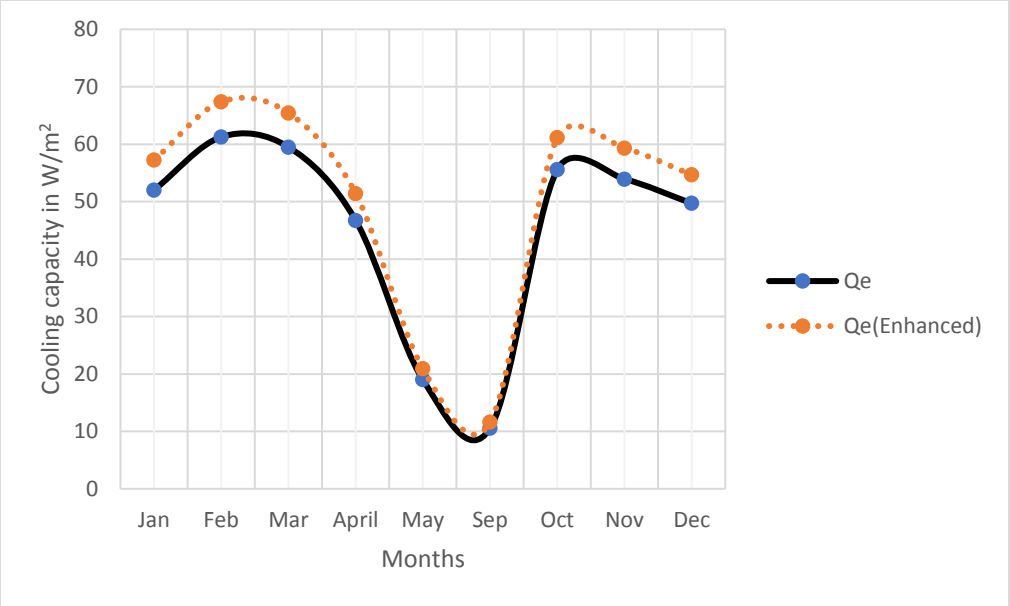

Fig 5.16 Monthly enhanced cooling capacity of the system on march

The maximum cooling capacity per unit collector area for march was 186.9 W/m^2 but after enhancing the system performance become 204.7 W/m^2 at 12:00. Monthly, in February cooling capacity enhanced from 61.26 W/m^2 to 67.39 W/m^2. It is better to use the mixer or it is better to induce a turbulence to the primary fluid flow inside the Ejector it increases the performance and mixing quality.

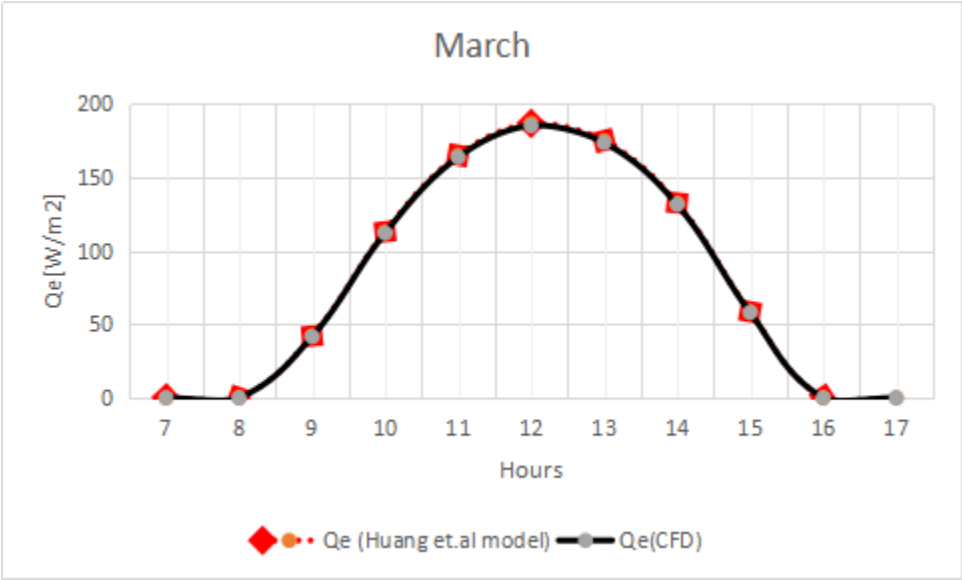

Fig 5.17 Verification with a well-known model

Chapter Six

6. Conclusion and Recommendation

6.1 Conclusion

In this present study the performance analysis of the solar ejector cooling system and enhancement of the component called ejector performance analysis has been carried out. The performance investigation of hourly and monthly SoECS is studied by taking Addis Ababa as a case study. The SoECS based on constant pressure ejector flow model and using refrigerant R-134a was considered. The maximum cooling capacity of the SoECS was calculated by means of the processed solar radiation and the ambient temperature data taken from the Ethiopian National Meteorological Agency (ENMA). The results can be summarized as follows.

Solar collector efficiency has been varied largely depending on the solar radiation and the ambient temperature for the month and day. The solar collector efficiency variation affected $COP_{overall}$. Q_e and q_{coll}.

- ✓ Solar collector efficiency varied from 0.1397 in July to 0.2631 in February monthly
- ✓ Solar collector efficiency reached 0.41 in hourly bases in march at 12:00
- ✓ The hourly maximum overall coefficient of the performance and the cooling capacity were obtained as 0.2049 and 186.9 W/m^2, respectively, at 12:00 in March.
- ✓ The monthly maximum overall coefficient of the performance and the cooling capacity were obtained as 0.1319 and 72.62 W/m^2, respectively, in February.
- ✓ The cooling capacities of the SoECS were very close to each other for the given conditions for most months.

The performance map for of the SoECS was derived for the off-design operating conditions to provide more useful information for designers and operators. The following conclusion drawn for the off-design operating conditions

- ✓ To increase the performance of the system generator temperature must decrease with constant evaporator and condenser temperature

- ✓ To increase the cooling capacity of the system generator and condenser temperature must decrease with constant evaporator temperature.
- ✓ In addition to that again to increase the cooling capacity of the system it is must to decrease the generator temperature and slight increase in evaporator temperature with constant condenser temperature.

To achieve the highest operation-efficiency, the temperatures of generator, condenser and evaporator should be automatically controlled according to the performance map. Therefore, the performance map will guide the automatic-control system of the Ejector Cooling System and helps the designers or operators to plant the system easily. By using this analysis researchers can enhance the system performance figuring out the problems easily.

The SoECS could be used for the office-cooling purpose for all Addis Ababa until 15:00 through the cooling season. For the given operating conditions, it was found that the SoECS would not sustain cooling in any months at 17:00. Moreover, the evacuated-tube solar collector efficiency approximately decreased to zero at 16:00. Therefore, in order to operate the system after 15:00, an auxiliary heat-source instead of solar energy should be employed. According to the obtained results, the necessary collector surface areas per ton cooling capacity for Addis Ababa at on-design operating conditions in Jan, Feb, March, April, May Sept, Oct and Nov are 23.18 m^2, 20.01 m^2, 18.72 m^2, 19.15 m^2, 23.72 m^2, 30.91 m^2, 20.25 m^2 and 22.26 m^2 at 12:00 in, respectively.

Finally, Ejector which is a part of SoECS which helps the system to drive is enhanced in present study. The Mixer is placed in the upstream of the primary nozzle which helps to introduces the turbulence which increases the amount of moment exchange between two fluid, enhance heat transfer, increase rate of energy and increases the contact time of the fluids. The results are expressed in terms of pressure, Velocity, Mach number and Turbulence Kinetic energy it showed a difference between two ejectors. The pressure is reduced along the primary nozzle for with mixer ejector than normal ejector this leads the quick recovery of the pressure along the mixing tube. The quick pressure recovery increases the two streams contact time. Mach number also increases along the primary nozzle and decrease from the mixing tube to diffuser due to a mixing effect. Entrainment ratio has been improved by 10.4 % using Curved blade mixer with camber angle of 14^0. The cooling capacity per unit collector area for march was 186.9 W/m^2 but after enhancing the system performance become 204.7 W/m^2 at 12:00.

6.2 Recommendation and future work

Recommendations for further work to enhance more research and improvements done on Solar ejector cooling system and particularly Ejector;

- ✓ The numerical performance analysis has been carried out here in this research and it is important to investigate it in experiments.
- ✓ The off-design operating condition map is derived in this study. By using this map, it is possible to create performance controlling mechanism.
- ✓ The investigation carried out here could be as a resource for the researchers and also will help the designers or the operators to plant the system with confidence.
- ✓ Since the solar energy is used in day time only and affects the performance in night time. It is better if auxiliary heater is used in night time. It is better if there is a mechanism provided which can replace the Ejector with compressor during the night.
- ✓ Variable area Ejector can perform better than the normal ejector due to this it is possible to increase the performance by varying one of the ejector parameters such as nozzle throat diameter, primary nozzle outlet diameter, the mixing tube diameter, the distance between the primary nozzle outlet to the mixing tube section, primary nozzle converging nozzle angle.
- ✓ It is better to use the hot water storage and cold-water storage to increase the system performance as well as to use the system at night time.
- ✓ The influence of mixer design and blade angle on the ejector performance can become a future work.
- ✓ Mixer can increase the system performance here as it showed 10.4% improvement due to this other type of mixer rather than curved blade hollow type mixer can be able to increase the performance even better.
- ✓ Here four blades are used to increase the system performance. It is possible to study the number of blades effect on the performance of the system.
- ✓ Still it can be possible to analyze the effect of blade angles of the mixer on the performance of the system.

References

[1] G. Grazzini et al.,(2018) Ejectors for Efficient Refrigeration, https://doi.org/10.1007/978-3- 319-75244

[2] Thévenot, R. (1979). *A History of Refrigeration Throughout the World*. Paris, International Institute of Refrigeration.

[3] Pedro DG & Pedro DS (2015), Handbook of Research on Advances and Applications in Refrigeration Systems and Technologies, ISBN 978-1-4666-8399-0 (set: Ebook)

[4] Dennis, M., &Garzoli, K. (2011). Use of variable geometry ejector with cold store to achieve high solar fraction for solar cooling. *international journal of refrigeration*, 34, 1626– 1632. Retrieved from www.elsev ier.com/locate/ijrefrig

[5] Kim, D.S., Infante Ferreira, C.A., (2008). Solar refrigeration options a state-of-the-art review. *International journal of Refrigeration*31, 3-15.

[6] Pridasawas, W., & Lundqvist, P. (2007). A year-round dynamic simulation of a solar-driven ejector refrigeration system with iso-butane as a refrigerant. *International Journal of Refrigeration*, *30*, 840–850. Retrieved from *www.elsevier.com/locate/ijrefrig*

[7] Prandecki, Konrad (25 May 2014*).*Theoretical Aspects of Sustainable Energy, *Energy and Environmental Engineering*. **2** (4): 83–90. doi*:*10.13189/eee.2014.020401.

[8] Chen LT(1978). A heat driven mobile refrigeration cycle analysis. Energy Convers ;18:25–9.

[9] Adnan, S., Mehmet, O., & Erol, A. (2004). Prospects for utilization of solar driven ejectorabsorption cooling system in Turkey. *Applied Thermal Engineering*, 24, 1019–1035. *https://doi.org/10.1016/j.applthermaleng.2003.11.011*

[10] Erosy HK, Yalcin S, & Ozgoren M (2007), Performance of a solar ejector cooling-system in the southern region of Turkey, *Applied Energy* 84, 971–983 doi:10.1016/j.apenergy.2006.10.001

[11] Pridasawas, W., & Lundqvist, P. (2007). A year-round dynamic simulation of a solar-driven ejector refrigeration system with iso-butane as a refrigerant. *International Journal of Refrigeration*, *30*, 840–850. Retrieved from *www.elsevier.com/locate/ijrefrig*

[12] Kim, D.S., Infante Ferreira, C.A., (2008). Solar refrigeration options a state-of-the-art review. *International journal of Refrigeration*31, 3-15.

[13] Alexis, G. K., & Karayiannis, E. K. (2005). A solar ejector cooling system using refrigerant R134a in the Athensarea. *Renewable Energy*, 30, 1457 1469.https://doi.org/10.1016/j.renene.2004.11.004

[14] Khaled A, & Charles, G. (2005). Effect of changing throat diameter ratio on a steam supersonic pressure exchange ejector. *Modern Physics*, 19(28), 1715–1718. Retrieved from *www.worldscientific.com*

[15] SzabolcsVarga, Armando C. Oliveir, Bogdan Diaconu (2 0 0 9), Numerical assessment of steam ejector efficiencies using CFD. *i n t e r n a t i o n a l j o u r n a l o f r e f r i g e r a t i o n* 3 2, 1 2 0 3 – 1 2 1 1.www.elsevier.com/locate/ijrefrig

[16] Amel, H., François, H., Sébastien, L., Jean-Marie, S., & Yann, B. (2009). CFD analysis of asupersonic air ejector. Part II: Relation between global operation and local flow features.*AppliedThermalEngineering*,29,2990-2998.doi.org/10.1016/j.applthermaleng.2009.03.019

[17] Dennis, M., &Garzoli, K. (2011). Use of variable geometry ejector with cold store to achieve high solar fraction for solar cooling. *international journal of refrigeration*, 34, 1626– 1632. Retrieved from www.elsev ier.com/locate/ijrefrig

[18] Szabolcs Varga1, Armando C. Oliveira and Bogdan Diaconu(2009), Analysis of a solar-assisted ejector cooling system for air conditioning, *International Journal of Low-Carbon Technologies*, 4, 2–8. doi:10.1093/ijlct/ctn001

[19] SzabolcsVarga , Armando C. Oliveira , Xiaoli Ma (2 0 1 1), Experimental and numerical analysis of a variable area ratio steam ejector, *i n t e r n a t i o n a l j o u r n a l o f r e f r i g e r a t i o n* 3 4 , 1 6 6 8 -1 6 7 5. doi:10.1016/j.ijrefrig.2010.12.020

[20] Varga, S., Pedro Lebre, M. S., & Oliveira Armando, C. (2013). CFD study of a variable area ratio ejector using R600a and R152a refrigerants. *Int j o u r n a l o f r e f r i g e r a t i o n*, 36, 4200–465. Retrieved from *www.elsevier.com/locate/ijrefrig*

[21] R.H. Yen , B.J. Huang , C.Y. Chen (2013). Performance optimization for a variable throat ejector in a solar refrigeration system.*i n t e r n a t i o n a l j o u r n a l o f r e f r i g e r a t i o n*, 3 6, 1 5 1 2 -1 5 2 0. *www.elsevier.com/locate/ijrefrig*

[22] Yusuke, S., Tatsuya, I., Akiko, M., & Haruki, S. (2014). Ejector Configuration for Designing a Simple and High Performance Solar Cooling System. Energy Procedia, 57, 2564–2571. Retrieved from *www.sciencedirect.com*

[23] Dennis, M., &Garzoli, K. (2011). Use of variable geometry ejector with cold store to achieve high solar fraction for solar cooling. *international journal of refrigeration*, 34, 1626– 1632. Retrieved from www.elsev ier.com/locate/ijrefrig

[24] Surya SD, Vasu TA, Raghavan KS and Murthy Ch (2017), CFD Simulation of Ejector in Steam Jet Refrigeration, *Journal of AppliedMechanical Engineering*, 6:263 doi:10.4172/2168

[25] Joe Hayton (2017), Solar Heating and Cooling Systems Fundamentals, Experiments and Applications, *Academic Press publications*, 293-294. ISBN: 978-0-12-811662-3

[26] J, Parveen, T Shaligram, & A Mani, (2014) Three-dimensional Numerical Investigations on Ejector of Vapour Jet Refrigeration System" . *International Refrigeration and Air Conditioning Conference.* 1433.

[27] M, Jawali, & M, Annamalai, (2016) Experimental And Numerical Investigations of Ejector Jet Refrigeration System With Primary Stream Swirl" (2016). *International Refrigeration and Air Conditioning Conference*.

[28] John A. Duffie and William A. (2013) Beckman Solar Engineering of Thermal Processes, Fourth Edition. ISBN 978-0-470-87366-3

[29] I. Sarbu & C. Sebarchievici (2017), Solar Heating and Cooling Systems ISBN: 978-0-12-811662-3

[30] Y. Allouche, C. Bouden & S.Riffat (2012), Asolar-Driven Ejector refrigeration system for Mediterranean climate, *Energy procedia* 18, 1115-1124

[21] H. Vidal, S. Colle & S. Pereirp (2006), Modelling and Hourly simulation of Solar ejector cooling system. *Applied Thermal Engineering* 26, 663-672

[32] MX, Zhang W, Omer S, Riffat B. (2010) Experimental investigation of a novel steam ejector refrigerator suitable for solar energy applications. *Appllied Thermal Engineering* 30:1320–5.

[33] Varga S, Oliveira AC, Diaconu B. (2009)Analysis of a solar-assisted ejector cooling system for air conditioning. *Int J Low-Carbon Technology*;4: 2–8.

[34] Dorantes R, Estrada CA, Pilatowsky I. (1996) Mathematical simulation of a solar ejector-compression refrigeration system. *Applied Thermal Engineering*.;16: 669–75.

[35] Tashtoush B, Alshare A, Al-Rifai S.(2015). Hourly dynamic simulation of solar ejector cooling system using TRNSYS for Jordanian climate. *Energy Convers Manag* 100:288–99.

[36] Tashtoush B, Alshare A, Al-Rifai S. (2015) Performance study of ejector cooling cycle at critical mode under superheated primary flow. *Energy Convers Manag* 94:300–10.

[37] Garg HP, Chakravertty S, Shukla AR, Agnihotri RC. (1983) Advanced tubular solar energy collector a state of the art. *Energy Conversion and Management* 23 (3):157-69.

[38] Kim Y, Seo T. (2007) Thermal performances comparisons of the glass evacuated tube solar collectors with shapes of absorber tube. *Renewable Energy* 32:772-95.

[39] Shah LJ, Furbo S. (2004) Vertical evacuated tubular-collectors utilizing solar radiation from all direction. *Appl Ene* 78:371-95.

[40] Ioan S & Calin S. Solar Heating and Cooling Systems Fundamentals, Experiments and Applications. ISBN: 978-0-12-811662-3

[41] Gaylon S & Campbell M. N (1998)An Introduction to Environmental Biophysics Second Edition ISBN 0-387-94937-2

[42] Ileri A.(1995) Yearly simulation of a solar-aided R22-DEGDME absorption heat-pump system. *Solar Energy* 55(4):255–65.

[43] Ibrahim A, Abdulvahap Y, (2003) Simulation of solar-powered absorption cooling system. *Renewable Energy* 28 1277–1293

[44] Keenan H, Neumann EP, Lustwerk F. (1950) An investigation of ejector design by analysis and experiment. J. *Appllied. Mechanical., Trans.* 72: 299–309.

[45] W Pridasawas (October 2006) Solar-Driven Refrigeration Systems with Focus on the Ejector Cycle *Division of Applied Thermodynamics and Refrigeration* ISBN 91-7178-449-7

[46] Munday, J, & Bagster, D (1977). A new ejector theory applied to steam jet refrigeration. *Industrial & Engineering Chemistry Process Design and Development*, 164, 442–449.

[47] Huang, B., Chang, J., Wang, C., & Petrenko, V. (1999). A 1-D analysis of ejector performance. *International Journal of Refrigeration*, 22, 354–364.

[48] E. Preisegger, R. Henrici, (1992) Refrigerant 134a: the first step into a new age of refrigerants, *International Journal of Refrigeration* 15 326-331

[49] A. Selvaraju, A. Mani, (2004) Analysis of an ejector with environment friendly refrigerants, *Applied Thermal Engineering.* 24 827-838.

Appendix A

a). Monthly Average Daily Sunshine Duration in Addis abeba

Months	Jan	Feb	Mar	April	May	Jun	Jul	Aug	Sept	Oct	Nov	Dec
n_s	8.94	9.04	7.98	7.48	6.07	4.54	2.67	2.8	4.59	7.88	8.28	9.17

b). Monthly Average daily horizontal and inclined surface solar radiation in Addis Ababa from excel

Months	Date	N for ith d	N	Latitude	ns	Declina	Ns	ns/Ns	a	b	Ws(degree)	w(rads)	Beta	cos beta	w's
Jan	17	i	17	9.01891	8.94	-20.92	11.53	0.78	0.37	0.36	86.52	1.51	22.01891	0.93	95.06
Feb	16	31+i	47	9.01891	9.04	-12.95	11.72	0.77	0.37	0.37	87.91	1.53	22.01891	0.93	93.04
Mar	16	59+i	75	9.01891	7.98	-2.418	11.94	0.67	0.34	0.44	89.62	1.56	9.01891	0.99	90.00
April	15	90+i	105	9.01891	7.48	9.4149	12.2	0.61	0.32	0.48	91.51	1.60	9.01891	0.99	90.00
May	15	120+i	135	9.01891	6.07	18.792	12.41	0.49	0.28	0.56	93.10	1.62	9.01891	0.99	90.00
Jun	11	151+i	162	9.01891	4.54	23.086	12.51	0.36	0.24	0.65	93.88	1.64	-3.98109	1.00	95.65
Jul	17	181+i	198	9.01891	2.67	21.184	12.47	0.21	0.19	0.75	93.53	1.63	-3.98109	1.00	95.13
Aug	16	212+i	228	9.01891	2.8	13.455	12.29	0.23	0.20	0.74	92.18	1.61	-3.98109	1.00	93.17
Sep	15	243+i	258	9.01891	4.59	2.2169	12.04	0.38	0.25	0.64	90.35	1.58	9.01891	0.99	90.00
Oct	15	273+i	288	9.01891	7.88	-9.599	11.79	0.67	0.34	0.44	88.46	1.54	9.01891	0.99	90.00
Nov	14	304+i	318	9.01891	8.28	-18.91	11.58	0.72	0.35	0.41	86.88	1.52	9.01891	0.99	90.00
Dec	10	334+i	344	9.01891	9.17	-23.05	11.48	0.80	0.38	0.35	86.13	1.50	22.01891	0.93	95.64

Costeta inci	cos teta z	Rb	reflectivity of	1+cosbeta	1-cosbeta	R	Isc(W/m2)	Ho(MJ/m2	H(MJ/m2 -day)	KT(H/Ho)or	I/Io	Hd/H	Hd -diffuse	Ho -again	Hb	HT -inclined surfac
0.91	0.92	0.99	0.2	0.96	0.04	0.99	1367	3.46E+07	2.26E+07	0.66	0.29	6.57E+06	0.346	7.84E+06	2.24E+07	
0.95	0.96	0.99	0.2	0.96	0.04	0.99	1367	3.61E+07	2.36E+07	0.65	0.29	6.87E+06	0.361	8.54E+06	2.34E+07	
1.00	0.99	1.01	0.2	0.99	0.01	1.01	1367	3.71E+07	2.34E+07	0.63	0.31	7.28E+06	0.371	8.69E+06	2.36E+07	
0.99	0.97	1.01	0.2	0.99	0.01	1.01	1367	3.66E+07	2.24E+07	0.61	0.33	7.34E+06	0.366	8.21E+06	2.26E+07	
0.95	0.94	1.01	0.2	0.99	0.01	1.01	1367	3.52E+07	1.95E+07	0.56	0.38	7.38E+06	0.352	6.88E+06	1.96E+07	
0.90	0.91	0.99	0.2	1.00	0.00	0.99	1367	3.41E+07	1.62E+07	0.48	0.45	7.35E+06	0.341	5.53E+06	1.61E+07	
0.91	0.92	0.99	0.2	1.00	0.00	0.99	1367	3.46E+07	1.22E+07	0.35	0.59	7.23E+06	0.346	4.23E+06	1.21E+07	
0.95	0.96	0.99	0.2	1.00	0.00	0.99	1367	3.61E+07	1.32E+07	0.37	0.58	7.60E+06	0.361	4.77E+06	1.31E+07	
1.00	0.99	1.01	0.2	0.99	0.01	1.01	1367	3.71E+07	1.81E+07	0.49	0.44	7.98E+06	0.371	6.72E+06	1.82E+07	
0.99	0.97	1.01	0.2	0.99	0.01	1.01	1367	3.66E+07	2.31E+07	0.63	0.31	7.18E+06	0.366	8.45E+06	2.33E+07	
0.94	0.93	1.01	0.2	0.99	0.01	1.01	1367	3.50E+07	2.26E+07	0.64	0.30	6.77E+06	0.35	7.90E+06	2.28E+07	
0.90	0.91	0.99	0.2	0.96	0.04	0.99	1367	3.40E+07	2.24E+07	0.66	0.29	6.44E+06	0.34	7.62E+06	2.22E+07	

c). Hourly average daily radiation in W/m^2 vs solar time from 2016-18 for all months

ST	Jan	Feb	March	April	May	June	July	Aug	Sept	October	Nov	Dec
7	95.06	110.25	124.17	136.02	131.10	111.78	82.89	82.75	100.78	113.83	99.55	90.79
8	267.33	292.48	311.30	319.91	294.47	246.97	184.41	190.54	246.53	296.25	275.23	260.55
9	464.83	500.97	525.32	528.18	478.04	398.74	298.40	312.11	412.78	505.04	476.40	455.54
10	647.43	693.54	722.96	719.53	646.03	537.55	402.67	423.57	566.09	697.92	662.29	635.99
11	776.02	829.08	862.05	853.84	763.68	634.74	475.68	501.72	673.91	833.69	793.15	763.13
12	822.32	877.87	912.11	902.13	805.94	669.65	501.91	529.80	712.70	882.56	840.26	808.92
13	776.02	829.08	862.05	853.84	763.68	634.74	475.68	501.72	673.91	833.69	793.15	763.13
14	647.43	693.54	722.96	719.53	646.03	537.55	402.67	423.57	566.09	697.92	662.29	635.99
15	464.83	500.97	525.32	528.18	478.04	398.74	298.40	312.11	412.78	505.04	476.40	455.54
16	267.33	292.48	311.30	319.91	294.47	246.97	184.41	190.54	246.53	296.25	275.23	260.55
17	95.06	110.25	124.17	136.02	131.10	111.78	82.89	82.75	100.78	113.83	99.55	90.79
18	0.00	0.00	0.00	8.86	16.12	16.44	11.32	7.52	1.63	0.00	0.00	0.00

d). For January hourly solar radiation calculation in excel

1	January	ST	hour angle (w)	Latitude	Altitude	declination	H-horizontal daily	HT -inclined su	ws	ws(rad)	a	b	cosw	cos ws
2	11:00	23	-165	9.01891	2.386	-20.92	2.26E+07	2.24E+07	86.52150927	1.51	0.417599634	0.652717474	-9.66E-01	0.06
3	10:00	22	-150	9.01891	2.386	-20.92	2.26E+07	2.24E+07	86.52150927	1.51	0.417599634	0.652717474	-8.66E-01	0.06
4	9:00	21	-135	9.01891	2.386	-20.92	2.26E+07	2.24E+07	86.52150927	1.51	0.417599634	0.652717474	-7.07E-01	0.06
5	8:00	20	-120	9.01891	2.386	-20.92	2.26E+07	2.24E+07	86.52150927	1.51	0.417599634	0.652717474	-5.00E-01	0.06
6	7:00	19	-105	9.01891	2.386	-20.92	2.26E+07	2.24E+07	86.52150927	1.51	0.417599634	0.652717474	-2.59E-01	0.06
7	6:00	18	-90	9.01891	2.386	-20.92	2.26E+07	2.24E+07	86.52150927	1.51	0.417599634	0.652717474	0.00	0.06
8	5:00	17	-75	9.01891	2.386	-20.92	2.26E+07	2.24E+07	86.52150927	1.51	0.417599634	0.652717474	0.26	0.06
9	4:00	16	-60	9.01891	2.386	-20.92	2.26E+07	2.24E+07	86.52150927	1.51	0.417599634	0.652717474	0.50	0.06
10	3:00	15	-45	9.01891	2.386	-20.92	2.26E+07	2.24E+07	86.52150927	1.51	0.417599634	0.652717474	0.71	0.06
11	2:00	14	-30	9.01891	2.386	-20.92	2.26E+07	2.24E+07	86.52150927	1.51	0.417599634	0.652717474	0.87	0.06
12	1:00	13	-15	9.01891	2.386	-20.92	2.26E+07	2.24E+07	86.52150927	1.51	0.417599634	0.652717474	0.97	0.06
13	12:00	12	0	9.01891	2.386	-20.92	3.26E+07	2.24E+07	86.52150927	1.51	0.417599634	0.652717474	1.00	0.06
14	11:00	11	15	9.01891	2.386	-20.92	2.26E+07	2.24E+07	86.52150927	1.51	0.417599634	0.652717474	0.97	0.06
15	10:00	10	30	9.01891	2.386	-20.92	2.26E+07	2.24E+07	86.52150927	1.51	0.417599634	0.652717474	0.87	0.06
16	9:00	9	45	9.01891	2.386	-20.92	2.26E+07	2.24E+07	86.52150927	1.51	0.417599634	0.652717474	0.71	0.06
17	8:00	8	60	9.01891	2.386	-20.92	2.26E+07	2.24E+07	86.52150927	1.51	0.417599634	0.652717474	0.50	0.06
18	7:00	7	75	9.01891	2.386	-20.92	2.26E+07	2.24E+07	86.52150927	1.51	0.417599634	0.652717474	0.26	0.06
19	6:00	6	90	9.01891	2.386	-20.92	2.26E+07	2.24E+07	86.52150927	1.51	0.417599634	0.652717474	0.00	0.06
20	5:00	5	105	9.01891	2.386	-20.92	2.26E+07	2.24E+07	86.52150927	1.51	0.417599634	0.652717474	-2.59E-01	0.06
21	4:00	4	120	9.01891	2.386	-20.92	2.26E+07	2.24E+07	86.52150927	1.51	0.417599634	0.652717474	-5.00E-01	0.06
22	3:00	3	135	9.01891	2.386	-20.92	2.26E+07	2.24E+07	86.52150927	1.51	0.417599634	0.652717474	-7.07E-01	0.06
23	2:00	2	150	9.01891	2.386	-20.92	2.26E+07	2.24E+07	86.52150927	1.51	0.417599634	0.652717474	-8.66E-01	0.06
24	1:00	1	165	9.01891	2.386	-20.92	2.26E+07	2.24E+07	86.52150927	1.51	0.417599634	0.652717474	-9.66E-01	0.06

sin ws	rt	I(j/m2-hour)(ho	rd diffuse	Hd	Id(J/m2-hour) horizontal	Id w/m2	Ib(J/m2-hour) horizontal	Ib w/m2 hor	IT(j/m2-hour)(Inclined)	IT W/m2 inclin
0.998157646	0.03	6.50E+05	-1.35E-01	6.57E+06	-8.86E+05	-2.46E+02	1.54E+06	426.65	6.43E+05	0.00
0.998157646	0.02	4.07E+05	-1.22E-01	6.57E+06	-8.00E+05	-2.22E+02	1.21E+06	335.20	4.03E+05	0.00
0.998157646	0.00	1.00E+05	-1.01E-01	6.57E+06	-6.63E+05	-1.84E+02	7.63E+05	211.92	9.93E+04	0.00
0.998157646	-6.72E-03	-1.52E+05	-7.36E-02	6.57E+06	-4.84E+05	-1.34E+02	3.32E+05	92.13	-1.51E+05	0.00
0.998157646	-1.04E-02	-2.36E+05	-4.20E-02	6.57E+06	-2.76E+05	-7.66E+01	3.94E+04	10.94	-2.34E+05	0.00
0.998157646	-3.33E-03	-7.54E+04	-7.97E-03	6.57E+06	-5.24E+04	-1.45E+01	-2.30E+04	-6.39E+00	-7.46E+04	0.00
0.998157646	0.02	3.46E+05	0.03	6.57E+06	1.71E+05	47.50	1.75E+05	48.53	3.42E+05	95.06
0.998157646	0.04	9.72E+05	0.06	6.57E+06	3.79E+05	105.31	5.93E+05	164.74	9.62E+05	267.33
0.998157646	0.07	1.69E+06	0.08	6.57E+06	5.58E+05	154.95	1.13E+06	314.60	1.67E+06	464.83
0.998157646	0.10	2.35E+06	0.11	6.57E+06	6.95E+05	193.05	1.66E+06	460.96	2.33E+06	647.43
0.998157646	0.12	2.82E+06	0.12	6.57E+06	7.81E+05	217.00	2.04E+06	566.91	2.79E+06	776.02
0.998157646	0.13	4.31E+06	0.12	6.57E+06	8.11E+05	225.16	3.50E+06	972.34	2.96E+06	822.32
0.998157646	0.12	2.82E+06	0.12	6.57E+06	7.81E+05	217.00	2.04E+06	566.91	2.79E+06	776.02
0.998157646	0.10	2.35E+06	0.11	6.57E+06	6.95E+05	193.05	1.66E+06	460.96	2.33E+06	647.43
0.998157646	0.07	1.69E+06	0.08	6.57E+06	5.58E+05	154.95	1.13E+06	314.60	1.67E+06	464.83
0.998157646	0.04	9.72E+05	0.06	6.57E+06	3.79E+05	105.31	5.93E+05	164.74	9.62E+05	267.33
0.998157646	0.02	3.46E+05	0.03	6.57E+06	1.71E+05	47.50	1.75E+05	48.53	3.42E+05	95.06
0.998157646	-3.33E-03	-7.54E+04	-7.97E-03	6.57E+06	-5.24E+04	-1.45E+01	-2.30E+04	-6.39E+00	-7.46E+04	0.00
0.998157646	-1.04E-02	-2.36E+05	-4.20E-02	6.57E+06	-2.76E+05	-7.66E+01	3.94E+04	10.94	-2.34E+05	0.00
0.998157646	-6.72E-03	-1.52E+05	-7.36E-02	6.57E+06	-4.84E+05	-1.34E+02	3.32E+05	92.13	-1.51E+05	0.00
0.998157646	0.00	1.00E+05	-1.01E-01	6.57E+06	-6.63E+05	-1.84E+02	7.63E+05	211.92	9.93E+04	0.00
0.998157646	0.02	4.07E+05	-1.22E-01	6.57E+06	-8.00E+05	-2.22E+02	1.21E+06	335.20	4.03E+05	0.00
0.998157646	0.03	6.50E+05	-1.35E-01	6.57E+06	-8.86E+05	-2.46E+02	1.54E+06	426.65	6.43E+05	0.00

d). Hourly average Solar radiation for all Months

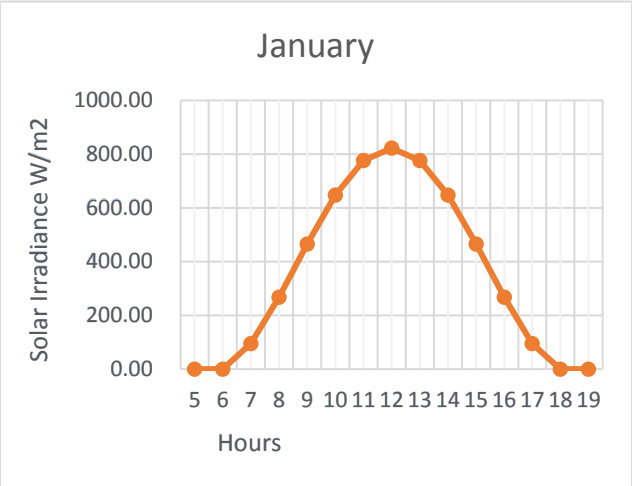

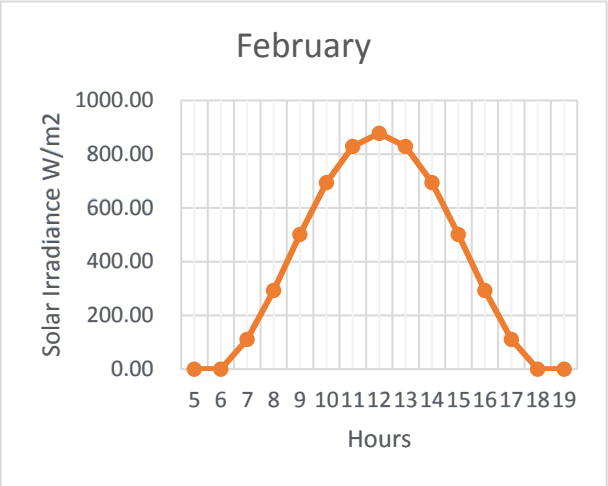

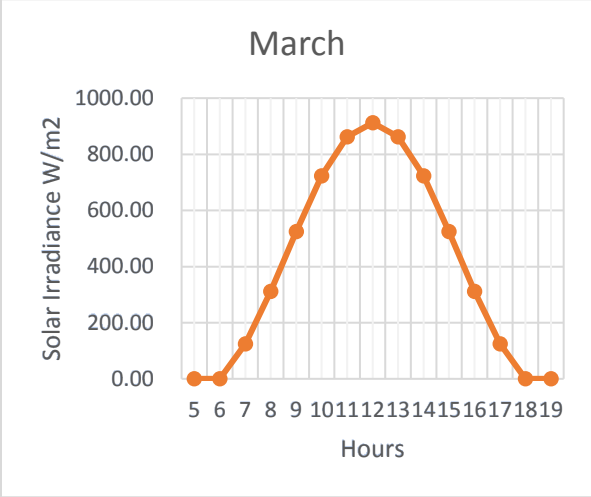

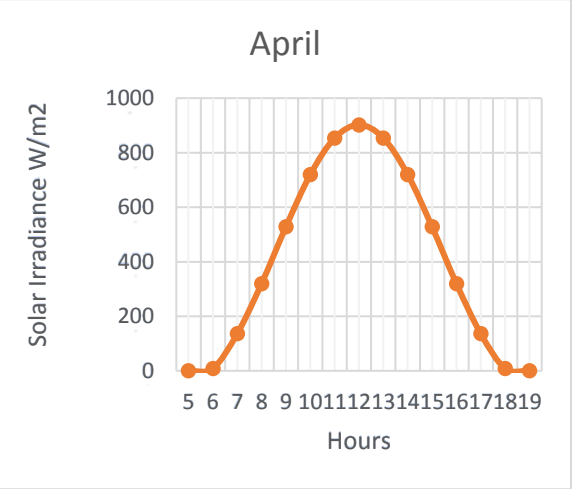

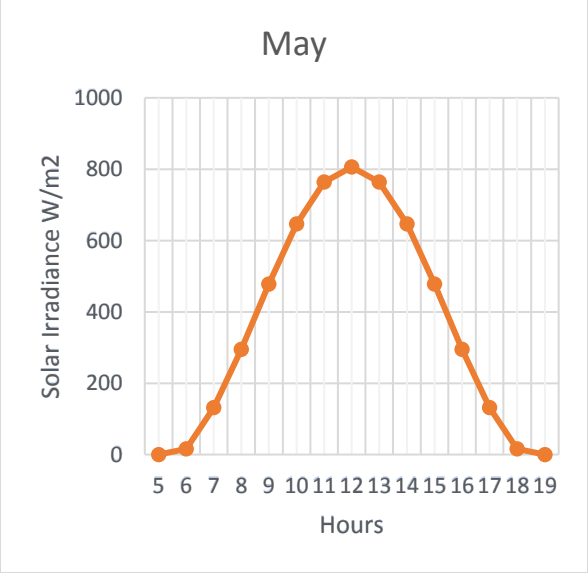

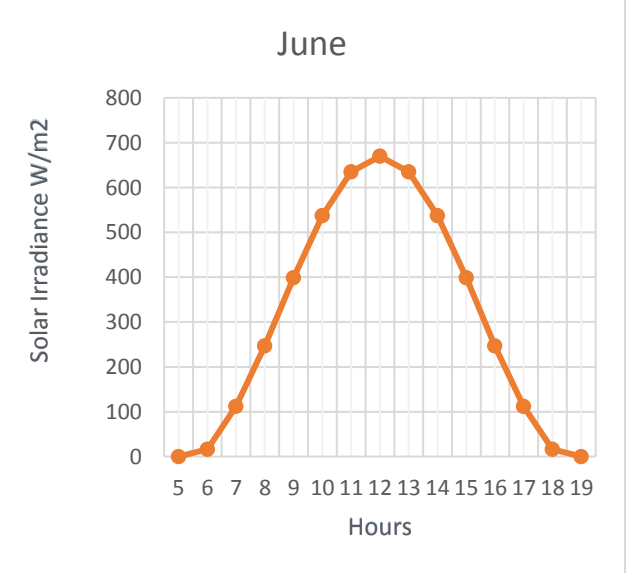

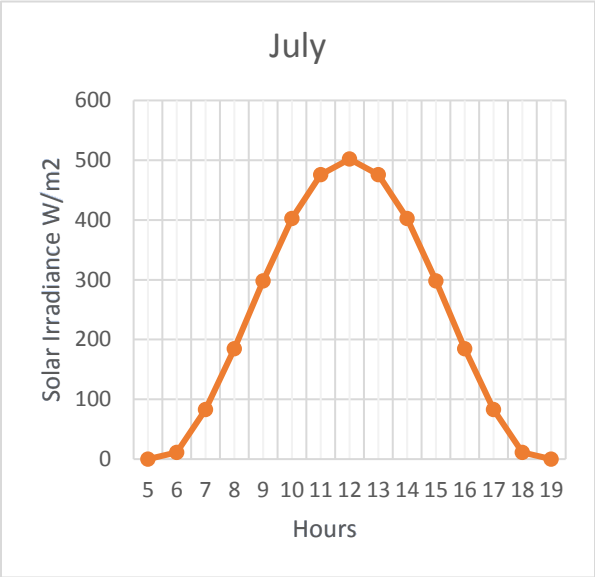
July
Solar Irradiance W/m2
600
500
400
300
200
100
0
5 6 7 8 9 10 11 12 13 14 15 16 17 18 19
Hours

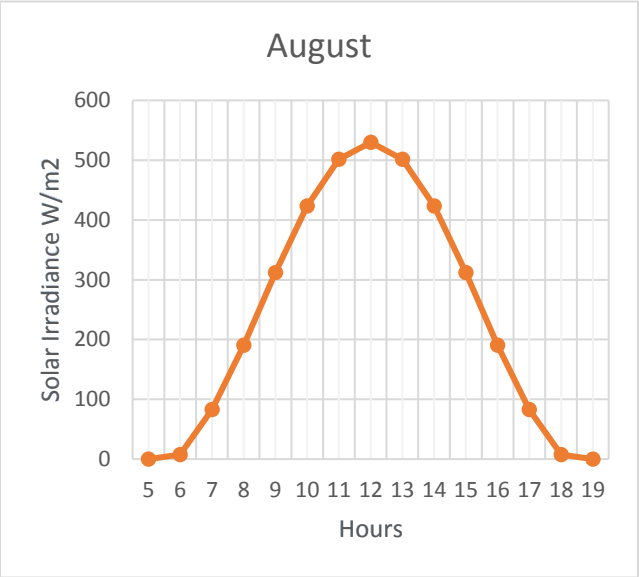
August
Solar Irradiance W/m2
600
500
400
300
200
100
0
5 6 7 8 9 10 11 12 13 14 15 16 17 18 19
Hours

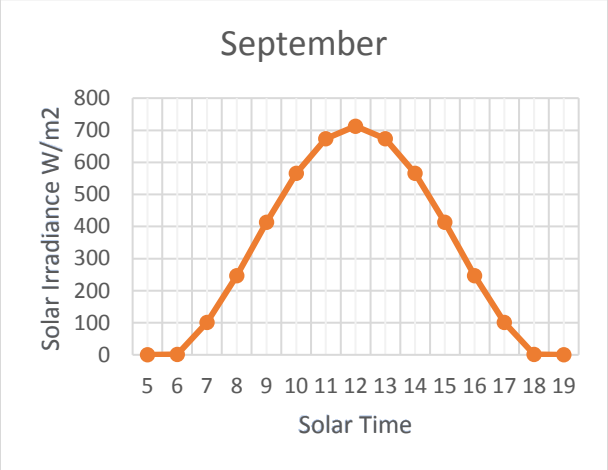
September
Solar Irradiance W/m2
800
700
600
500
400
300
200
100
0
5 6 7 8 9 10 11 12 13 14 15 16 17 18 19
Solar Time

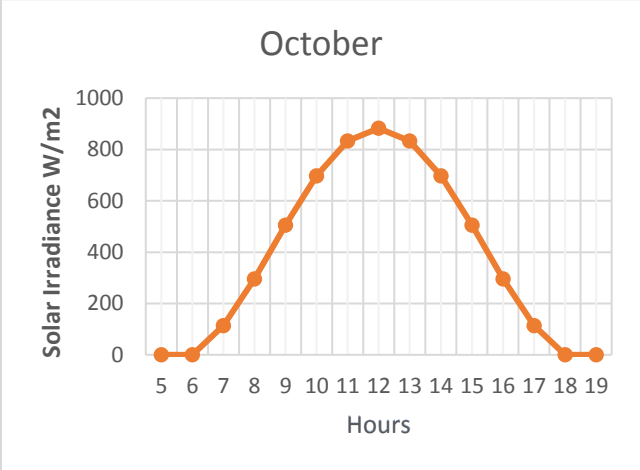
October
Solar Irradiance W/m2
1000
800
600
400
200
0
5 6 7 8 9 10 11 12 13 14 15 16 17 18 19
Hours

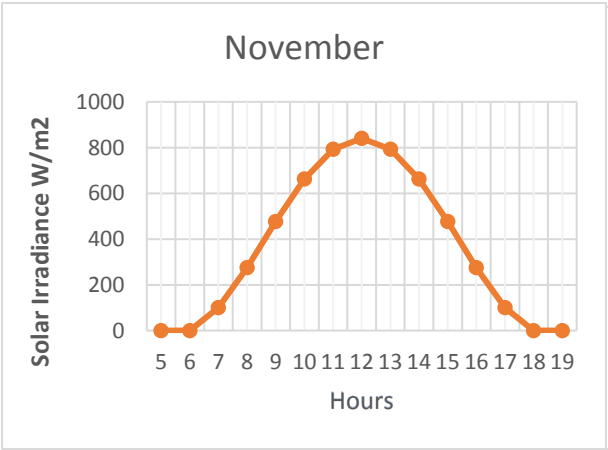
November
Solar Irradiance W/m2
1000
800
600
400
200
0
5 6 7 8 9 10 11 12 13 14 15 16 17 18 19
Hours

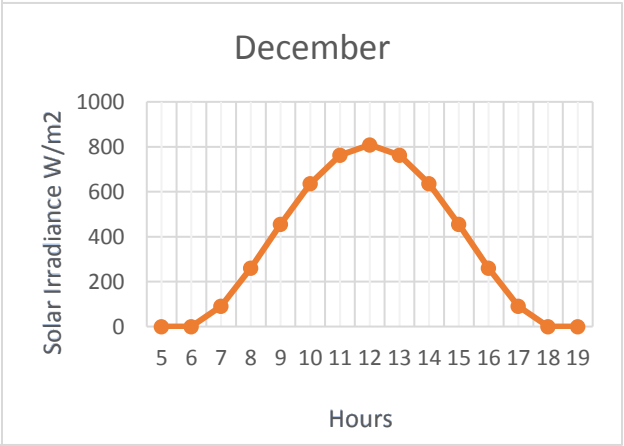
December
Solar Irradiance W/m2
1000
800
600
400
200
0
5 6 7 8 9 10 11 12 13 14 15 16 17 18 19
Hours

e). Monthly Maximum, minimum and average temperature

Months	**T max**	**T min**	**T aver**
Jan	24.62	9.15	16.88
Feb	26.13	10.6	19.48
Mar	26.82	12.15	19.45
April	25.25	12.91	19.08
May	23.13	13.26	18.19
Jun	23.09	12.53	17.81
Jul	23.17	12.14	17.65
Aug	22.1	11.89	16.99
Sep	22.73	11.69	17.21
Oct	23.37	11.02	17.19
Nov	24.13	9.36	16.74
Dec	23.82	8.36	16.09

Appendix B

a). Solar ejector cooling system performance analysis EES programming code

"Ejector Performnace anlysis under design and off-design operating conditions Programming in EES by Mihretab Woldetsadik Thermal systems "

T_g=363[K];

x_1 = 1;

P_g = pressure (R134a, T=T_g, x = x_1) ;

h_g1=Enthalpy(R134a,T=T_g,x=x_1);

s_g1=Entropy(R134a,T=T_g,x=x_1);

v_g1=Volume(R134a,T=T_g,x=x_1);

G=1.2;"Specific Ratio "

E_ffN=0.95;"isentropic efficiency of nozzle Assuming that the nozzle efficiency is close to unity 0.95"

R=0.0815[KJ/Kg*K];

c_p=0.489;

A_t=0.000003938[m^2];"2.24mm"

m_g=((P_g*A_t)/(T_g)^(1/2))*((G*E_ffN/R)*(2/(G+1))^((G+1)/(G-1)))^(1/2);"The mass flow is proportional to the nozzle throat area Ath. An isentropic Efficiency ηp introduces a first parameter to be found "

A_p1=0.000009616[m^2];"3.5mm"

A=A_p1/A_t;"Area ratio for sample"

(A*M_p1)=((0.909*(1+0.1*M_p1^2))^5.5);"Assuming that the nozzle efficiency is close to unity, the conditions at nozzle exit (section p1) are evaluated by classic gas-dynamic isentropic relations"

P_g/P_p1=(1+0.1*M_p1^2)^6;"From section Pp1, the primary flow is thought to continue its expansion in exit of the nozzle"

"Entrained flow from inlet to section y-y From assumption (6), the entrained flow reaches choking condition at the y-y section, i.e. Msy =1. For a given inlet stagnant pressure Pe, we have"

M_sy=1;"Msy =1. For a given inlet stagnant pressure Pe"

T_e=285[K];

x_2 = 1;

P_e = pressure (R134a, T=T_e, x = x_2) ;

h_g2=Enthalpy(R134a,T=T_e,x=x_2);

S_g2=Entropy(R134a,T=T_e,x=x_2);

v_g2=Volume(R134a,T=T_e,x=x_2);

" Psy may be found considering that at section y the entrained flow reaches sonic velocity, that is, for an approximately isentropic flow,"

P_e/P_sy=(1+((G-1)/2)*M_sy^2)^(G/(G-1));

"Primary-flow core (from section 1-1 to section y-y)"

"The Mach number Mpy of the primary flow at the y-y section follows the isentropic relations as an approximation"

"At this section, primary and secondary flows have the same pressure Ppy = Psy and start to mix."

P_sy=P_py;

P_py/P_p1=((1+((G-1)/2)*M_p1^2)^(G/(G-1)))/(1+((G-1)/2)*M_py^2)^(G/(G-1));

"The flow area, on the other hand, is evaluated introducing in the isentropic relation a coefficient ϕp that should count for viscous loss at the boundary between primary and secondary flow"

E_ffp=0.88;"isentropic relation a coefficient ϕp assumed as"

A_py/A_p1=(E_ffp*M_p1/M_py)*((2/(G+1))*((1+0.1*M_py^2)/(1+0.1*M_p1^2)))^5.5;

"Cross-sectional area at section y-y"

"The geometrical cross-sectional area at section y-y is A3 that is the sum of the areas for the primary flow Apy and for the entrained flow Asy. That is"

A_3=0.000020578[m^2]"5,12mm Given that the section y has been assumed to stay in the cylindrical portion of the ejector, the area of this portion is now specified as D3=5mm"

A_3=A_py+A_sy;"A tentative value of area A3 is used to calculate secondary flow area Asy"

"if A_sy<0;"

"The best values of the empirical parameters are ηP = 0.95, ηS =0.85, and ϕP =0.88. [Ejectors for Efficient Refrigeration Design, Applications and Computational Fluid Dynamics by Federico Mazzelli]"

E_ffS=0.85;

m_s=((P_e*A_sy)/(T_e)^(1/2))*((G*E_ffS/R)*(2/(G+1))^((G+1)/(G-1)))^(1/2);

"Temperature and Mach number at section y-y"

"The temperature and the Mach number of the two stream at section y-y follows"

T_g/T_py=1+((G-1)/2)*M_py^2;

T_e/T_sy=1+((G-1)/2)*M_sy^2;

"Mixed flow at section m-m before the shock"

"wo streams starts to mix from section y-y. A shock then takes place with a sharp pressure rise at section s-s. A momentum balance relation thus can be derived as"

"where Um is the velocity of the mixed flow and ϕm is the coefficient accounting for the frictional loss Similarly, an energy balance relation can be derived as"

Q=A_3/A_t;

" We choose ϕm or Effm = (0:80; for Q > 8:3) & (0:82; for 6.96 < Q < 8:3) & (0:84; for Q < 6:9):"

E_ffm=0.4;

U_py=M_py*(G*R*T_py)^0.5;

U_sy=M_sy*(G*R*T_sy)^0.5;

E_ffm*(m_g*U_py+m_s*U_sy)=(m_g+m_s)*U_m; "where Upy and Usy are the gas velocities of the primary and entrained flow at the section y-y , Um is mixed fluid velocity "

"Similarly, an energy balance relation can be derived as"

m_g*(C_p*T_py+((U_py^2)/2))+m_s*(C_p*T_sy+((U_sy^2)/2))=(m_g+m_s)*(C_p*T_m+((U_m^2)/2));

"The Mach number of the mixed flow can be evaluated using the following relation:

M_m=(U_m)/((G*R*T_m)^0.5);

"After mixing, the flow undergoes a normal shock in section s. Assuming an isentropic flow before and after the shock, the pressure rise is concentrated in this section and brings the stream from the mixed flow pressure Pm = Ppy =Psy to the final value P3 at the end of the cylindrical duct. The classic gas dynamic relations give Mixed flow across the shock from section m-m to section 3-3 "

P_m=P_py;

P_3/P_m=1+(2*G/(G+1))*((M_m^2)-1);

M_3=((1+((G+1)/2)*M_m^2)/((G*M_m^2)-((G-1)/2)))^0.5;

"Mixed flow through diffuser The pressure at the exit of the diffuser follows the relation, assuming isentropic process Finally, the conical diffuser produces a further pressure recovery up to"

P_c/P_3=(1+((G-1)/2)*M_3^2)^(G/(G-1));"backward pressure"

"condensor temperature 34oC"

T_c=303[K];

X_3=0;

P_con = pressure (R134a, T=T_c, x = x_3) ;

h_fc=Enthalpy(R134a,T=T_c,x=x_3);

s_fc=Entropy(R134a,T=T_c,x=x_3);

v_fc=Volume(R134a,T=T_c,x=x_3);

{Pcon is - critical back pressure of the ejector, Pc * }

"If the value of pc is higher than the Pcod then i will decreas the assumption of the A3 but here the pc value is less than pcod then it is possible if we take any value of A3 until it reachs Pco but it shoudnt go beyond pcod"

"Pc=602690 Pa and Pcon=59497 Pa , THEREFORE Pc<Pcon(P crit) then A3 + is possible as much as it is less than Pcod . but it should not exceed it "

{The authors suggest to use the above described set of equations to calculate the entrainment ratio and the diameter D3 of the ejector from the knowledge of the boundary conditions and of the nozzle geometry. The procedure works as follows:}

r_p=P_c/P_e;"Compression ratio"

w=m_s/m_g;"Entrainment ratio"

" COP is the coefficient of performance of the ECS."

W_pum1=v_fc*(P_g-P_con)/1000;

h_6=(h_fc+W_pum1);"State six or h6 which inters to generator "

h_5=h_fc;

h_1=h_g1;

h_2=h_g2;

Cop_ECS=w*(h_2-h_5)/(h_1-h_6);

"The overall coefficient of performance (COPo) of the SECS"

"where FR(sa) and FRUL are collector characteristic coefficients for evacuted tube collector is 0.7 and 3.3"

F_sa=0.7;"FR(sa)"

F_UL=3.3;

“I_T=700;”

“T_a=293;”

T_i=T_g+10;

"The solar collector efficiency g was defined as follows "

coll_eff=(F_sa)-((F_UL)*((T_i-T_a)/I_T));

"The overall coefficient of performance (COPo) of the SECS:"

COP_overall=(coll_eff)*(Cop_ECS);

"The useful energy output of the collector per unit collector area Qcoll and the cooling capacity per unit collector area Qe are"

Q_coll=(coll_eff)*(I_T);

Q_e=(COP_overall)*(I_T);